

**Parameter Establishment and Verification of a
Fabrication Stress Model and a Thermo-Kinetic
Cure Model for Filament Wound Structures**

by

Russell Kent Call

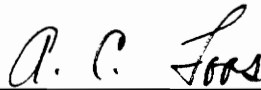
Thesis submitted to the Faculty of the
Virginia Polytechnic Institute and State University
in partial fulfillment of the requirements for the degree of

MASTER OF SCIENCE


in

Engineering Mechanics

APPROVED:



A. C. Loos, Chairman


C. E. Knight
O. H. Griffin

September, 1991

Blacksburg, Virginia

LD
5655
V855
1991
@34
c-2

**Parameter Establishment and Verification of a
Fabrication Stress Model and a Thermo-Kinetic
Cure Model for Filament Wound Structures**

by

Russell Kent Call

Committee Chairman: Alfred C. Loos
Engineering Mechanics

(ABSTRACT)

Two comprehensive composite fabrication simulation computer codes have been written. These codes when coupled together have the capability to model the filament winding and curing processes for composite structures. The "Filament Winding Cure" (FWCURE) code is a thermo-kinetic model. FWCURE models the resin viscosity, percent of cure, temperature, resin flow, and layer location. As these characteristics change, they have an effect on the fiber tension within the composite. The "Winding and Curing Stress Analysis Finite Element" (WACSAFE) code models the filament winding process and predicts manufacturing stresses and strains based on material properties, lay-down tension and wind angle.

The permeability model in FWCURE requires constants that are found experimentally. The WACSAFE code requires an input tension that is equivalent to the initial spool tension minus the instantaneous tension losses.

The permeability constants and the instantaneous tension losses were found experimentally. The codes were then used to predict fiber tension, tension losses and mandrel strains for experimental test cylinders. The predictions were compared to test data.

Acknowledgements

I would like to express my appreciation to Dr. A. C. Loos and Dr. C. E. Knight for not giving up on me when I left VPI&SU after my course work was completed. Their guidance and support in finishing this thesis is greatly appreciated.

I would also like to thank Dr. O. H. Griffin for willingly filling a vacancy on my committee at the last minute.

This work was supported by Thiokol Corporation. I wish to express my thanks to Thiokol for their financial support and to Mr. W. T. Berndt for his support and guidance.

There are many people in my current job at Thiokol who have encouraged me and helped me to finish. Their names are too numerous to mention here, but I sincerely appreciate each of them.

Finally I would like to thank my wife Dana, and my daughter Kelsee. They have willingly supported me through graduate school and in finishing this thesis. I could not have completed this work without their support.

Table of Contents

1.0 INTRODUCTION	1
2.0 TEST SETUP	6
2.1 WIND SETUP	6
2.2 RESIN CONTENT CONTROL	9
2.3 FIBER TENSION MEASUREMENT	9
2.4 WINDING MANDRELS	16
3.0 TIME-DEPENDENT TENSION LOSS	20
3.1 TIME-DEPENDENT TENSION LOSS TEST MATRIX	22
3.2 RESIN VISCOSITIES	26
3.3 FWCURE VERIFICATION	31
3.3.1 Single Layer Low Viscosity Winds	32
3.3.2 Single Layer High Viscosity Winds	40
3.3.3 Multi-Layer Winds	41

4.0 MODELING THE WINDING PROCESS	46
4.1 WINDING TEST MATRIX AND EXPERIMENTAL RESULTS	47
4.2 SEPARATION OF THE WINDING TENSION LOSSES	58
4.2.1 Parametric Sensitivity Study	61
4.2.2 Side-by-Side Tension Losses	69
4.2.3 Instantaneous Tension Losses	75
4.3 WACSAFE VERIFICATION	86
5.0 SUMMARY AND CONCLUSIONS	98
5.1 SUMMARY	98
5.2 CONCLUSIONS	100
5.3 RECOMMENDATIONS	102
BIBLIOGRAPHY	104
APPENDIX A	106
APPENDIX B	120
VITA	165

List of Figures

Figure 2.1	Schematic of the Winding Setup	7
Figure 2.2	Tension Measuring Device	11
Figure 2.3	Load Cell Output Versus Applied Load	12
Figure 2.4	Fiber Tension Versus Load Cell Output	15
Figure 2.5	Fiber Tension Test Setup	17
Figure 2.6	Mandrel Strain Gage Locations	18
Figure 3.1	Viscosity of EPON 826-RD2 Resin	27
Figure 3.2	Viscosity of EPON 826 and 828 Resin	29
Figure 3.3	Viscosity of EPON 826-A Resin	30
Figure 3.4	Single Layer AS4W-12K/826-RD2 Tension Loss	33
Figure 3.5	Single Layer IM6W-12K/826-RD2 Tension Loss	34
Figure 3.6	Single Layer AS4W-12K/826 Tension Loss	35
Figure 3.7	Single Layer AS4W-12K/826-A Tension Loss ..	36
Figure 3.8	Single Layer P55S-2K/826-RD2 Tension Loss .	37
Figure 3.9	Single Layer P55S-2K/826-RD2 Tension Loss Verification	38
Figure 3.10	Multi-Layer AS4W-12K/826-RD2 Tension Loss .	42

Figure 3.11	Multi-Layer AS4w-12K/826-RD2 Tension Loss Verification	43
Figure 4.1	Stress Retention Factor Versus Spool Tension for AS4W-12K/826-RD2	50
Figure 4.2	Stress Retention Factor Versus Spool Tension for IM6W-12K/826-RD2	51
Figure 4.3	Stress Retention Factor Versus Spool Tension for P55S-2K/826-RD2	52
Figure 4.4	Finite Element Model of the $\frac{1}{2}$ -inch Wind ...	57
Figure 4.5	WACSAFE Model of the Thin-Walled Mandrel Experiments	59
Figure 4.6	WACSAFE Model of the Thick-Walled Mandrel Experiments	60
Figure 4.7	Theoretical Tension Versus Input Tension for AS4W-12K/826-RD2	70
Figure 4.8	Theoretical Tension Versus Input Tension for IM6W-12K/826-RD2	71
Figure 4.9	Theoretical Tension Versus Input Tension for P55S-2K/826-RD2	72
Figure 4.10	Percent Side-by-Side Tension loss Versus Input Tension	73
Figure 4.11	Lay-down Tension Versus Spool Tension for AS4W-12K/826-RD2	77
Figure 4.12	Lay-down Tension Versus Spool Tension for IM6W-12K/826-RD2	78
Figure 4.13	Lay-down Tension Versus Spool Tension for P55S-2K/826-RD2	79
Figure 4.14	Lay-down Tension Retention Factor Versus Spool Tension for AS4W-12K/826-RD2.....	80
Figure 4.15	Lay-down Tension Retention Factor Versus Spool Tension for IM6W-12K/826-RD2.....	81
Figure 4.16	Lay-down Tension Retention Factor Versus Spool Tension for P55S-2K/826-RD2.....	82

Figure 4.17	Instantaneous Tension Loss Versus Spool Tension for AS4W-12K/826-RD2	83
Figure 4.18	Instantaneous Tension Loss Versus Spool Tension for IM6W-12K/826-RD2	84
Figure 4.19	Instantaneous Tension Loss Versus Spool Tension for P55S-2K/826-RD2	85
Figure 4.20	Mandrel Hoop Strain Through the Thickness After Eight Circuits	88
Figure 4.21	Mandrel Hoop Strain Through the Thickness After Twenty-one Circuits	89
Figure 4.22	Averaged Lay-down Tension Retention Factor for AS4W-12K/826-RD2	91
Figure 4.23	Averaged Lay-down Tension Retention Factor for IM6W-12K/826-RD2	92
Figure 4.24	Thin-Walled Mandrel Strain Comparisons for AS4W-12K/826-RD2	94
Figure 4.25	Thick-Walled Mandrel Strain Comparisons for AS4W-12K/826-RD2	95
Figure 4.26	Mandrel Strain Comparisons for IM6W-12K/826-RD2	96
Figure 4.27	Mandrel Strain Comparisons for P55S-2K/826-RD2	97

List of Tables

Table 3.1 Time Dependent Tension Loss Test Matrix 23

Table 4.1 Instantaneous Tension Loss test Matrix 48

Table 4.2 Uncured Mechanical Property Limits
for T1000/974 64

Table 4.3 Fractional Factorial Test Matrix 67

Table 4.4 Uncured Composite Mechanical Properties 74

1.0 INTRODUCTION

For the past twenty-five years, composite materials have been used where high strength-to-weight and stiffness-to-weight ratios are required. Typical uses are in space and aerospace vehicles. As the number of composite structures in use has increased, there has been increasing interest in incorporating composite materials in land and sea vehicles as well. The prime motivator for using composites over a light weight alloy is generally an economic one, i.e. additional fuel savings or increased payload. In the past the manufacturing methods and materials were expensive and often excluded many potential uses. However, with more and more composite structures being used the amount of material being produced has increased, causing a decrease in the unit cost. The cost of manufacturing has also been reduced as more operations have become automated.

Some of the manufacturing processes that are now automated include; pultrusion, braiding, tape laying and filament winding. All of these processes have advantages and limitations. Filament winding is one of the older technologies for modern composite structures, having origin dating back to the 1950's. The winding machines have changed from the gear and chain type of control to highly versatile computer control. Filament winding has the capability of laying down a large amount of fiber in a relatively short period of time, making it a viable candidate for high speed production of composite structures.

During the past 20 to 25 years there has been much effort to understand and control the effect of filament winding process variables on the final structure and to optimize those variables. In the past this effort was largely an empirical one. Subscale models were fabricated varying tension, wind angles, ply thicknesses and cure cycles until an acceptable result was obtained. The effort then shifted to scaling up to the full scale model. The scaling up process was also a trial and error method. This empirical approach for establishing the process variables has proved to be inefficient and costly.

Recently efforts have been made to develop computer codes

that could model the filament winding and curing processes. These codes can predict the manufacturing stresses, resin flow, resin viscosity, percent of cure, temperature at any location within the composite during cure, layer location within the composite and the changes in fiber tension. Two one-dimensional codes have been written allowing the modeling of composite cylinders only. Calius and Springer^{1,2} have written a computer code for modeling composite cylinders which will yield the aforementioned results. The ability of this code to predict the temperatures within the composite and at the mandrel surface, along with the residual curing stresses has been verified^{3,4}. A similar model has been written by Spencer⁵. The two codes are similar in what they attempt to model but their approaches are different. Also, the codes are limited to a one-dimensional analysis.

Two axisymmetric codes have been written by Tzeng⁶ and Nguyen⁷. These codes when coupled together have the capability to model the manufacturing and curing processes. The first code is a thermo-kinetic code, "Filament Winding Cure" (FWCURE). The second code is the manufacturing stress model, "Winding and Curing Stress Analysis Finite Element" (WACSAFE).

The two computer codes are based on input parameters that

need to be determined experimentally. It is the scope of this thesis to determine these parameters and verify the results of these two codes. The FWCURE program models the resin flow, viscosity, percent of cure, temperature and layer location. As these parameters change they will have an affect on the tension loss of the fibers in the composite. The parameters will vary with the cure cycle while the resin flow is also dependent on the permeability of the composite. FWCURE incorporates a permeability model. The model requires a constant that is established through experimentation. A series of experiments was run in which the fiber tension was monitored with time. The spool tension, fiber modulus, initial resin viscosity and number of layers were changed to determine usable values of the permeability constant. The parameters in the model were adjusted until the model data matched the experimental data.

The WACSAFE program predicts the manufacturing stresses and strains based on cured and uncured composite material properties, lay-down tension and wind angle. The lay-down tension is a function of the initial spool tension and an instantaneous tension loss. This instantaneous tension loss is caused by the flattening of the fiber bundle and the instantaneous resin flow due to sudden application of pressure on the fiber bundle. A second tension loss effect

occurs simultaneously, caused by multiple circuits laying down next to each other. Both tension loss effects are explained in detail in section 4.0 and also by Nguyen⁷. The instantaneous tension loss and the tension loss due to multi-circuit effects were determined experimentally. A series of specimens were wound in which both tension loss effects were present. WACSAFE was used to determine the multi-circuit effect for each material at various tension levels. The multi-circuit effect was subtracted from the total tension loss and the lay-down tension as a function of spool tension was established.

Throughout this report three types of fiber tension are referred to. To aid the reader, a definition for the three types is provided here. Spool tension is defined to be the tension in the fiber prior to mandrel contact. Lay-down tension is defined to be the tension in the fiber after mandrel contact and after any instantaneous tension losses. Winding tension is the tension in the fiber when winding is complete. Both instantaneous and side-by-side tension loss effects are present in winding tension.

2.0 TEST SETUP

All experimental specimens were wound with the same basic setup. The setup consisted of a spool holding device, a fiber tensioning system, a resin impregnation cup, a tension measuring device, a mandrel and the winding machine. A schematic of the winding process is shown in Figure 2.1.

2.1 WIND SETUP

Each experiment was wound using only one spool of fiber. The spool was mounted on a shaft which was free to rotate. The distance from the spool to the first redirect roller was maximized to reduce the variations in the fiber pay out angle. The fiber pay out angle varies as the fiber moves from end to end of the spool. This variation of the fiber pay out angle causes the fiber tension to vary. Therefore as the variations in the fiber pay out angle are minimized,

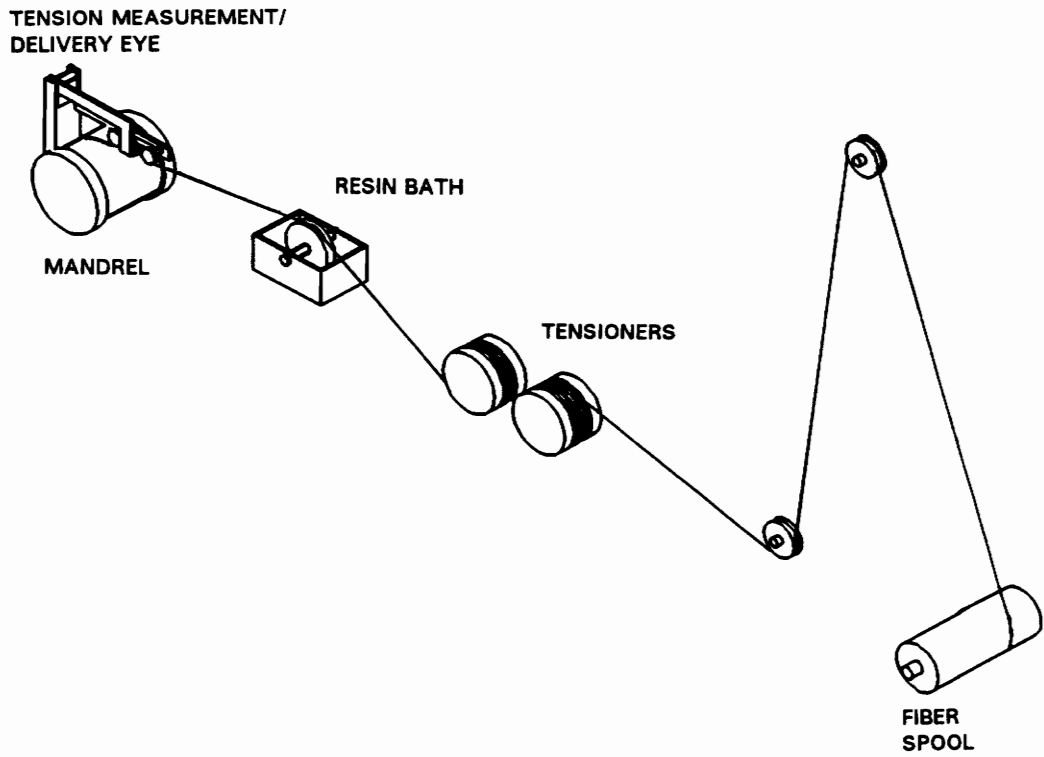


Figure 2.1 Schematic of the Winding Setup

the changes in tension due to this angle changing are also minimized.

From the spool the fiber passed over two redirect rollers onto the two tensioning rollers. The first roller was attached to a Magtrol 1-2046 electric torque motor. The torque was varied by a Magtrol 4636 torque adjust unit. This change in torque translated to a change in the fiber tension. The second roller was free to rotate allowing several wraps of the fiber to be made around the first roller to prevent slippage. After the fiber was tensioned it was impregnated with resin at the resin cup. The resin cup consisted of a resin pick up roller partially immersed in a resin bath. A scraper bar was positioned next to the surface of the pick up roller, controlling the amount of resin allowed on the roller surface. The resin content in the fiber was controlled by changing the distance between the scraper bar and the pick up roller.

The winding machine used was a Southbend model A lathe. All windings were hoop winds (90° to mandrel axis). The band advance was changed depending on the type and size of fiber being wound.

2.2 RESIN CONTENT CONTROL

The resin content was determined by taking a 150-inch dry fiber sample and weighing it. The appropriate wet sample weight was calculated for the desired resin content. The scraper bar was then adjusted until a 150-inch wet sample weight met the calculated results. The equation to determine the wet sample weight is shown in Equation (2.1).

$$W-D\left(1+\frac{\rho_r V_r}{\rho_f(1-V_r)}\right) \quad (2.1)$$

W = wet sample weight
D = dry sample weight
 V_r = resin volume fraction
 ρ_r = resin density
 ρ_f = fiber density

Use of this equation will yield an ideal resin content by volume assuming no voids. The presence of any voids will lower the resin volume and the fiber volume. The derivation for Equation (2.1) is shown in Appendix A.

2.3 FIBER TENSION MEASUREMENT

After the fibers were impregnated they passed through the tension measuring device. This device served two purposes. The first was to measure the tension in the fiber. The

second purpose was to work the resin into the fibers by passing through the series of rollers. The tension measuring device consisted of two fixed rollers and one roller supported by a Revere MCBU-.025 load cell. The output of the load cell was monitored by a Vishay/Ellis-11 strain indicator. A sketch of the tension measuring device is shown in Figure 2.2. The position of the load cell may be changed to vary the ratio between the force on the roller and the force on the load cell. For the experiments presented here, the position of the load cell was such that the load on the load cell was approximately three times the load on the pivot roller.

As the fiber tension increases, the force on the load cell also increases. Tests were conducted to verify that the load cell output versus the applied load was a linear function. Calibrated weights were suspended from the load cell, and the output was recorded. The results are plotted in Figure 2.3. The linearity shown in Figure 2.3 yields a constant ratio between the output of the load cell and the applied load of 26.36/lbs. This ratio was used to derive Equation (2.2) relating the load cell output to fiber tension.

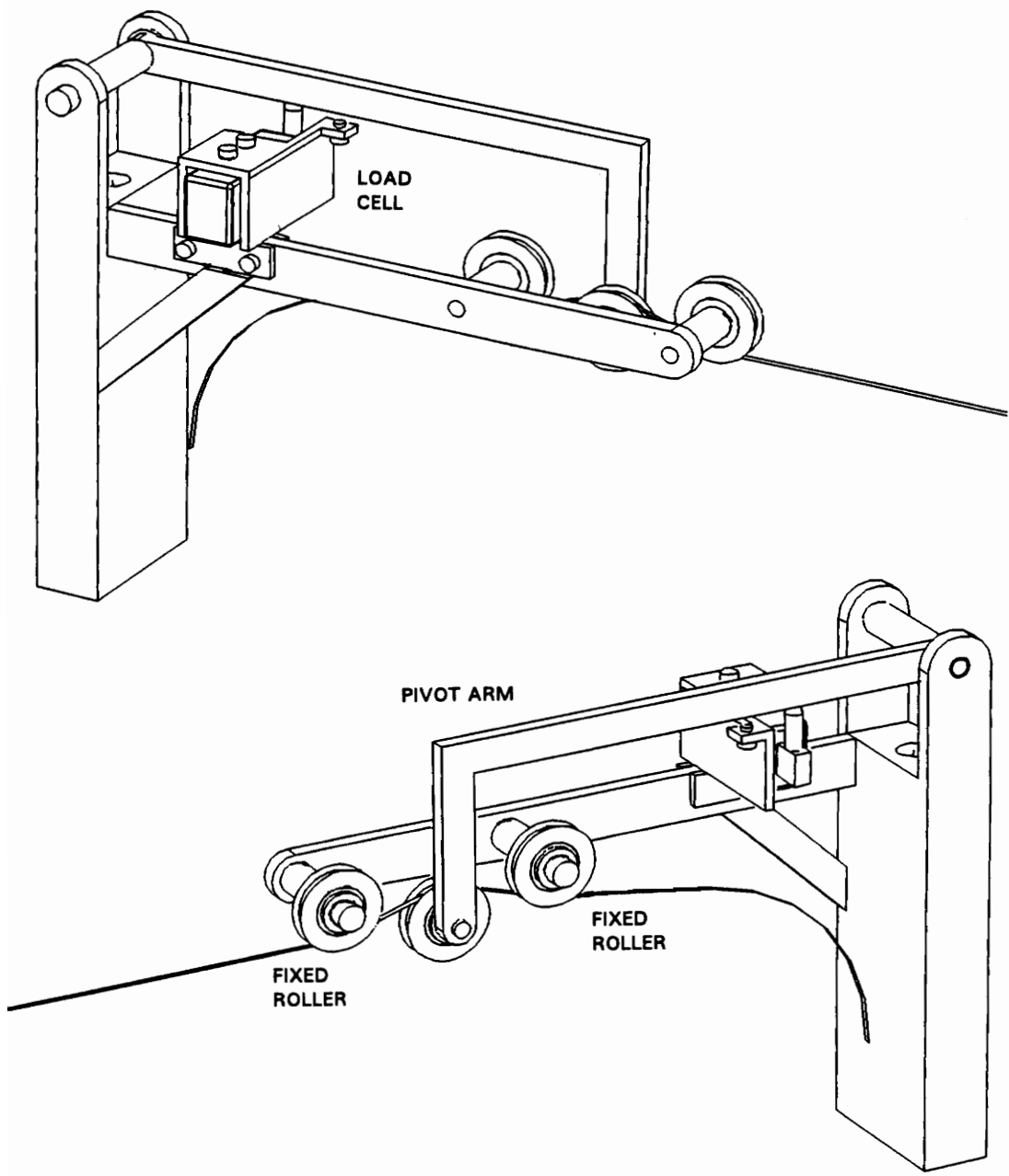


Figure 2.2 Tension Measuring Device

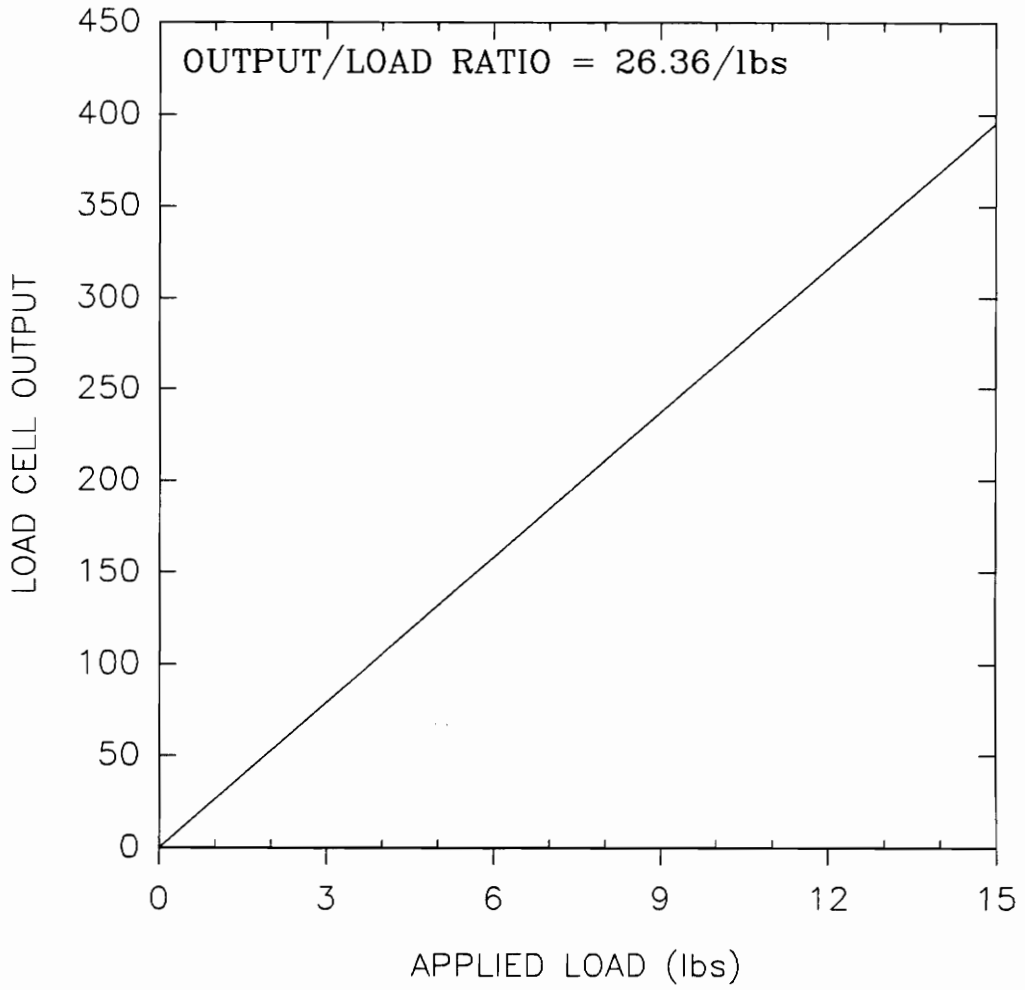


Figure 2.3 Load Cell Output Versus Applied Load

$$T = \frac{X O_{LC}}{R(\sin\alpha_1 + \sin\alpha_2) \left[W \cos\left(\tan^{-1} \frac{O_{LC}}{2500RX}\right) - Z \sin\left(\tan^{-1} \frac{O_{LC}}{2500RX}\right) \right]} \quad (2.2)$$

T = fiber tension
 X = load cell location (2.405-in)
 O_{LC} = load cell output reading
 R = output over load ratio (26.36/lbs)
 α_1 = fiber angle between pivot roller and roller #1
 α_2 = fiber angle between pivot roller and roller #2
 W = pivot arm length (7.625-in)
 Z = pivot arm stub length (2.625-in)

The fiber angles, α_1 and α_2 , are found by satisfying Equations (2.3).

$$\begin{aligned}
 L_1 \sin\alpha_1 + (D+R) \cos\alpha_1 - 2R &= 0 \\
 L_2 \sin\alpha_2 + (D+R) \cos\alpha_2 - 2R &= 0
 \end{aligned} \quad (2.3)$$

L_1 = length between pivot roller and roller #1
 L_2 = length between pivot roller and roller #2
 D = displacement of pivot roller
 R = roller radius (.5")

The pivot roller displacement, D, is determined using Equation (2.4). The lengths between the pivot roller and the fixed rollers are found using Equations (2.6).

$$D = D_i + D_{PR} \quad (2.4)$$

D_i = initial pivot roller vertical displacement (.04")
 D_{PR} = pivot roller vertical displacement caused by the applied load. Determined from Equation (2.5)

$$D_{PR} = W \sin\left(\tan^{-1} \frac{O_{LC}}{2500RX}\right) - Z \left[1 - \cos\left(\tan^{-1} \frac{O_{LC}}{2500RX}\right)\right] \quad (2.5)$$

W = pivot arm length (7.625-in)
 O_{LC} = load cell output
 R = output over load ratio (26.36/lbs)
 X = load cell location
 Z = pivot arm stub length (2.625-in)

$$L_1 = l_1 - W \left[1 - \cos\left(\tan^{-1} \frac{O_{LC}}{2500RX}\right)\right] - Z \sin\left(\tan^{-1} \frac{O_{LC}}{2500RX}\right) \quad (2.6)$$

$$L_2 = l_2 + W \left[1 - \cos\left(\tan^{-1} \frac{O_{LC}}{2500RX}\right)\right] + Z \sin\left(\tan^{-1} \frac{O_{LC}}{2500RX}\right)$$

l₁ = initial horizontal distance between pivot roller and roller #1 (1.592")
 l₂ = initial horizontal distance between pivot roller and roller #2 (1.644")
 W = pivot arm length (7.625-in)
 O_{LC} = load cell output
 R = output over load ratio (26.36/lbs)
 X = load cell location
 Z = pivot arm stub length (2.625-in)

The derivations for Equations (2.2), (2.3), (2.5), and (2.6) are presented in Appendix A. A graph of fiber tension versus load cell output is displayed in Figure 2.4. The graph and equations are a close approximation of the fiber tension. The load cell output through the Vishay/Ellis-11 strain indicators would vary from day to day. To obtain a more accurate reading of the fiber tension, a simple test was performed. A fiber was threaded through the tension

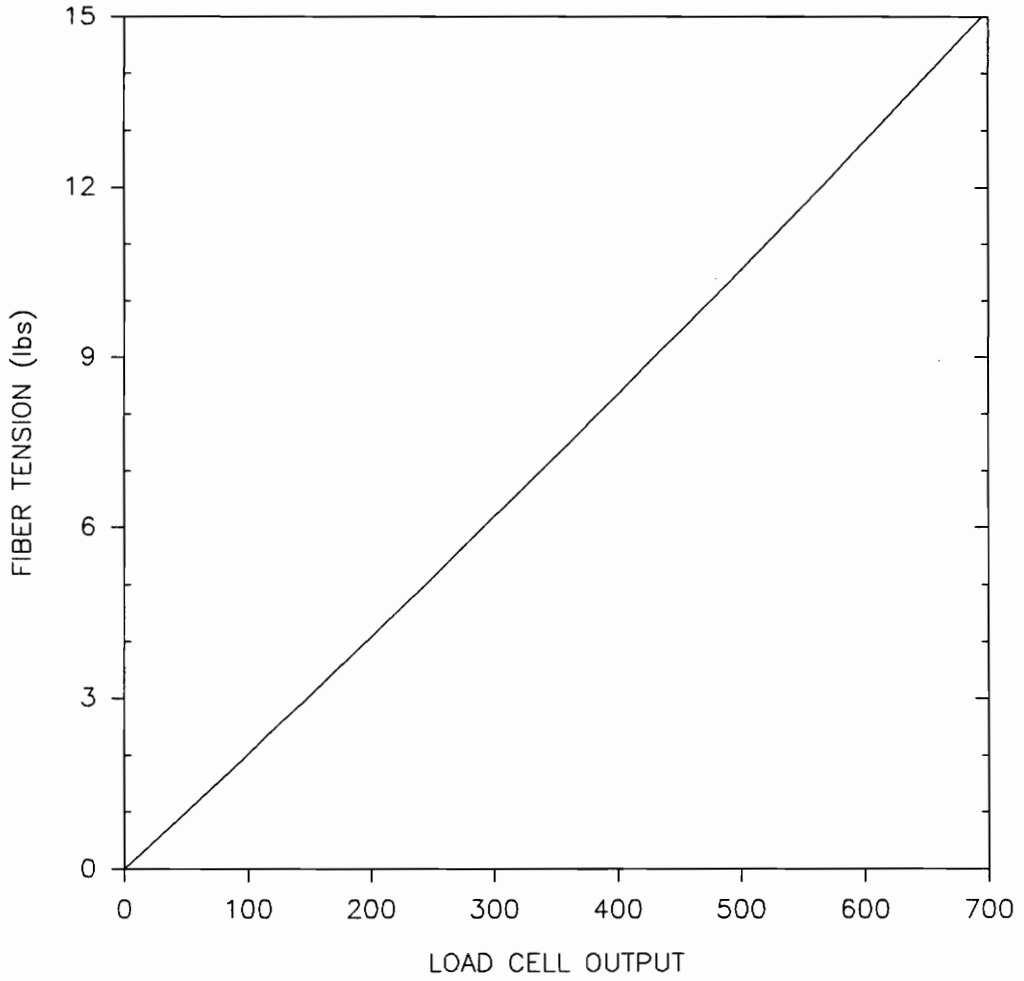


Figure 2.4 Fiber Tension Versus Load Cell Output

measuring rollers with one end fixed and the other end attached to a weight as shown in Figure 2.5. The weight was equivalent to the desired fiber tension. The load cell output was noted and the same output was matched during the winding operation.

The tension measuring device was the last contact the fiber made with the winding apparatus prior to contacting the mandrel. By having the device as the last fiber contact prior to mandrel lay-down, the actual fiber tension could be measured without concern of any influence from other rollers or contact points.

2.4 WINDING MANDRELS

Two different aluminum mandrels were used for winding. Both mandrels were cylindrical, four inches long and had an outside diameter of six inches. One mandrel was .050-inch thick and the other was .250-inch thick. Two Micro-Measurements strain gages type EA-13-250AP-120 were mounted on the inside surface of each mandrel. The gages were mounted mid length at 0° and 90°. The orientation of the gages was such that circumferential strain could be measured. The location of the gages on the mandrel is shown in Figure 2.6. The leads from the strain gages were

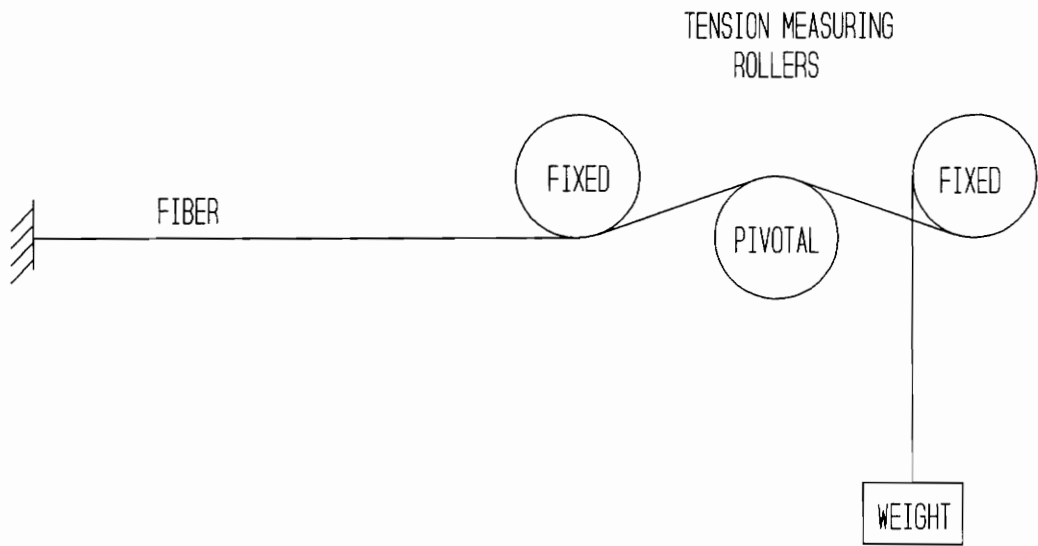
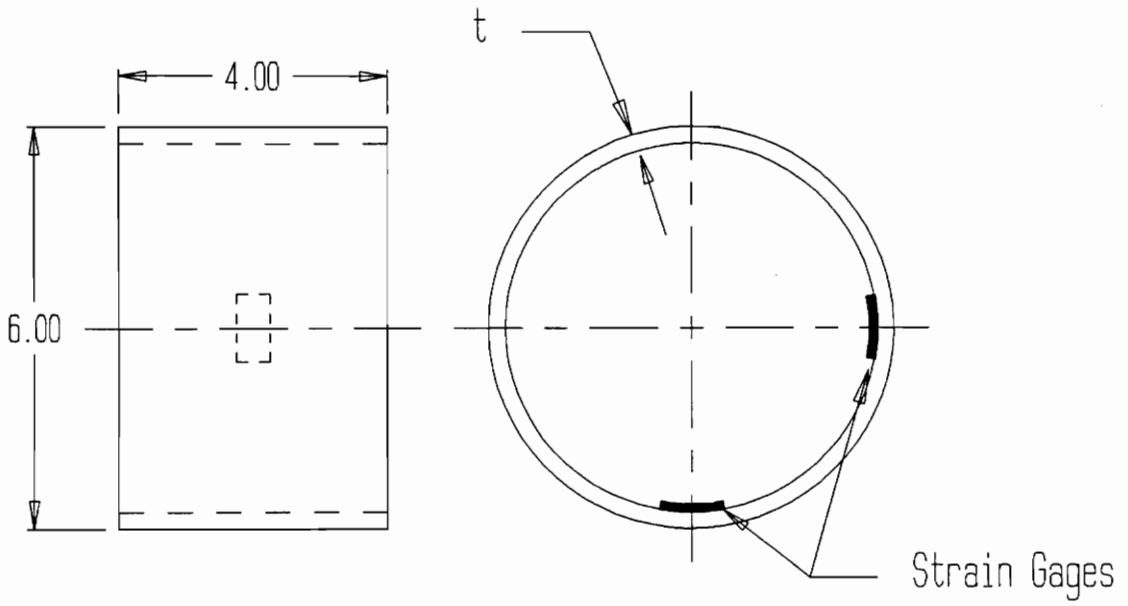


Figure 2.5 Fiber Tension Test Setup



MANDREL MATERIAL : ALUMINUM
 $t = 0.050$ in. and 0.250 in.

Figure 2.6 Mandrel Strain Gage Locations

attached to a Vishay/Ellis-20 switch and Vishay/Ellis-21 balance unit. The mandrel strains were monitored during and after winding. These mandrel strains were used to determine the winding tension in the fibers.

3.0 TIME-DEPENDENT TENSION LOSS

Filament winding requires that resin impregnated fibers be wound over a mandrel under tension. The tension ensures that the fibers are placed on the desired path without any buckling. The curvature of the mandrel and the tension in the fibers result in radial pressures that aid in the debulking of the composite. Debulking of the composite is accomplished through the nestling of the individual fiber bundles, resin flowing radially outward and the individual layers moving radially inward. The movement of the layers radially inward results in fiber tension loss. The resin flow and layer location are dependent on the fiber tension, resin viscosity and the permeability of the composite. The viscosity is in turn dependent on the temperature and percent of cure. It is possible for fiber tension levels to be such that the outer layers create a radial pressure of a magnitude that will cause the inner plies to lose all their tension and be put in compression. The fiber/resin system

in the uncured state cannot support compressive loads and the inside layers will buckle. This buckling results in a greatly reduced composite strength.

The FWCURE program models the resin flow, viscosity, percent of cure, temperature and layer location. As these parameters change they will affect the tension loss of the fibers in the composite. These parameters vary with the cure cycle, while the resin flow is also dependent on the permeability of the composite. FWCURE incorporates a permeability model. The model is based on the Kozeny-Carman equation. Using the proper values for porosity of the porous medium will result in an equation yielding the permeability parallel to the fibers or normal to the fibers. The permeability normal to the fibers (Equation 3.1) is the more dominate and is the one of interest in the study.

$$S_n = \frac{d^2 P_n^3}{C'' (1 - P_n)^2} \quad (3.1)$$

S = permeability of the porous medium
d = filament diameter
C'' = permeability constant
P_n = porosity normal to the fibers

The derivation of Equation (3.1) and a more complete explanation of the permeability model is explained by Tzeng⁶. For FWCURE to model the permeability, the permeability constant needs to be established through

experimentation. The role of the permeability constant is to shift the tension loss with time curve. It does not affect the shape of the curve.

A series of experiments was run in which the fiber tension, fiber modulus, initial resin viscosities and number of layers were changed to determine applicable permeability coefficients. An initial estimate was made based on the first set of experiments. The code was then run incorporating these coefficients and a prediction was made for similar sets of experiments. An iterative process was then involved to determine the coefficient values which most closely fit the data. Good agreement between the test data and the predictions was found for all test cases.

3.1 TIME-DEPENDENT TENSION LOSS TEST MATRIX

The series of experiments used in this study is listed in Table 3.1. The raw data is listed in Appendix B. In Table 3.1 set number refers to the number identifying the different combinations of listed parameters. The "826" and "828" shown under the resin type column refer to different Shell Epon epoxy resin systems made by the Shell Chemical Company. "RD2" is a reactive diluent used to lower the viscosity of the resin. "A" is a curing agent. "RD2" and

Table 3.1 Time Dependent Tension Loss Test Matrix

SET #	FIBER TYPE	FIBER E1 (msi)	RESIN TYPE	RESIN VISC. (poise)	SPOOL TENSION (lbs)	INITIAL TENSION/PRESSURE	# LAYERS
1	AS4W-12K	34	826/RD2	6.16	10.0	5.8 lbs	1
2	AS4W-12K	34	826/RD2	6.16	5.0	2.9 lbs	1
3	AS4W-12K	34	826/RD2	6.16	7.5	4.4 lbs	1
4	AS4W-12K	34	826/RD2	6.16	12.3	6.2 lbs	1
5	AS4W-12K	34	826/RD2	6.16	3.0	1.8 lbs	1
6	IM6W-12K	40.4	826/RD2	6.16	5.0	3.3 lbs	1
7	P55S-2K	55	826/RD2	6.16	3.0	1.9 lbs	1
8	AS4W-12K	34	826	80	5.0	2.9 lbs	1
9	AS4W-12K	34	828	145	5.0	2.7 lbs	1
10	AS4W-12K	34	826/A	20-1900	5.0	3.0 lbs	1
11	AS4W-12K	34	826/RD2	6.16	5.0	10.83 psi 13.67 psi 14.92 psi 15.17 psi	18 layer 1 layer 2 layer 3 layer 4

"A" are product codes of the Miller Stephenson Chemical Company Incorporated. Set #10 is the only set to incorporate the curing agent (20% by weight). The viscosity shown in set #10 is shown as a parameter representing the measured ranges for the resin as it advances through cure. Spool tension is defined to be the tension on the fiber prior to contact with the mandrel. Initial tension is defined to be the tension of the fibers just after winding is completed and the first mandrel strain reading is taken. The difference between the spool tension and the initial tension is covered in section 4.0. Initial mandrel pressures are listed in set #11 rather than tension. Set #11 is the only set to contain more than one layer of material. The tension in any given layer cannot be determined from closed form solutions once more than one layer is wound on the mandrel. Therefore, to validate the model the mandrel pressures were used. Initial pressure is defined to be the pressure on the mandrel immediately following winding when the first mandrel strain reading is taken.

Spool tension was determined from the tension measuring device described in the test set up, section 2.0. The tension in the fiber after winding has been completed is determined from mandrel hoop strain readings using Equation (3.2).

$$T = E \epsilon t W \quad (3.2)$$

T = fiber winding tension
E = modulus of mandrel
 ϵ = hoop strain of the mandrel
t = mandrel thickness
W = single fiber bundle width
(on mandrel)

The equation is only valid for thin-walled mandrels. The derivation is shown in Appendix A. For thick-walled mandrels an equation based on elasticity theory would be used, (See Equation (4.1) in section 4.1).

Mandrel pressure is also determined from the mandrel hoop strain readings. The relationship shown in Equation (3.3) relates mandrel strain readings to mandrel pressure. The derivation for this equation is also shown in Appendix A.

$$P = \frac{T}{R W} \quad (3.3)$$

P = mandrel pressure
T = fiber tension
R = mandrel external radius
W = single fiber bundle width
(on mandrel)

3.2 RESIN VISCOSITIES

The viscosities of the different resins were measured using a Rheometrics RMS 800 rheometer. Resin samples, used in the viscosity measurements, were taken from the same batch of resin used in winding the test specimens. The baseline resin system consisted of Epon 826 resin with 5% RD2 by weight, a reactive diluent added to lower the resin viscosity to a level normally used in "wet" filament winding. Five different samples were mixed and tested at different frequencies. A small amount of resin was placed between a fixed disk and an oscillating disk. Increasing the frequency of the oscillating disk corresponds to increasing the rate of shear strain which is calculated by the software of the Rheometrics RMS 800. The results of the tests are shown graphically in Figure 3.1. The large scatter is normal for low viscosity materials tested at low frequencies. As the frequency increases the scatter in the viscosity measurement decreases. The value used, listed in Table 3.1, is an average viscosity of the five samples taken at the highest tested frequency.

The viscosities of Shell Epon 826 and 828 resin systems were also measured at different frequencies on the Rheometrics machine. The same resin lots for each of the 826 and 828 resin systems were used throughout the testing. These are

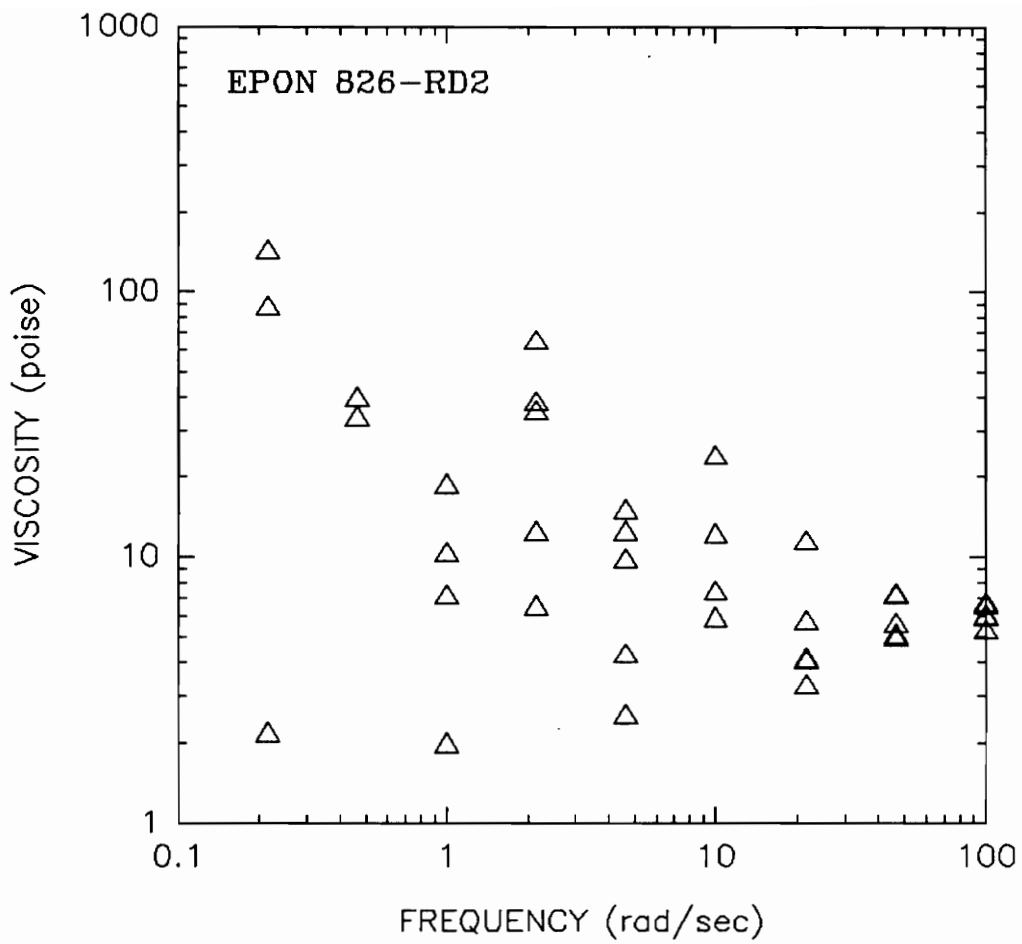


Figure 3.1 Viscosity of Epon 826-RD2 Resin

base resins shipped as is from the manufacturer and, when used in their base form, require no mixing. Therefore, only one test sample was used for each resin type. The results are illustrated in Figure 3.2. It is not expected that additional samples would vary significantly from these results. Due to the higher viscosity of the resins the scatter is reduced at the lower frequencies. The values used in the FWCURE model are the average of the last six data points on each curve.

Epon 826 with curing agent "A" was tested at a constant frequency, 10 radians/second. The frequency used during testing was chosen by the technician operating the Rheometrics machine as a good median value. Too low a frequency, with a low viscosity fluid, would yield highly scattered measurements as seen in Figure 3.1. Too high of a frequency, with a high viscosity fluid, would be hard on the testing equipment. The resin was mixed with 20% by weight curing agent "A". A sample was taken to the Rheometrics machine, and its viscosity was measured with time. Winding and tension loss data were simultaneously being gathered using the remainder of the resin. The measured viscosities are shown in Figure 3.3.

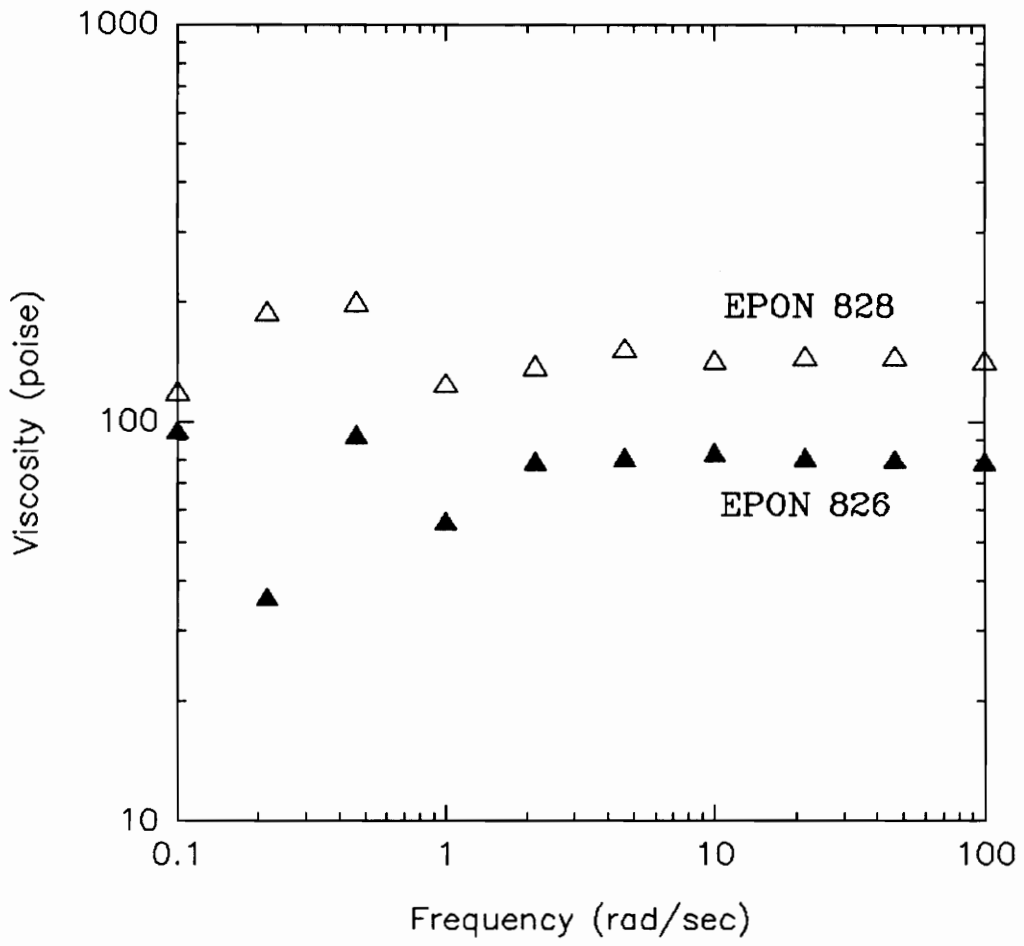


Figure 3.2 Viscosity of Epon 826 and 828 Resins

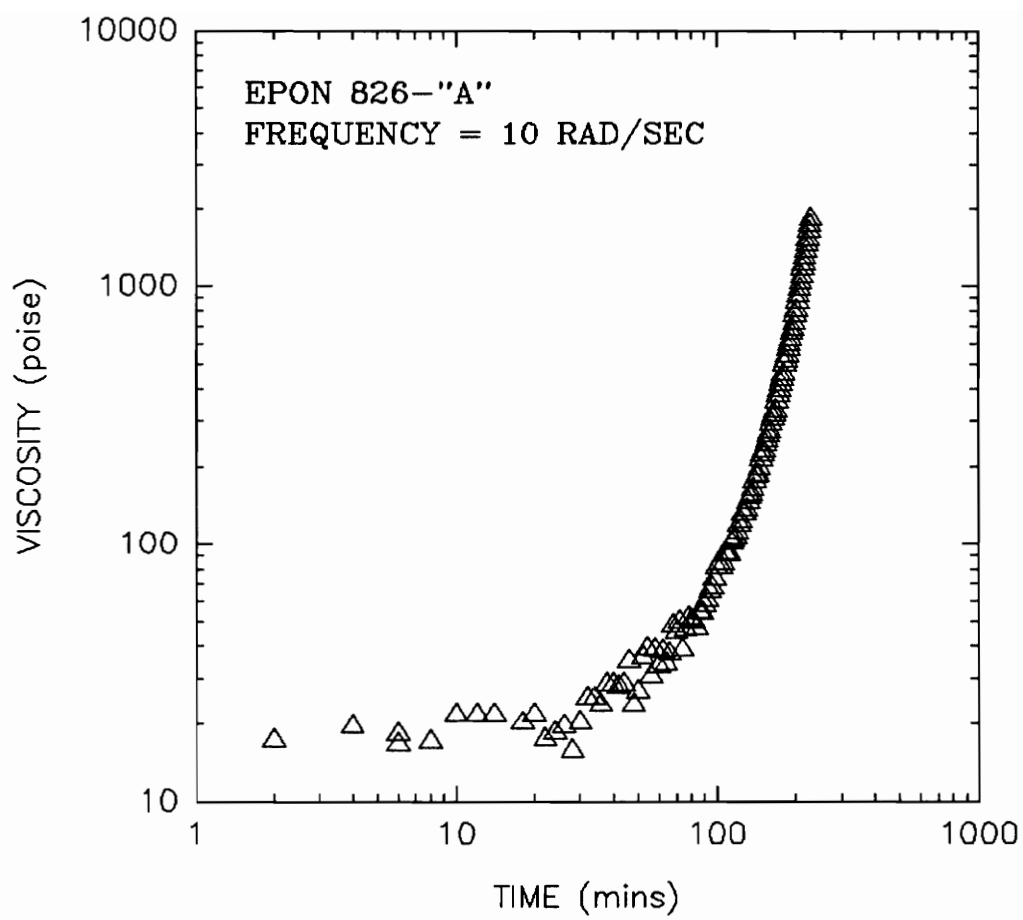


Figure 3.3 Viscosity of Epon 826-A Resin

3.3 FWCURE VERIFICATION

While trying to determine the coefficients for the permeability model, it was found that the model's predictions for tension loss with time, when using the measured resin content, did not correspond well with the measured tension loss with time curve. It was suggested that resin would migrate to the surface almost instantaneously upon mandrel lay-down, leaving a lower, fairly constant resin content within the fiber bundle. The amount of resin migration would be expected to depend on the winding tension which provides the driving force for the migration. Observation during the winding process showed that some resin would indeed migrate to the surface instantaneously leaving a resin rich surface. A portion of the remaining resin within the fiber bundle will continue to migrate to the surface with time as the fibers move radially inward displacing the resin. The radial movement of the fibers is caused by the imposed tension and results in the tension loss with time. A relationship between resin volume within the fiber bundle and the spool tension was established empirically. The coefficients for the permeability model were then determined.

3.3.1 Single Layer Low Viscosity Winds

There is excellent agreement between the measured tension loss with time and the predicted loss for the majority of the experiments using FWCURE. These include; single layer winds using the 826/RD2, 826, and 826/"A" resin systems and single layer winds using the Hercules AS4 and IM6 fibers. The correlation between the predicted results and the measured data are shown in Figures 3.4 through 3.7.

The test data for the P55 fiber, shown in Figure 3.8, shows a flatter curve for tension loss than that predicted by the model. A second test was wound to verify the data trend, Figure 3.9. Both tests show the same flat curve. A flat curve for tension loss with time suggests that the majority of the resin is migrating to the surface instantaneously leaving a lower resin content within the fiber bundle. The discrepancy between predicted values and measured values suggests a problem with the relationship between spool tension and resin content within the fiber bundle at lay-down.

There are two possible improvements to this relationship. The first would be to base the relationship on spool stress (spool tension divided by the cross sectional area of the fiber) rather than on spool tension only. The P55 fiber has

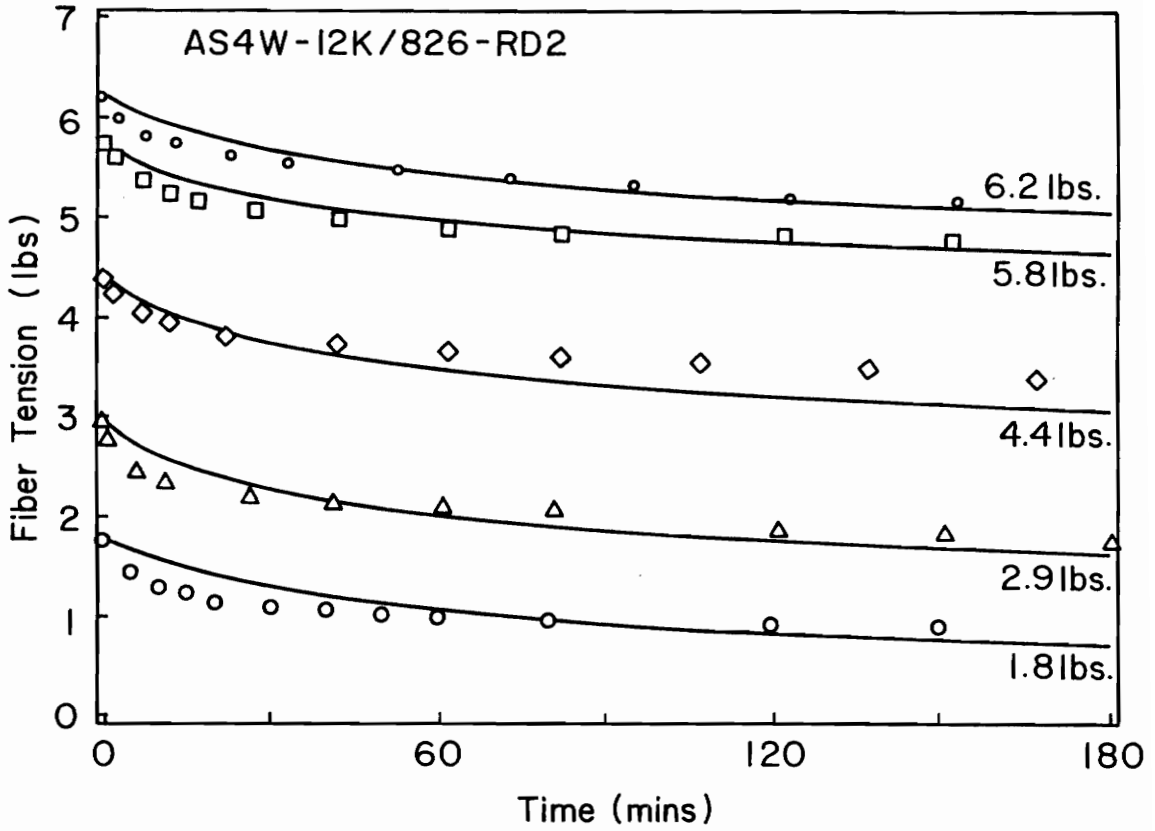


Figure 3.4 Single Layer AS4W-12K/826-RD2 Tension Loss

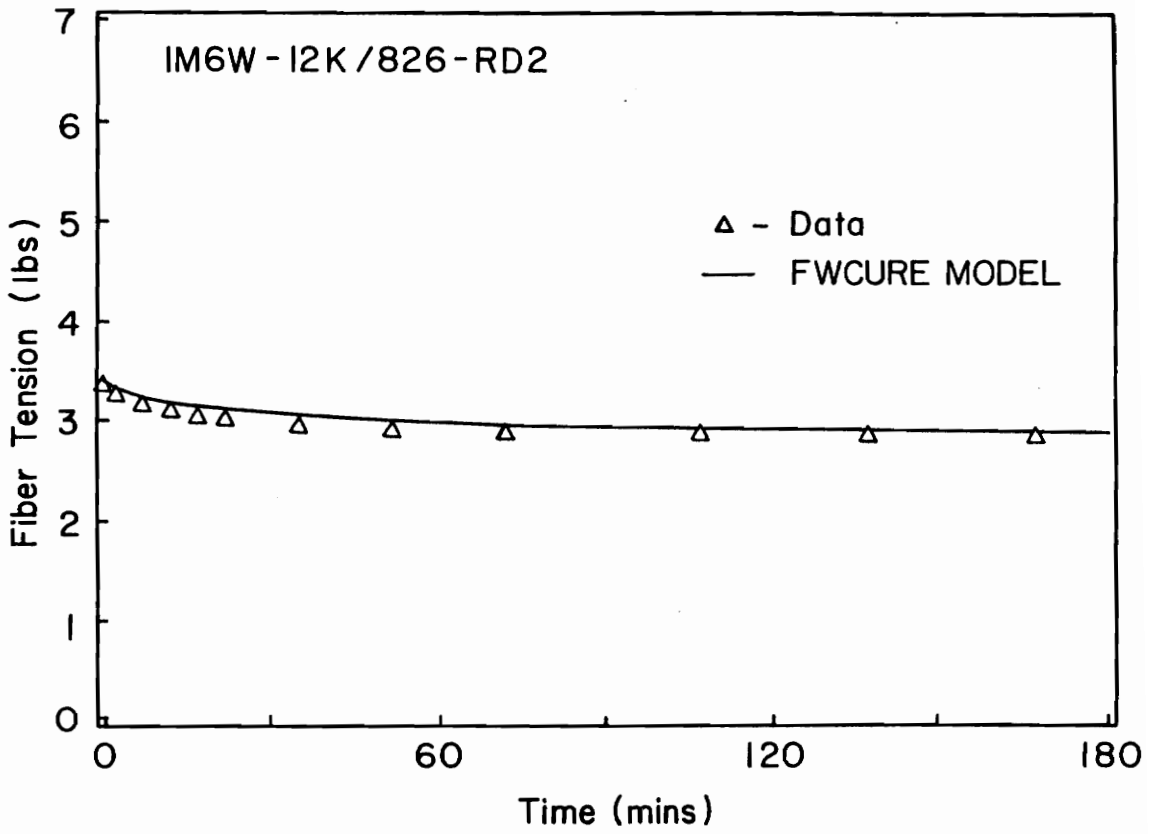


Figure 3.5 Single Layer IM6W-12K/826-RD2 Tension Loss

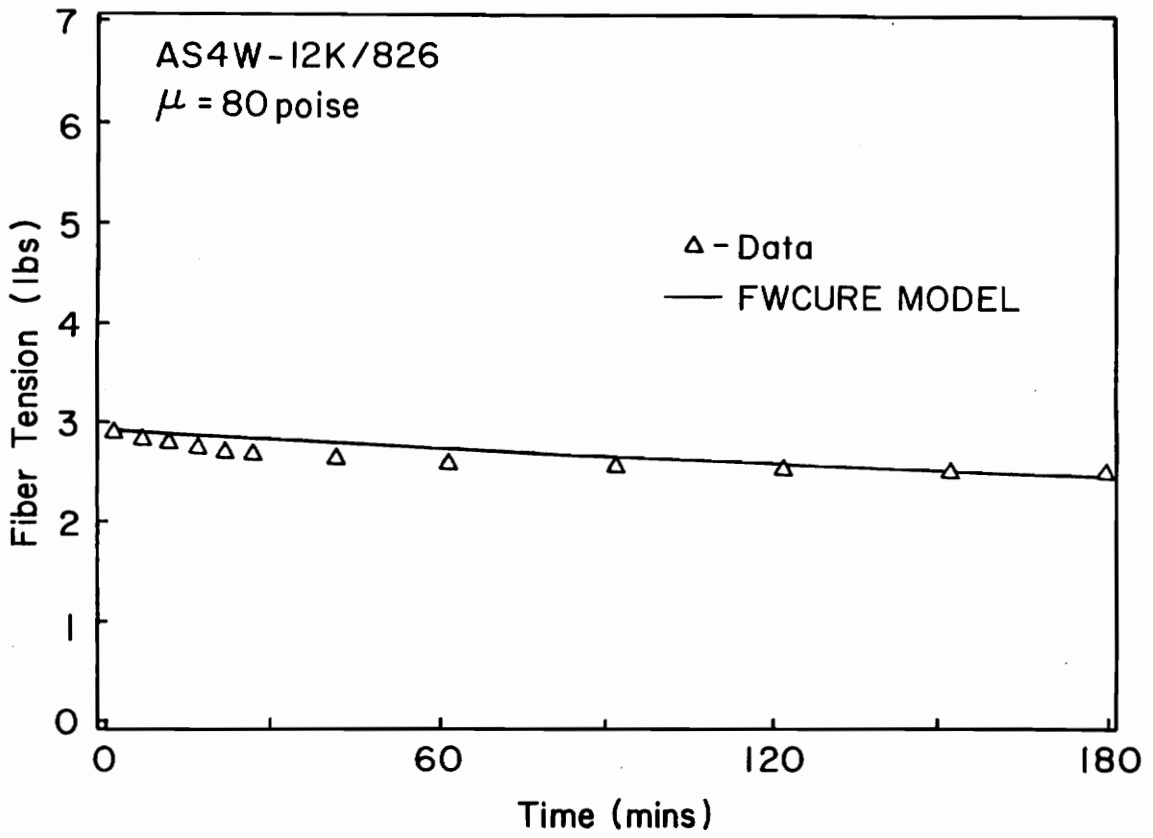


Figure 3.6 Single Layer AS4W-12K/826 Tension Loss

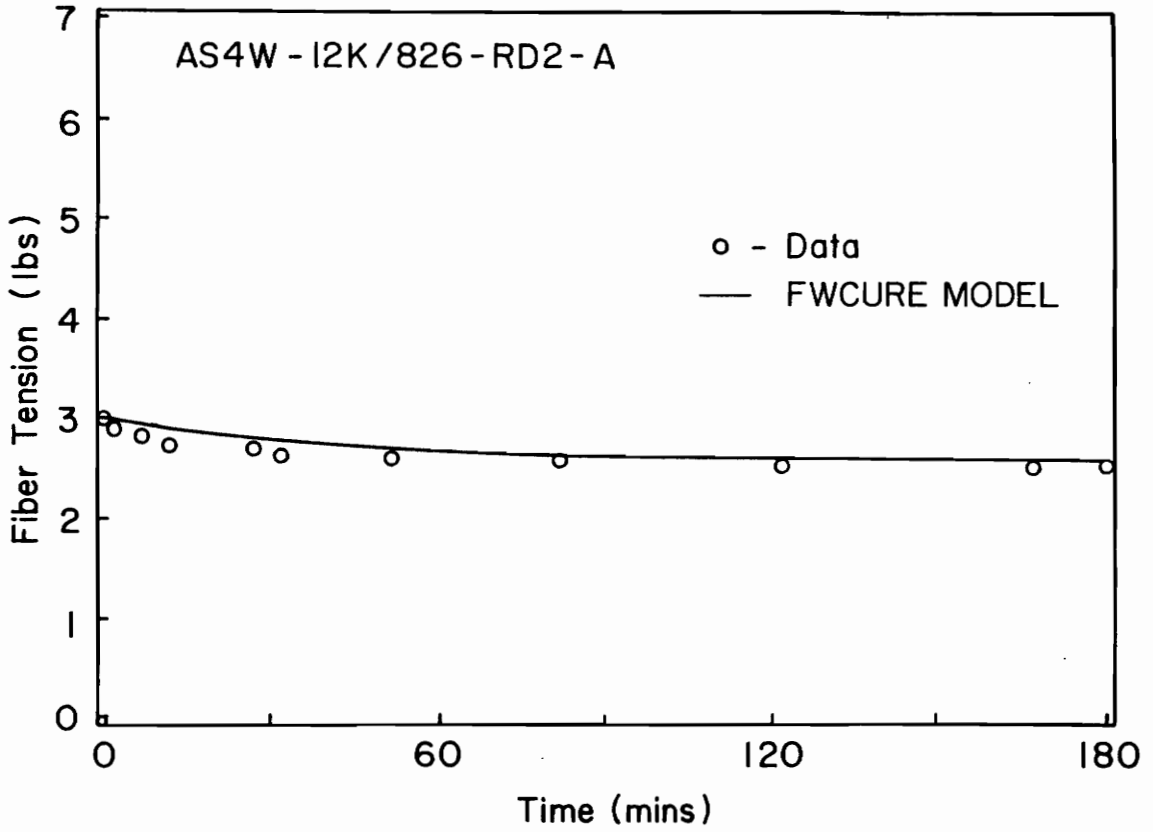


Figure 3.7 Single Layer AS4W-12K/826-A Tension Loss

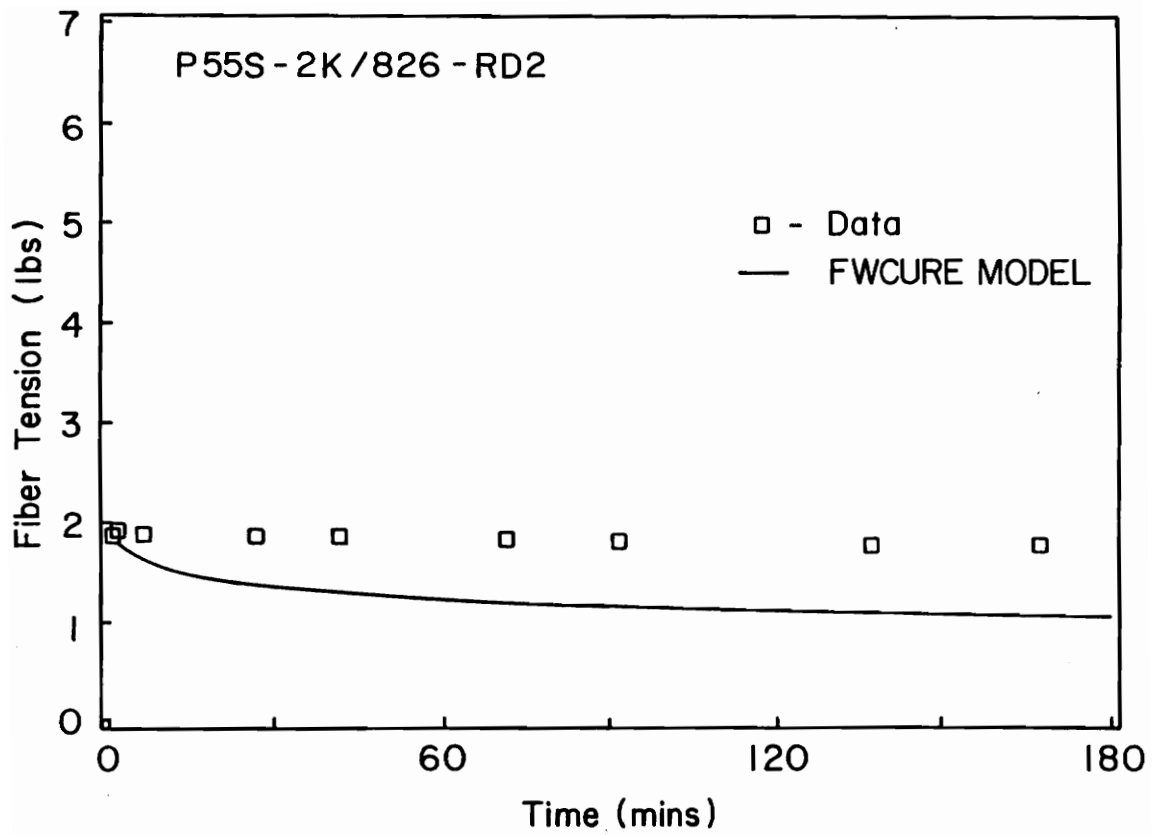


Figure 3.8 Single Layer P55S-2K/826-RD2 Tension Loss

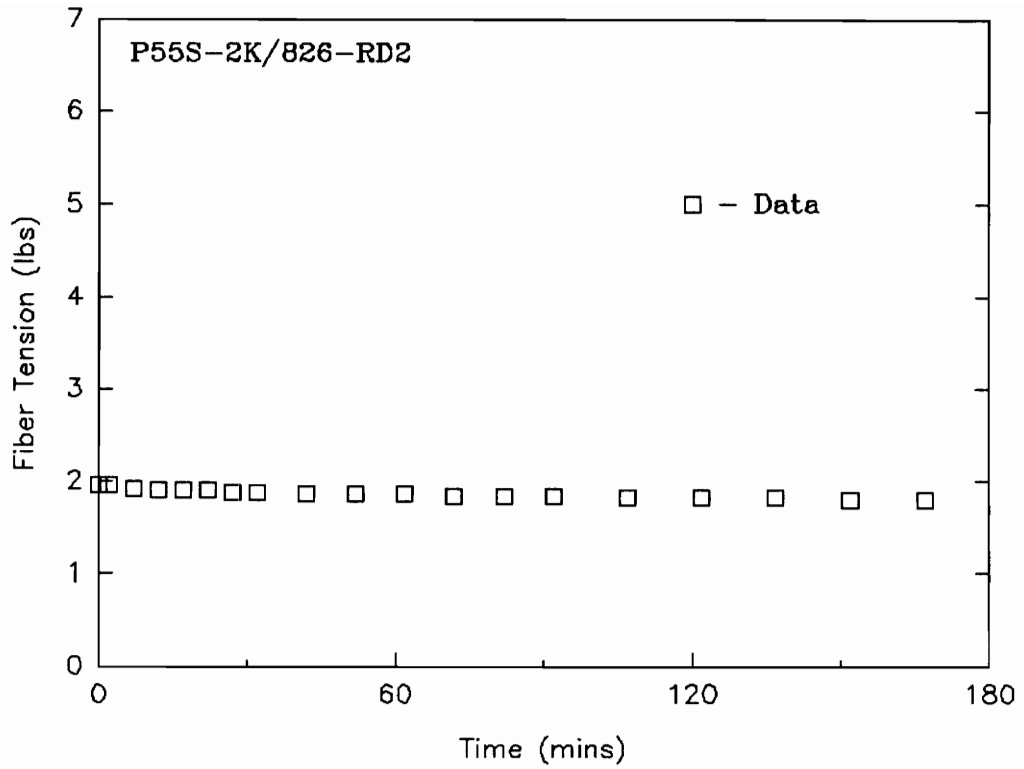


Figure 3.9 Single Layer P55S-2K/826-RD2
Tension Loss Verification

a cross sectional area that is only 33% as large as the AS4 fiber. The IM6 fiber also has a smaller cross sectional area than AS4. The IM6 cross sectional area is only 55% as large as the AS4. The excellent agreement for both the AS4 and IM6 fibers between the test data and the predicted values suggests that the difference in cross sectional areas is not a significant factor in determining a relationship between spool tension and fiber bundle resin content. If there were such a correlation, then a discrepancy would have been apparent for the experiments using the IM6 fiber as well as the experiments using the P55 fiber.

An improved relationship that appears to be more probable is to base the relationship on the spool tension and the number of filaments in the fiber bundle. The AS4 and IM6 fibers both have fiber bundles containing 12,000 filaments (12K) as opposed to only 2,000 filaments (2K) in the P55 bundle. For a given tension the fewer the filaments the higher the load on each individual filament. The higher load on individual filaments will cause them to "seat" faster resulting in more resin migrating to the surface instantaneously and a lower resin content within the fiber bundle will result. Fewer filaments within a fiber bundle will also offer less resistance (less congestion) to resin migration to the surface allowing more of the resin to migrate instantaneously. This would explain the excellent agreement

for the AS4-12k and IM6-12k fibers and the poor agreement for the P55-2k fiber. This could be verified by repeating the experiments using an AS4 fiber with 3,000 filaments (3K).

3.3.2 Single Layer High Viscosity Winds

Winding becomes extremely difficult using wet resins with high viscosities. Repeatable tests could not be obtained while winding with the Epon 828 resin system which has a viscosity of 145 poise. The high viscosity caused large variations in the winding tension making it impossible to get duplicate winds with the same tension throughout. The viscosity of the 828 resin system is much higher than that used in a wet winding system. This fact coupled with the difficulty in getting duplicate winds caused the termination of quantifying the tension loss with time for the experiments using the Epon 828 resin system.

Very high viscosity resin systems, such as prepreg resin systems, have viscosities high enough that the problems experienced with winding the 828 system do not present themselves. The very high viscosities of prepreps are due to the advancement of the resin to a B-stage. B-stage is an intermediate stage in the reaction of a thermosetting resin

in which it changes from a liquid (A-stage) to a soft solid. Prepregs tend to behave more like dry fibers, allowing the winding tension and processing to be reliably controlled. It would be expected that a new relationship between winding tension and fiber bundle resin content would be required for prepreg resin systems. It would also be expected that this fiber bundle resin content after mandrel lay-down would closely if not exactly match the resin content prior to lay down.

3.3.3 Multi-Layer Winds

There is a good agreement between the model prediction and the measured tension loss with time for the first layer of the multi-layer wind, Figure 3.10. The agreement deteriorates with each succeeding layer. The model predicts that the curve should flatten out to a greater extent than that indicated by the test data. An additional cylinder was wound to verify the shape of the tension loss curve for the additional layers being wound. The results of this experiment are shown in Figure 3.11.

Figures 3.10 and 3.11 show the same trend for the tension loss suggesting a problem with the permeability model or with the predicted fiber bundle resin content for

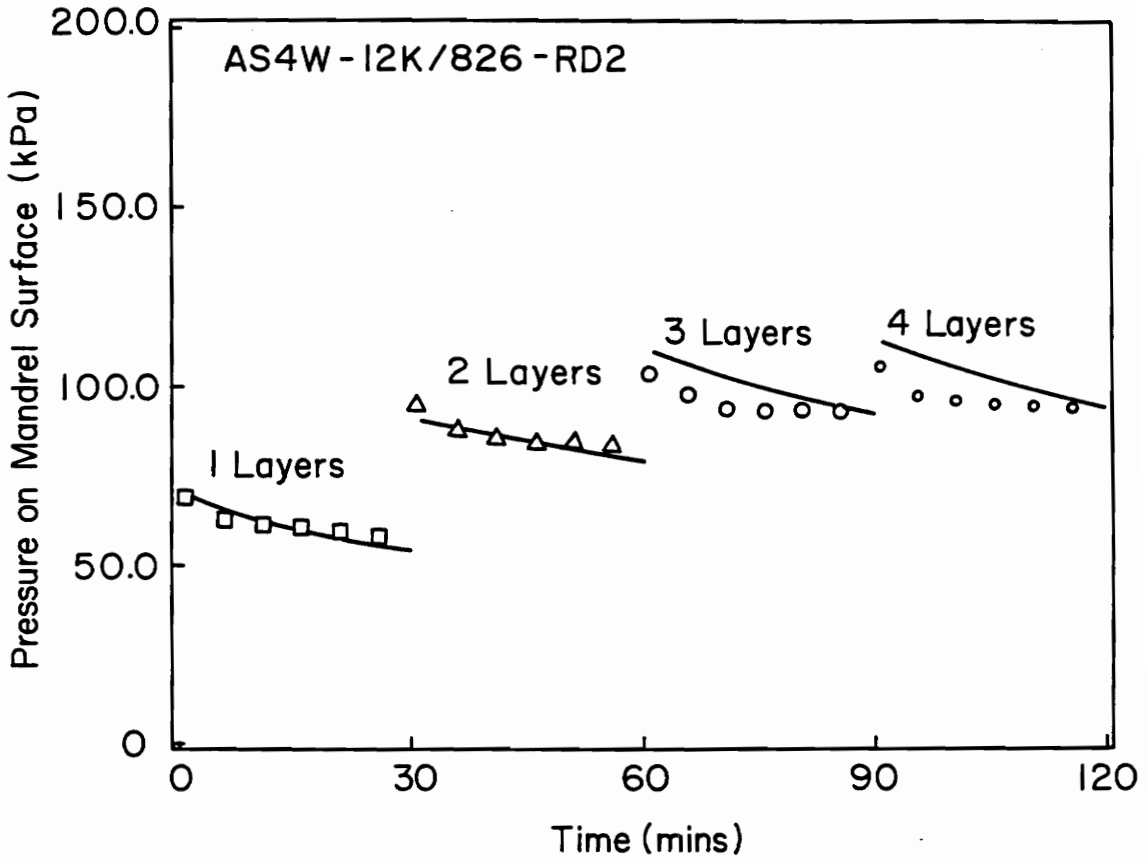


Figure 3.10 Multi-Layer AS4W-12K/826-RD2 Tension Loss

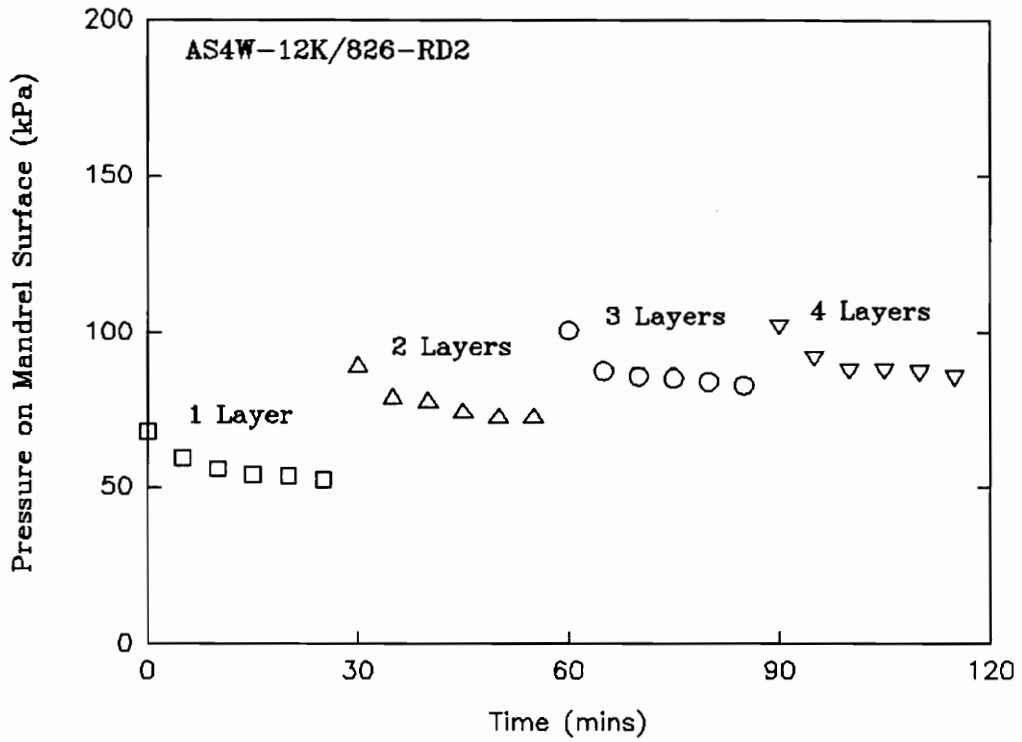


Figure 3.11 Multi-Layer AS4W-12K/826-RD2 Tension Loss Verification

multi-layer windings. It is this author's belief that the relationship between spool tension and fiber bundle resin content used for single layer winds is not valid for multi-layer wet winding. In the single layer winding the fiber bundle was wound against a "dry" mandrel. In multi-layer winding subsequent layers are wound against a resin rich surface due to resin migration from previous layers. The additional resin on the winding surface could result in a higher fiber bundle resin content. Thus, winding on a resin rich surface would probably produce a different relationship between spool tension and fiber bundle resin content. The higher resin content within the fiber bundle would result in more resin migrating to the surface with time resulting in a more pronounced tension loss curve as shown by the test data. A more pronounced tension loss curve correlates to a faster rate of tension loss.

The permeability model and the relationship between spool tension and fiber bundle resin content appear to be quite good for single layer winds using 12K fibers and resin systems with viscosities in the "wet" winding range (≤ 80 poise). The predictions for the P55 fiber and the multi-layer winds are not as good as the single layer 12K fiber winds, but they are still respectable. Some improvement may be possible with an improved relationship between spool tension and fiber bundle resin content.

It should be noted that the relationships and coefficients used in this study were based on wet winding resin systems. If prepreg systems are used (much higher viscosities) new coefficients and relationships between fiber bundle resin content and spool tension will need to be made based on prepreg test winding.

4.0 MODELING THE WINDING PROCESS

The WACSAFE program predicts the manufacturing stresses and strains based on cured and uncured composite material properties, lay-down tension, and wind angle. The lay-down tension is a function of the initial spool tension and an instantaneous tension loss. This instantaneous tension loss is caused by the flattening of the fiber bundle, the instantaneous resin flow due to sudden application of pressure on the fiber bundle and the mandrel deformation.

A second tension lessening effect occurs simultaneously caused by multiple circuits laying down next to each other. A previously wound circuit will lose tension when a circuit is wound next to it. This circuit will cause additional mandrel deformation, decreasing the load placed on the previously wound circuit. The load reduction translates to a tension loss. The effect diminishes as the distance increases between circuits. Nguyen⁷ stated that the side-

by-side tension loss depends on the relative stiffnesses of the underlying structure and the composite layer being wound. These relative stiffnesses are in turn dependent on the engineering properties of the mandrel and the composite, the thicknesses of the mandrel and composite, and the size of the structure.

The WACSAFE program has the capability to account for side-by-side effects. The instantaneous loss must be determined experimentally. A series of experiments were wound in which both tension loss effects were present. These effects were separated and the lay-down tension for each experiment was determined. The WACSAFE program was then used to model the filament winding process. The results were compared to mandrel strain readings taken during the winding process.

4.1 WINDING TEST MATRIX AND EXPERIMENTAL RESULTS

The series of experiments used in this study is listed in Table 4.1. The raw data is listed in Appendix B. In Table 4.1 set number refers to the number identifying the different combinations of listed parameters. Wind length refers to the length the fiber was wound on the cylinder. The 0.5-inch length windings were centered on the mandrel to be over the mandrel strain gage locations. Circuit or band

Table 4.1 Instantaneous Tension Loss Test Matrix

SET #	WIND LENGTH (inch)	FIBER TYPE	CIRCUIT WIDTH (inch)	MANDREL THICK. (inch)	SPOOL TENSION	
					FORCE (lb)	STRESS (psi)
1	4.0	AS4W-12K	1/10	0.05	12.3	9788
2	4.0	AS4W-12K	1/10	0.05	10.0	7958
3	4.0	AS4W-12K	1/10	0.05	7.5	5968
4	4.0	AS4W-12K	1/10	0.05	5.0	3979
5	4.0	AS4W-12K	1/10	0.05	2.5	1989
6	4.0	AS4W-12K	1/10	0.05	2.0	1592
7	4.0	AS4W-12K	1/10	0.05	1.75	1393
8	4.0	AS4W-12K	1/10	0.05	0.875	696
9	4.0	AS4W-12K	1/10	0.25	10.0	7958
10	4.0	AS4W-12K	1/10	0.25	5.0	3979
11	4.0	IM6W-12K	1/13	0.05	10.0	14423
12	4.0	IM6W-12K	1/13	0.05	5.0	7212
13	4.0	IM6W-12K	1/13	0.25	10.0	14423
14	4.0	IM6W-12K	1/13	0.25	5.0	7212
15	4.0	P55S-2K	1/25	0.05	3.0	7200
16	4.0	P55S-2K	1/25	0.25	5.0	12000
17	4.0	P55S-2K	1/25	0.25	3.0	7200
18	0.5	AS4W-12K	1/10	0.05	10.0	7958
19	0.5	AS4W-12K	1/10	0.05	5.0	3979
20	0.5	AS4W-12K	1/10	0.05	2.5	1989
21	0.5	IM6W-12K	1/13	0.05	10.0	14423
22	0.5	IM6W-12K	1/13	0.05	5.0	7212
23	0.5	AS4W-12K	1/10	0.25	10.0	7958
24	0.5	AS4W-12K	1/10	0.25	5.0	3979
25	0.5	IM6W-12K	1/13	0.25	10.0	14423
26	0.5	IM6W-12K	1/13	0.25	5.0	7212
27	0.5	P55S-2K	1/25	0.25	5.0	12000
28	0.5	P55S-2K	1/25	0.25	3.0	7200

width refers to the band spacing. This is dependent on the fiber used and the amount it flattens or spreads out during winding. The objective in winding is to eliminate any band gaping or overlapping. Mandrel thickness refers to the two different thicknesses of mandrels used. Spool tension lists both the force and stress applied to the fiber prior to mandrel lay-down.

The experiments wound in set numbers 1 through 17 employed different fibers wound at different tensions on both a thin-walled and a thick-walled mandrel. The thicker mandrel was used to minimize the side-by-side tension loss effects. The results of these experiments are illustrated in Figures 4.1 through 4.3. Plotted are the mean values for the set numbers listed in Table 4.1. The error bars correspond to the statistical upper and lower limits, three standard deviations away from the mean. No error bars are shown when only one experiment was made for a specific combination of parameters shown in Table 4.1. This also holds for the remaining figures in this section.

Shown in the graphs are the retention factors for various levels of spool tension. The spool tension is shown both as a force and as a stress, the spool tension force divided by the fiber/resin area. The retention factor is the ratio of winding tension divided by the spool tension. Winding

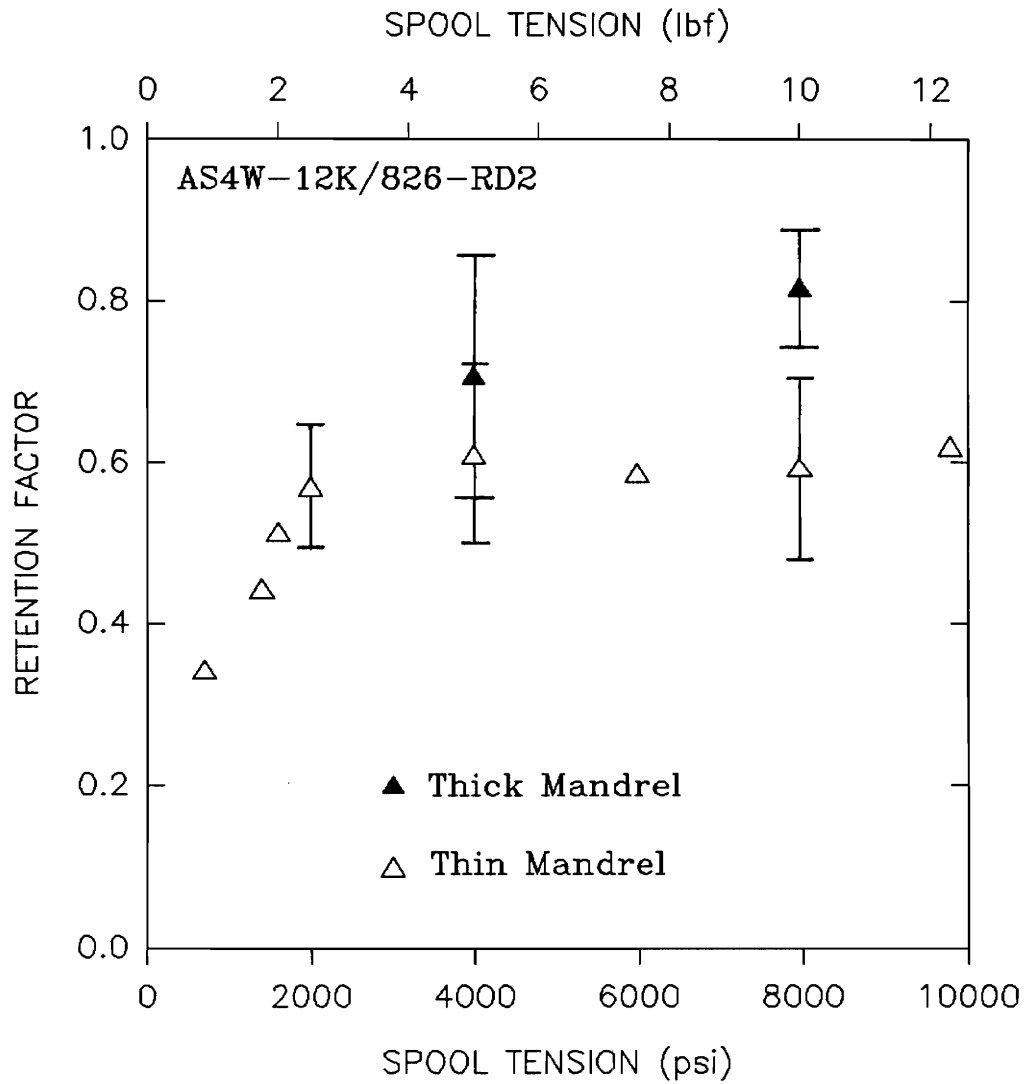


Figure 4.1 Stress Retention Factor Versus Spool Tension for AS4W-12K/826-RD2

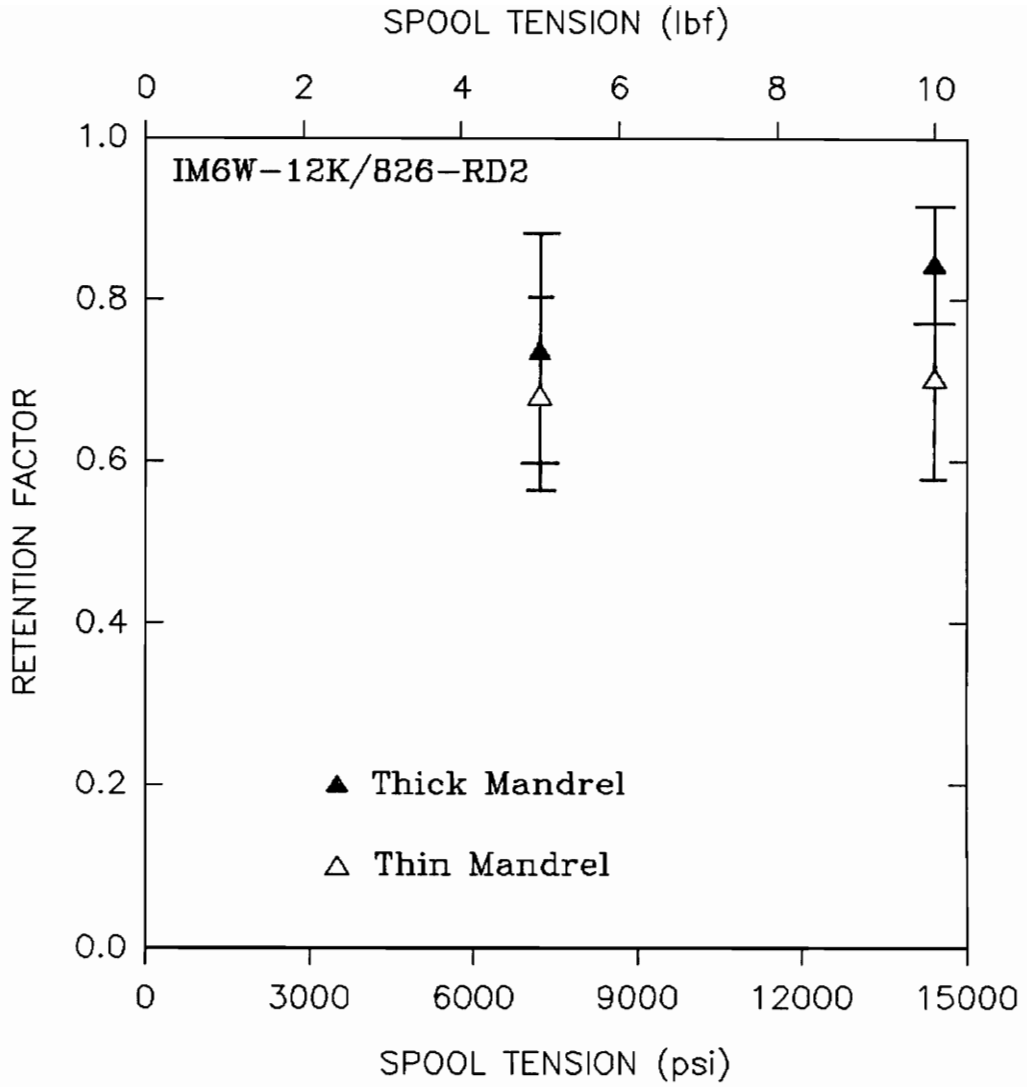


Figure 4.2 Stress Retention Factor Versus Spool Tension for IM6W-12K/826-RD2

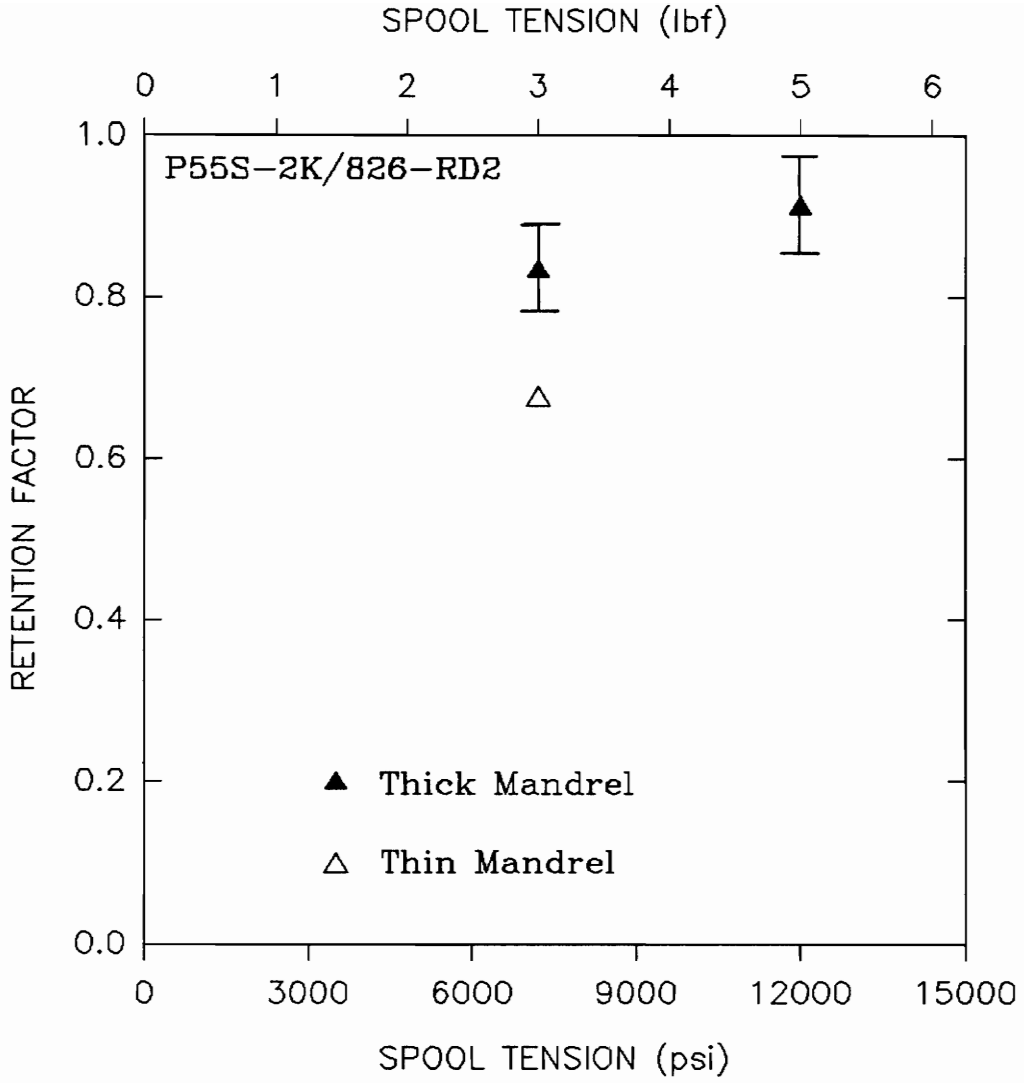


Figure 4.3 Stress Retention Factor Versus Spool Tension for P55S-2K/826-RD2

tension is defined to be the tension in the fiber after winding. Winding tension is different from the lay-down tension discussed previously in that the winding tension includes both the instantaneous losses and the side-by-side losses. The lay-down tension does not include the side-by-side losses. The winding tension (lbf) for the thin-walled mandrel was found using Equation (3.1). Winding tension (lbf) for the thick-walled mandrel was found using Equation (4.1). Equation (4.1) is based on elasticity theory for external pressure applied to an axisymmetric surface as explained by Timoshenko and Goodier⁸. Combining the theory of elasticity pressure equation with Equation (3.2) yields Equation (4.1).

$$T = \frac{W e_{\theta_i} E (b^2 - a^2)}{-2b} \quad (4.1)$$

- T = Fiber winding tension
- W = Fiber width (on mandrel)
- E = Elastic modulus of the mandrel
- a = Mandrel inside radius
- b = Mandrel outside radius
- e_{θ_i} = Mandrel hoop strain on inside surface

The experiments wound in set numbers 18 through 28 were an attempt to minimize the side-by-side tension losses by minimizing the numbers of adjacent circuits wound. The windings were centered on the mandrel over the strain gages.

The difficulty in performing this type of experiment is in applying the proper tension to the fiber as it is applied to the mandrel and as it is removed from the mandrel and then maintaining the correct tension level after winding is complete and mandrel strain readings are being taken. The leading circuit, as it enters the mandrel, should have the same tension as the spool tension. The lagging circuit as it is removed from the mandrel should maintain its as wound or winding tension.

Maintaining the spool tension on the leading circuit, as it enters the mandrel during winding, was easily accomplished with the tensioning rollers. The tensioning rollers also maintained spool tension in the leading circuit after winding and during the mandrel strain readings, provided the fiber was not cut. Maintaining the correct tension on the lagging circuit, as it was removed from the mandrel, proved to be so questionable that the results of these experiments were not used.

Circumferential winding requires two to three revolutions before the circuits start laying down next to each other in a uniform pattern. The winding is started by wrapping two to three extra circuits around the mandrel by hand. These "starting" circuits transition from the tension level applied to them during wrapping to the winding tension level

resulting from the winding operation.

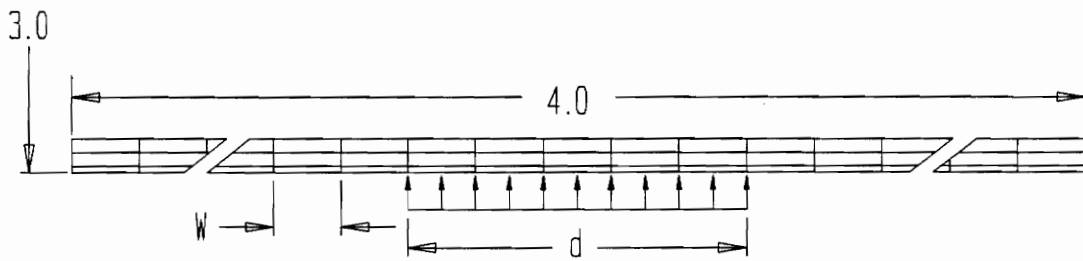
For the 1/2-inch winds, centered on the mandrel, the circuits caused from the extra revolutions and the "starting" circuits needed to be stripped off prior to reading the mandrel strain. If the circuits were left on the mandrel they would influence the mandrel strain readings. The problem in stripping the extra circuits is in determining how much tension to apply to the free end of the lagging circuit. The tension applied to the free end had a large influence on the mandrel strain readings.

An attempt was made to leave the extra circuits on the mandrel and account for their effect on the mandrel strains. This also proved to be unreliable since the actual tension in these circuits was unknown. The circuits were initially wrapped on the mandrel by hand at an unknown tension. When winding begins, the tension level transitions to the winding tension. The number of revolutions for this transition to take place cannot be determined without knowing the starting value.

A different attempt was made by starting the wind at one edge of the mandrel and continuing until a 1/2-inch width was achieved. The trailing end of the wind was then removed as the winding progressed leaving a 1/2-inch width advancing

down the length of the mandrel. When the winding was centered on the mandrel, the lathe was stopped and strain gage readings were taken. The tension applied while stripping the trailing edge would have an effect on the strain readings in the same way as reported in the previous case.

The 1/2-inch wind was modeled using finite element techniques and is shown in Figure 4.4. A 1/2-inch wide pressure load, simulating the composite, was applied to the mandrel model. The pressure load was adjusted until the mandrel strains in the model matched the mandrel strains from the experiments. The tensile load on the fibers was calculated using Equation (3.2) and the pressure load from the model. The resulting tensile load on the fiber was calculated to be higher than the spool tension. This condition is impossible to achieve without the additional load applied from stripping either the extra circuits or the trailing edge. The correct tension to apply during stripping is not only impossible to determine but it is done by hand and a measure of the tension applied would only be a gross approximation. For these reasons the data from these experiments were not used.



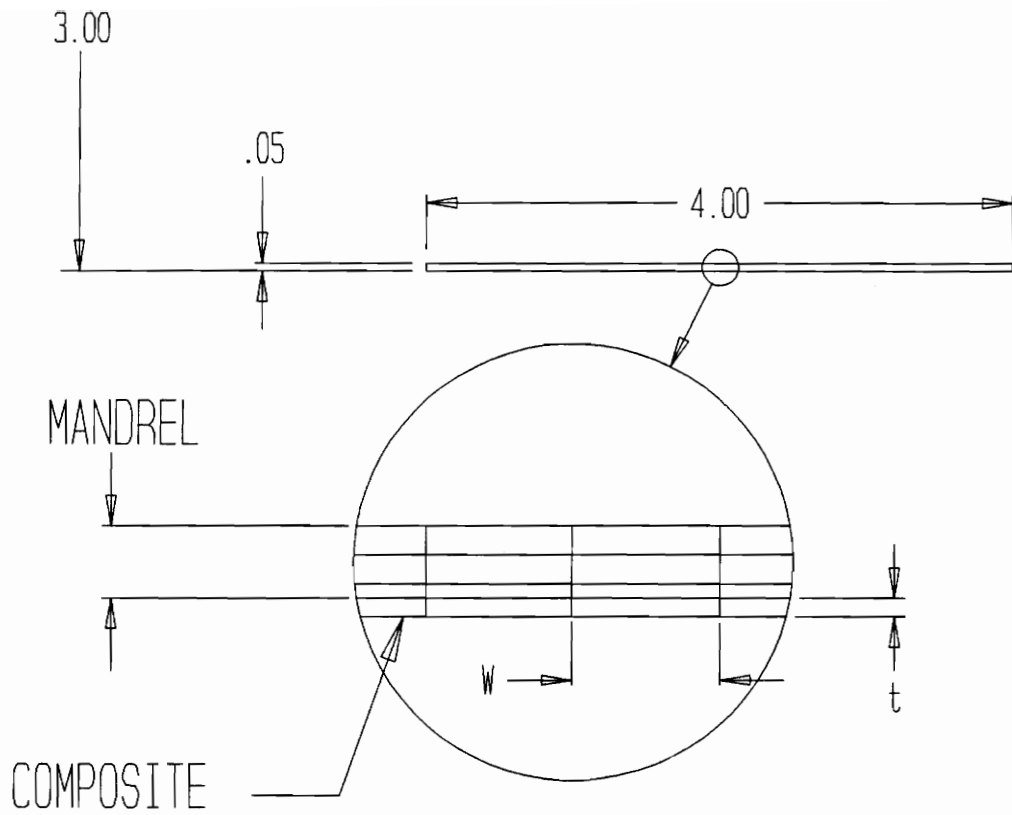
AS4W-12K	$W = 1/10$	$d = 5/10$
IM6W-12K	$W = 1/13$	$d = 6/13$
P55S-2K	$W = 1/25$	$d = 12/25$

Figure 4.4 Finite Element Model of the 1/2-inch Wind

4.2 SEPARATION OF THE WINDING TENSION LOSSES

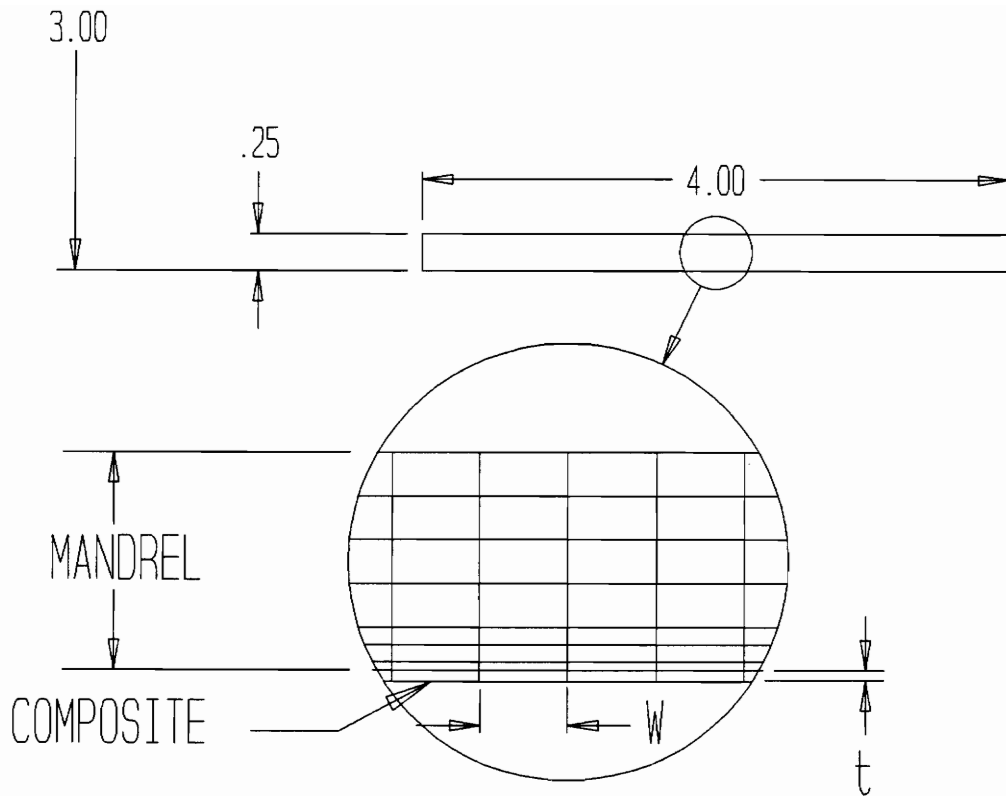
The tension loss, shown graphically in Figures 4.1 through 4.3, includes both the instantaneous tension loss as well as the side-by-side tension losses. The WACSAFE program has the capability to account for side-by-side losses for a given input tension, mandrel size and properties for the mandrel and for the uncured composite. By determining side-by-side losses using WACSAFE for different materials wound at various tension levels, the results can be subtracted out from the total tension loss leaving the values for the instantaneous tension loss. The WACSAFE input tension value for each experiment could then be determined by subtracting the instantaneous loss from the spool tension.

WACSAFE models of the experiments, set numbers one through seventeen, were created and are shown in Figures 4.5 and 4.6. Figure 4.5 represents the thin-walled mandrel models and Figure 4.6 represents the thick-walled mandrel models. The filament winding process was simulated by activating the composite elements one at a time down the length of the mandrel. The composite elements were prestressed at the input tension.



AS4W-12K	$W = 1/10$	$t = 0.01257$
IM6W-12K	$W = 1/13$	$t = 0.009013$
P55S-2K	$W = 1/25$	$t = 0.01042$

Figure 4.5 WACSAFE Model of the Thin-Walled Mandrel Experiments



AS4W-12K	$W = 1/10$	$t = 0.01257$
IM6W-12K	$W = 1/13$	$t = 0.009013$
P55S-2K	$W = 1/25$	$t = 0.01042$

Figure 4.6 WACSAFE Model of the Thick-walled Mandrel Experiments

4.2.1 Parametric Sensitivity Study

Modeling of the filament winding process using WACSAFE requires uncured composite mechanical properties. Little is known about the mechanical properties of composites in the uncured state. For some properties a rational argument can be made for establishing upper and lower limits. For other properties establishing limits is nothing more than a guess. With so little known about composite mechanical properties in the uncured state, it is desirable to know what impacts these properties have on the output of the side-by-side tension losses.

To determine the effects that the uncured composite properties have on side-by-side tension loss, a three level fractional factorial design of experiments approach was used. Box and Behnken⁹ developed a method for setting up and analyzing 3 level fractional factorial test matrices. Their method was utilized in this study.

The usual approach in designing a test matrix, involving several variables, is to change one variable at a time while holding the others constant. Although this approach is intuitive and easy to do, there are two serious drawbacks: 1) there is no capability for estimating variable interactions, and 2) there is no mathematical model capable

of predicting the response to unexpected combinations of variables.

A class of experimental designs which eliminate the two problems mentioned above is known as "factorial designs". In a factorial design, a predetermined number of levels is chosen for each variable in the study, and then all possible combinations are run.

Factorial designs in which all k variables are run at three levels are called "three-level factorials," or " 3^k factorials." As the number of k variables in a study increases, the number of possible experimental combinations increases geometrically. The time required to run a full factorial and the cost involved soon become prohibitive. As an example, a full three-level factorial with five variables would require $3^5 = 243$ runs. However, as k increases it turns out that most of the information from a three-level design can be obtained by performing only a fraction of the possible combinations. This is possible because main effects tend to be larger than two-variable interactions, which in turn tend to be larger than three-variable interactions, etc. Also, when k is moderately large, it often happens that some of the variables have no distinguishable effect.

To begin a three-level fractional factorial design of experiments, limits on the uncured material properties needed to be set. It was determined that one limit on the properties would be set by the cured properties. The rationale being that the uncured properties could not be any "better" than the cured properties.

A fiber resin system with known cured material properties was chosen for this analysis. The cured properties are shown in Table 4.2.

The other limits on uncured material properties are also listed in Table 4.2 and were determined as follows:

Using a rule of mixtures approach and assuming only the fiber carries any load:

$$E_1 = V_f E_f + V_m E_m \quad (4.2)$$

$V_f = 0.60$	Fiber Volume Fraction
$E_f = 42.0E+06$	Fiber Modulus
$V_m = 0.40$	Resin Volume Fraction
$E_m = 0.0$	Resin Modulus

**Table 4.2 Uncured Mechanical Property Limits
for T1000/974**

UPPER LIMIT		
T1000/974 CURED COMPOSITE MECHANICAL PROPERTIES		
$E_1 = 26.1$ msi	$\nu_{12} = 0.253$	$G_{12} = 0.7284$ msi
$E_2 = 1.231$ msi	$\nu_{13} = 0.253$	$G_{13} = 0.7284$ msi
$E_3 = 1.231$ msi	$\nu_{23} = 0.392$	$G_{23} = 0.4422$ msi
LOWER LIMIT		
T1000/974 UNCURED COMPOSITE MECHANICAL PROPERTIES		
$E_1 = 25.2$ msi	$\nu_{12} = 0.362$	$G_{12} = 0.007284$ msi
$E_2 = 0.01231$ msi	$\nu_{13} = 0.362$	$G_{13} = 0.007284$ msi
$E_3 = 0.01231$ msi	$\nu_{23} = 0.500$	$G_{23} = 0.041033$ msi

Assuming transverse isotropy and that E_2 and E_3 are not more than two orders of magnitude lower than the cured value:

$$E_2 = 1.231E+06/100 \quad \text{From Table 4.2} \quad (4.3)$$

$$E_3 = 1.231E+06/100 \quad \text{From Table 4.2}$$

Using a rule of mixtures approach and assuming the Poisson's ratio for liquid resin equals 0.500, the Poisson's ratio for T1000 equals 0.270 and that ν_{12} equals ν_{13} :

$$\begin{aligned} \nu_{12} &= V_f \nu_f + V_m \nu_m & V_f &= 0.60 & \text{Fiber Volume Fraction} & (4.4) \\ \nu_{13} &= V_f \nu_f + V_m \nu_m & V_m &= 0.40 & \text{Resin Volume Fraction} \\ & & \nu_f &= 0.270 & \text{Fiber Poisson's Ratio} \\ & & \nu_m &= 0.500 & \text{Resin Poisson's Ratio} \end{aligned}$$

Assuming the Poisson's ratio in the transverse direction is dominated by the resin and that the Poisson's ratio for uncured resin equals 0.500:

$$\nu_{23} = 0.500 \quad (4.5)$$

Assuming G_{12} and G_{13} are not more than two orders of magnitude lower than the cured value:

$$G_{12} = 0.7284E+06/100 \quad \text{From Table 4.2} \quad (4.6)$$

$$G_{13} = 0.7284E+06/100 \quad \text{From Table 4.2}$$

Assuming the shear modulus in the transverse plane maintains a similar relationship to the orthotropic relationship:

$$G_{23} = \frac{E_2}{2(1+\nu_{23})} \quad (4.7)$$

The shear modulus input to WACSAFE requires only the in-plane value (G_{12}). This coupled with the transverse isotropy assumption, i.e., E_2 equals E_3 and ν_{12} equals ν_{13} , resulted in only five variables for the fractional factorial test matrix. Using the methods of Box and Behnken⁹, the test matrix shown in Table 4.3 was employed. The plus sign ("+") represents the high parameter value, the minus sign ("-") represents the low parameter value and the zero ("0") represents the median value. The stiffness and compliant matrices for each combination of elastic constants used in Table 4.3 were verified to be positive definite using the methods presented by Jones¹⁰ pages 42 through 44.

The WACSAFE code was used to determine the theoretical

Table 4.3 Fractional Factorial Test Matrix

RUN NO.	V A R I A B L E S				
	E ₁	E ₂	ν_{12}	ν_{23}	G ₁₂
1	+	+	0	0	0
2	+	-	0	0	0
3	-	+	0	0	0
4	-	-	0	0	0
5	0	0	+	+	0
6	0	0	+	-	0
7	0	0	-	+	0
8	0	0	-	-	0
9	0	+	0	0	+
10	0	+	0	0	-
11	0	-	0	0	+
12	0	-	0	0	-
13	+	0	+	0	0
14	+	0	-	0	0
15	-	0	+	0	0
16	-	0	-	0	0
17	0	0	0	+	+
18	0	0	0	+	-
19	0	0	0	-	+
20	0	0	0	-	-
21	0	0	0	0	0
22	0	+	+	0	0
23	0	+	-	0	0
24	0	-	+	0	0
25	0	-	-	0	0
26	+	0	0	+	0
27	+	0	0	-	0
28	-	0	0	+	0
29	-	0	0	-	0
30	0	0	+	0	+
31	0	0	+	0	-
32	0	0	-	0	+
33	0	0	-	0	-
34	+	0	0	0	+
35	+	0	0	0	-
36	-	0	0	0	+
37	-	0	0	0	-
38	0	+	0	+	0
39	0	+	0	-	0
40	0	-	0	+	0
41	0	-	0	-	0

tension in the fiber for each combination. The difference between the input tension and the theoretical tension was caused by the side-by-side tension loss effect. The amount the theoretical tension varied between combinations was a result of the different elastic constants. An input tension of 5 pounds (8786 psi) was used in all cases along with the thin-walled mandrel model shown in Figure 4.4. The composite stresses at the center of the mandrel were recorded at the end of each run and then analyzed to determine main effects and any interactions.

The results of the analysis showed that the theoretical tension varied between 4.33 pounds (7602psi) and 4.30 pounds (7548psi). This means that the side-by-side tension loss varied between 0.67 pounds (1184 psi) and 0.70 pounds (1238 psi). E_1 accounts for 75.9 per cent of the variation and E_2 accounts for 23.8 per cent. The remaining 3 parameters (ν_{12} , ν_{23} , and G_{12}) and all interactions were negligible. The variation in the side-by-side tension loss, due to the different combinations of uncured composite material properties, when compared to the total side-by-side loss is only 4.4 per cent and is insignificant. Any value used within the ranges shown in Table 4.2 will yield good results for T1000/974. Similar results will be obtained for other fiber/resin systems.

4.2.2 Determination of Side-by-Side Tension Losses

WACSAFE was used to determine the side-by-side tension losses for each fiber/resin combination at different input tension levels and using both the thin-walled and thick-walled mandrel models. The results are shown in Figures 4.7 through 4.10. Illustrated in the first three figures are the WACSAFE theoretical tension (input tension minus the side-by-side losses) as a function of input tension for the three fiber/resin systems. Shown in Figure 4.10 are the side-by-side losses presented as a percentage of the input tension. The linearity exhibited in Figures 4.7, 4.8 and 4.9 resulted in the constant percent tension loss shown in Figure 4.10.

The uncured composite material properties used in the WACSAFE models are listed in Table 4.4. E_1 was determined using the rule of mixtures approach shown in Equation (4.2). E_2 and G_{12} were predicted using the mechanics of materials approach to micromechanics explained by Jones¹⁰ pages 90 through 97. The micromechanical values were reduced by one order of magnitude to approximate the uncured condition. ν_{12} was determined using the rule of mixtures approach shown in Equation (4.4). ν_{23} was assumed to be 0.50 using the same rationale as Equation (4.5). Transverse isotropy was assumed to obtain values for the remaining properties.

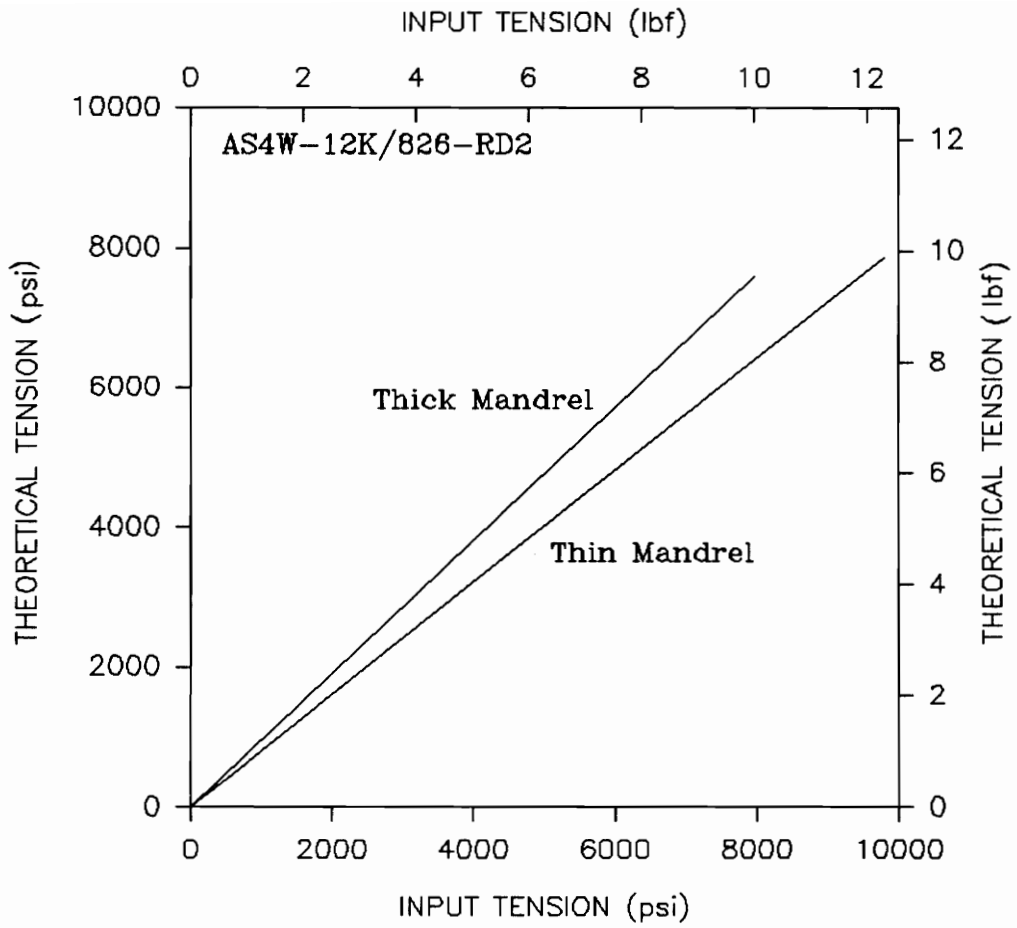


Figure 4.7 Theoretical Tension Versus Input Tension for AS4W-12K/826-RD2

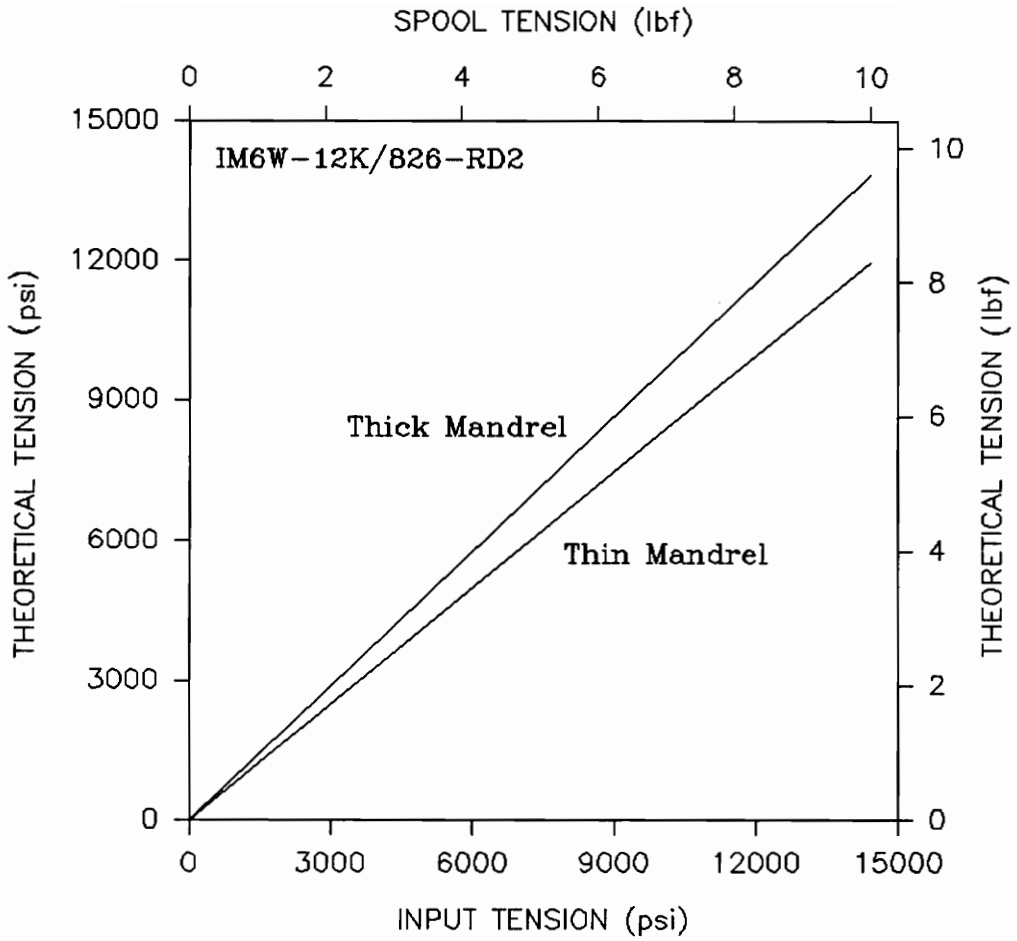


Figure 4.8 Theoretical Tension Versus Input Tension for IM6W-12K/826-RD2

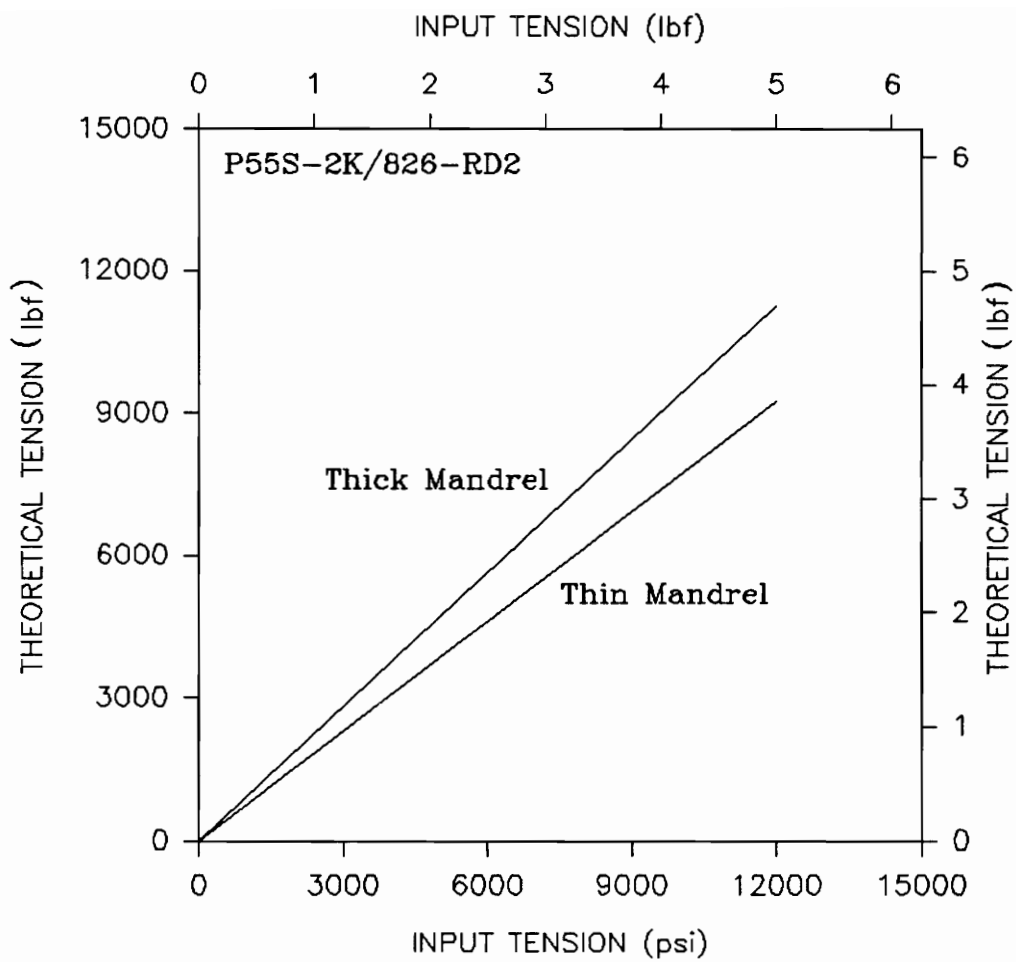


Figure 4.9 Theoretical Tension Versus Input Tension for P55S-2K/826-RD2

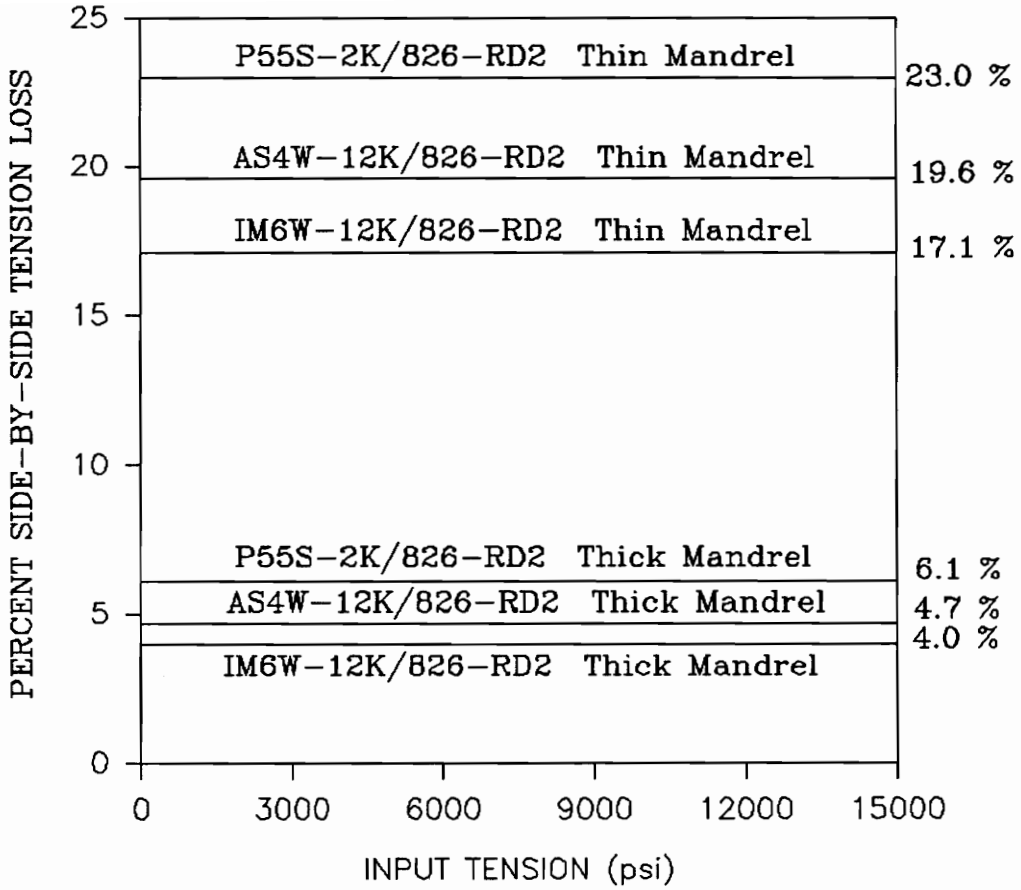


Figure 4.10 Percent Side-by-Side Tension Loss Versus Input Tension

Table 4.4 Uncured Composite Mechanical Properties

AS4W-12K/826-RD2		
$E_1 = 20.4$ msi	$\nu_{12} = 0.320$	$G_{12} = 0.04452$ msi
$E_2 = 0.1199$ msi	$\nu_{13} = 0.320$	
$E_3 = 0.1199$ msi	$\nu_{23} = 0.500$	
IM6W-12K/826-RD2		
$E_1 = 24.24$ msi	$\nu_{12} = 0.362$	$G_{12} = 0.04461$ msi
$E_2 = 0.1203$ msi	$\nu_{13} = 0.362$	
$E_3 = 0.1203$ msi	$\nu_{23} = 0.500$	
P55S-2K/826-RD2		
$E_1 = 33.0$ msi	$\nu_{12} = 0.362$	$G_{12} = 0.04481$ msi
$E_2 = 0.1209$ msi	$\nu_{13} = 0.362$	
$E_3 = 0.1209$ msi	$\nu_{23} = 0.500$	

4.2.3 Instantaneous Tension Losses

The instantaneous tension loss can be determined by taking the difference between the spool tension and the winding tension and then subtracting out the side-by-side effects. The winding tension was determined experimentally using the experiments shown in Table 4.1. Side-by-side tension losses as a function of input tension were found through analysis as explained in the previous section. To obtain the instantaneous tension loss the correct input tension must be established to determine the side-by-side tension loss.

A method to determine the input tension was suggested by Stein and Knight¹¹. They suggested that a ratio between experimental results and WACSAFE theoretical results be used. Define lay-down tension to be the tension on the fiber after instantaneous tension loss. Lay-down tension is equivalent to the input tension for WACSAFE. Input tension is the tension value used in the WACSAFE analysis. For these purposes let the input tension equal the spool tension. Experimental tension is the tension in the fibers after winding, found experimentally. Theoretical tension is the tension in the fiber after winding for the given input tension using WACSAFE. The ratio is shown in Equation (4.8).

$$\frac{\text{Lay-down Tension}}{\text{Experimental Tension}} = \frac{\text{Input/Spool Tension}}{\text{Theoretical Tension}} \quad (4.8)$$

The difference between lay-down tension and experimental tension and the difference between input tension and theoretical tension are both due only to the side-by-side tension loss effects. Using the ratio from Equation (4.8) the lay-down tension can be determined.

Lay-down tensions, for each of the experiments shown in Table 4.1, are illustrated in Figures 4.11 through 4.16. Shown in the first three figures are the lay-down tensions as a function of spool tension. Shown in the last three graphs are the lay-down tension retention factors versus spool tension. The tension retention factor is defined as the lay-down tension divided by spool tension.

The instantaneous tension loss may be determined by subtracting the lay-down tension from the spool tension shown in Figures 4.11 through 4.13. The percent instantaneous tension loss shown in Figures 4.17 through 4.19 were determined by taking one minus the Retention factor, from Figures 4.14 through 4.16, and multiplying by one-hundred.

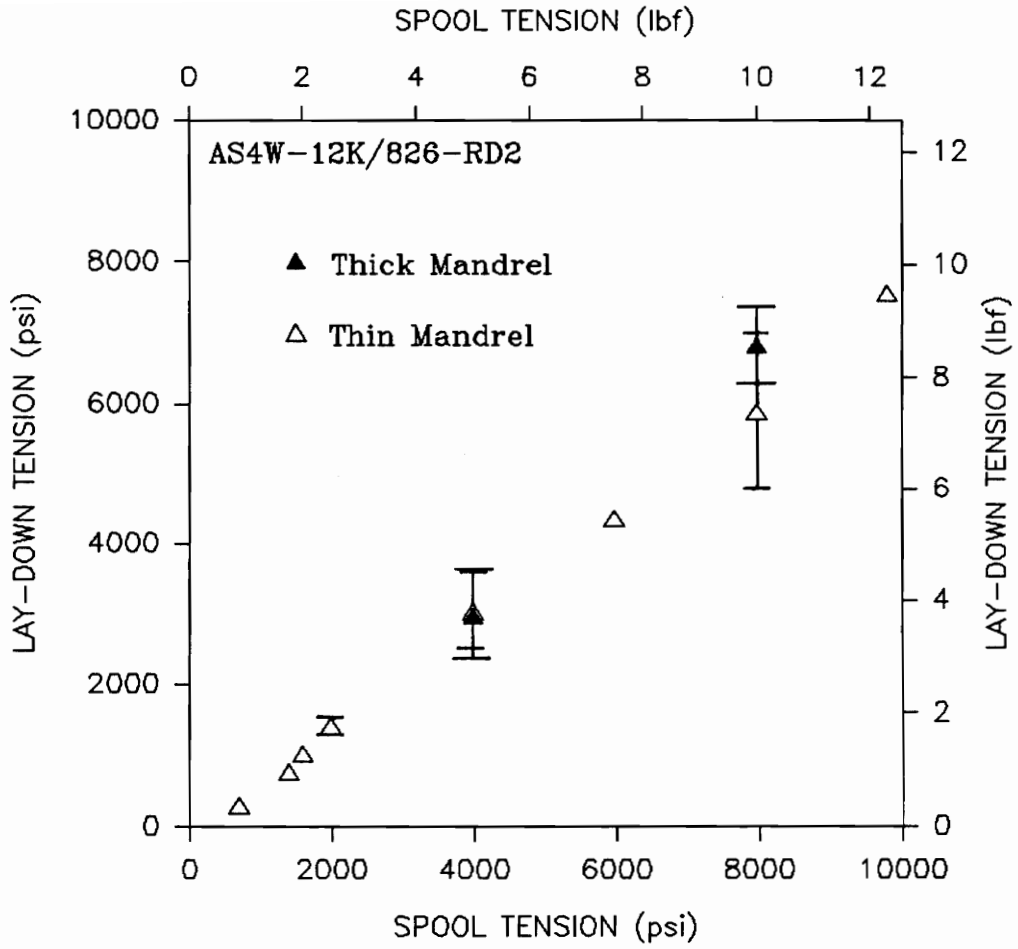


Figure 4.11 Lay-down Tension Versus Spool Tension for AS4W-12K/826-RD2

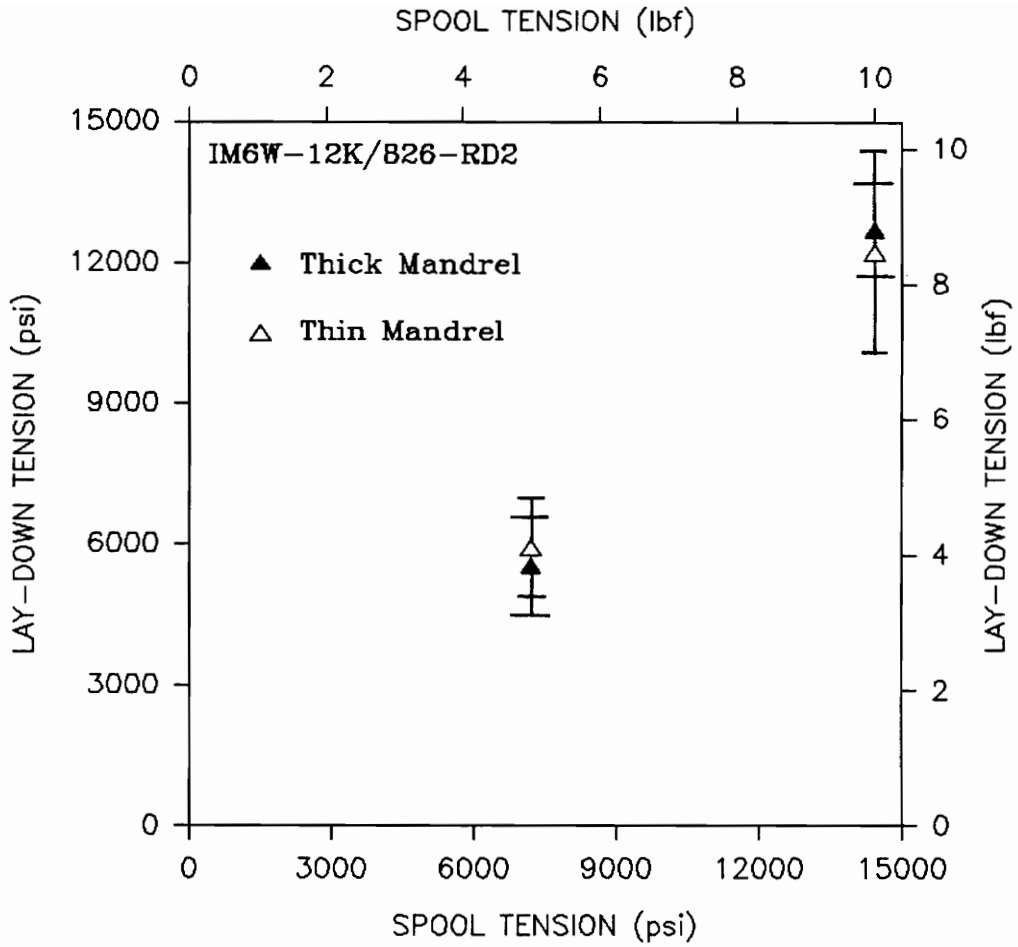


Figure 4.12 Lay-down Tension Versus Spool Tension for IM6W-12K/826-RD2

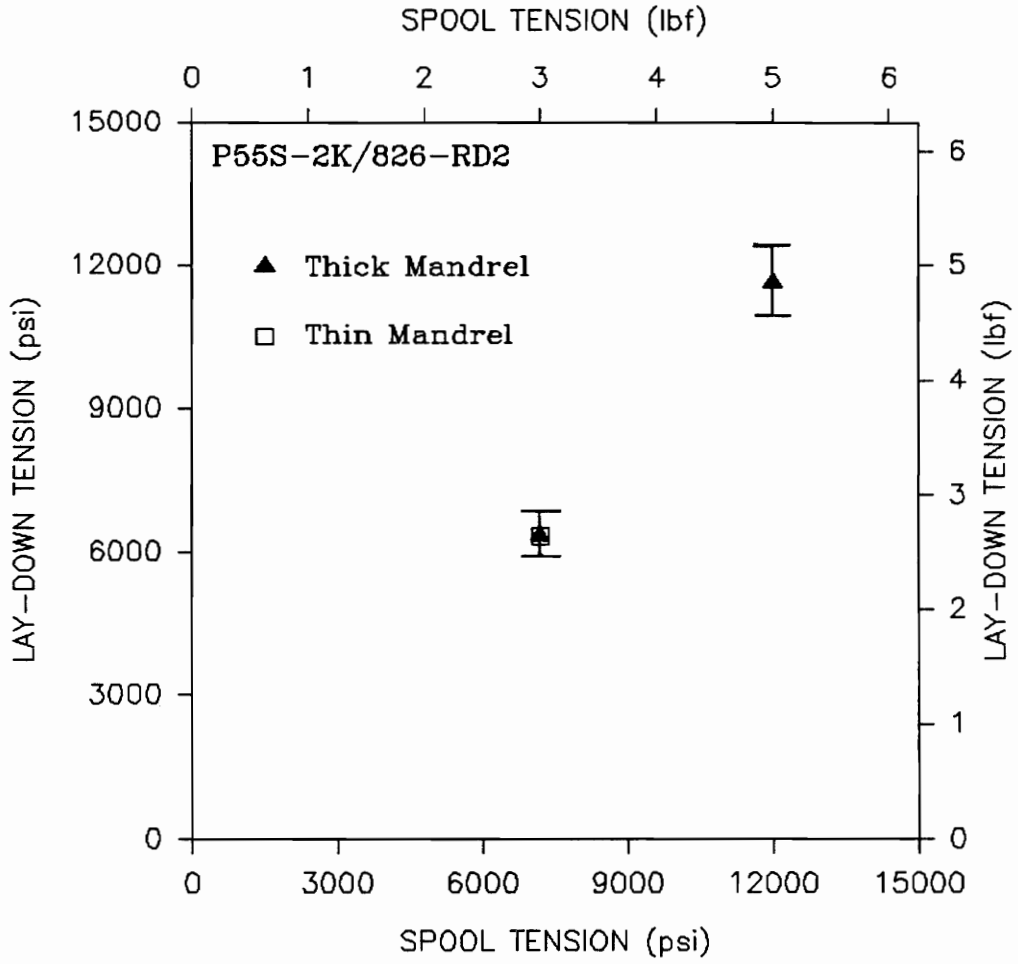


Figure 4.13 Lay-down Tension Versus Spool Tension for P55S-2K/826-RD2

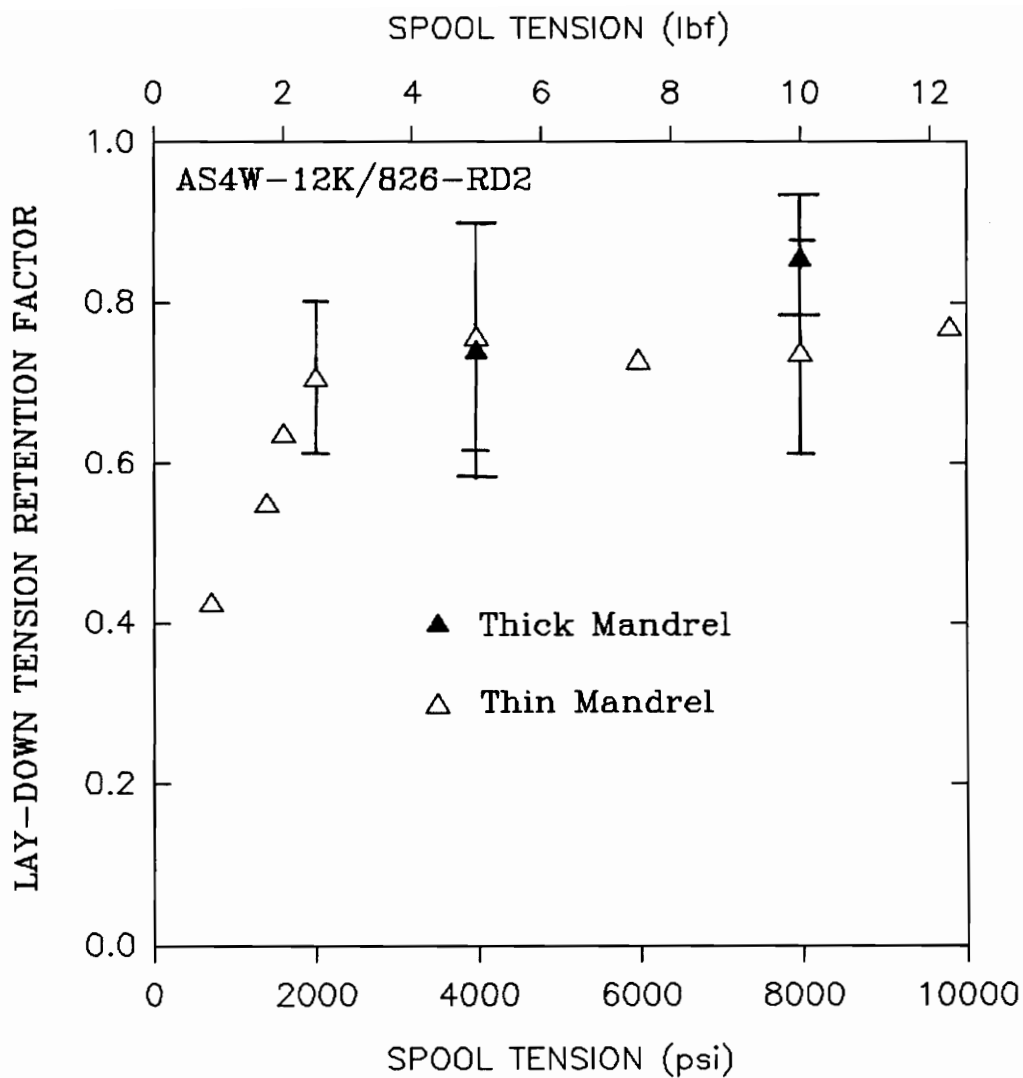


Figure 4.14 Lay-down Tension Retention Factor Versus Spool Tension for AS4W-12K/826-RD2

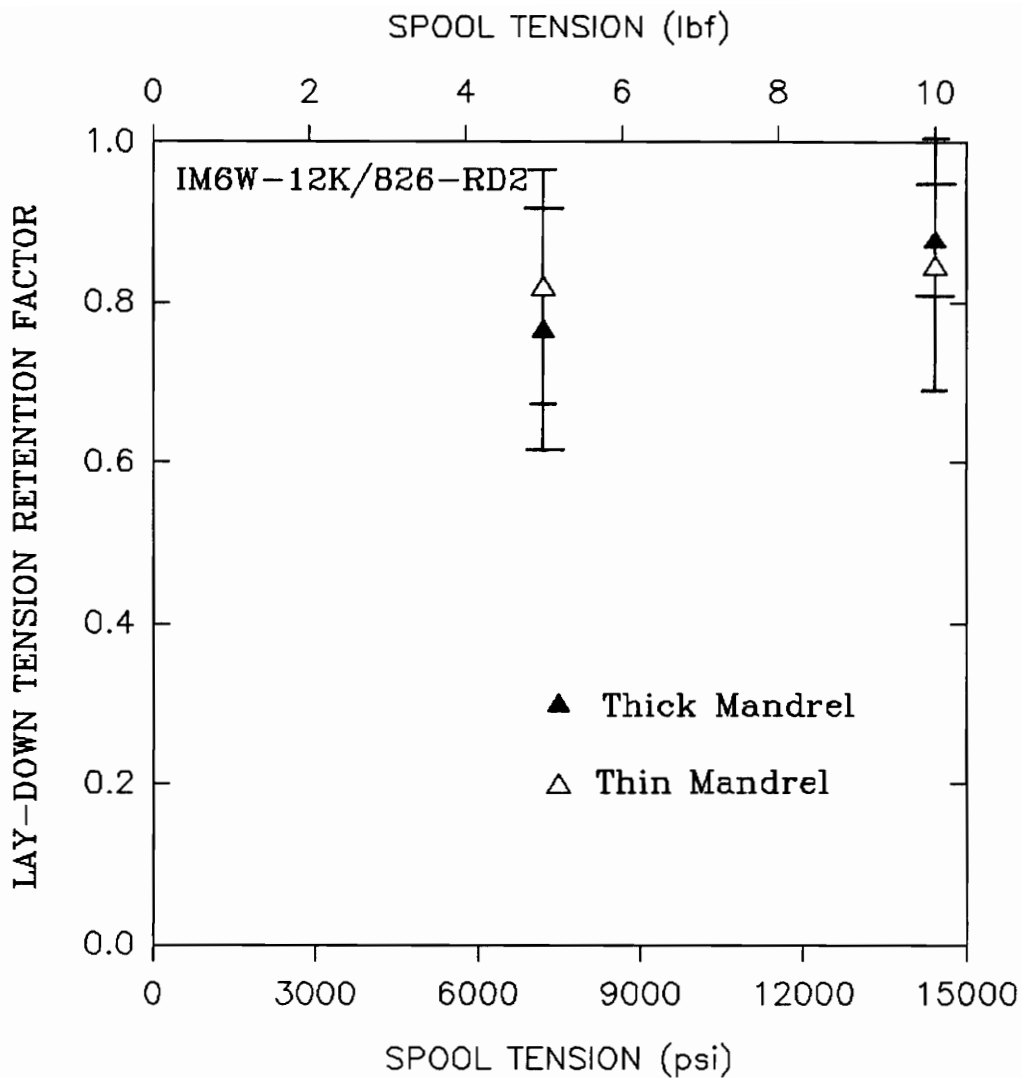


Figure 4.15 Lay-down Tension Retention Factor Versus Spool Tension for IM6W-12K/826-RD2

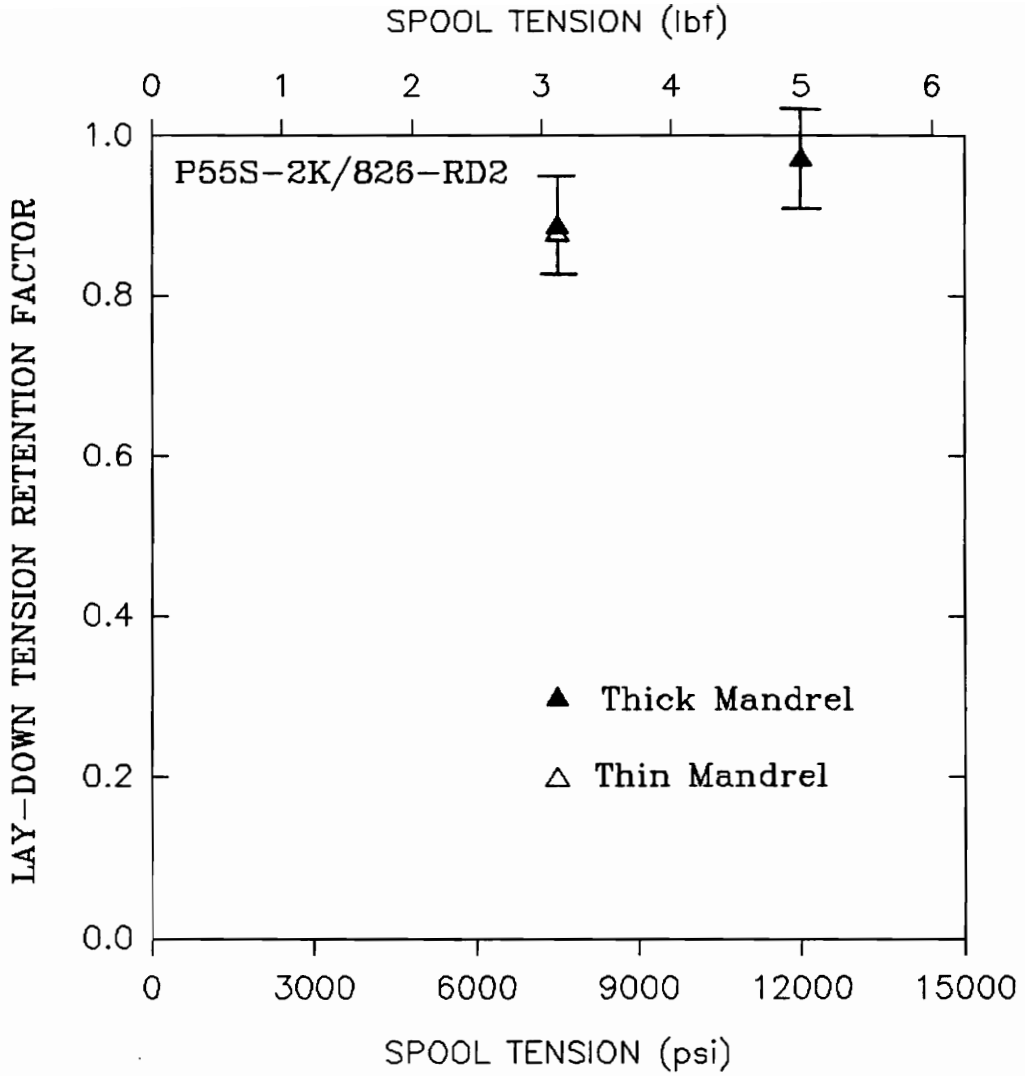


Figure 4.16 Lay-down Tension Retention Factor Versus Spool Tension for P55S-2K/826-RD2

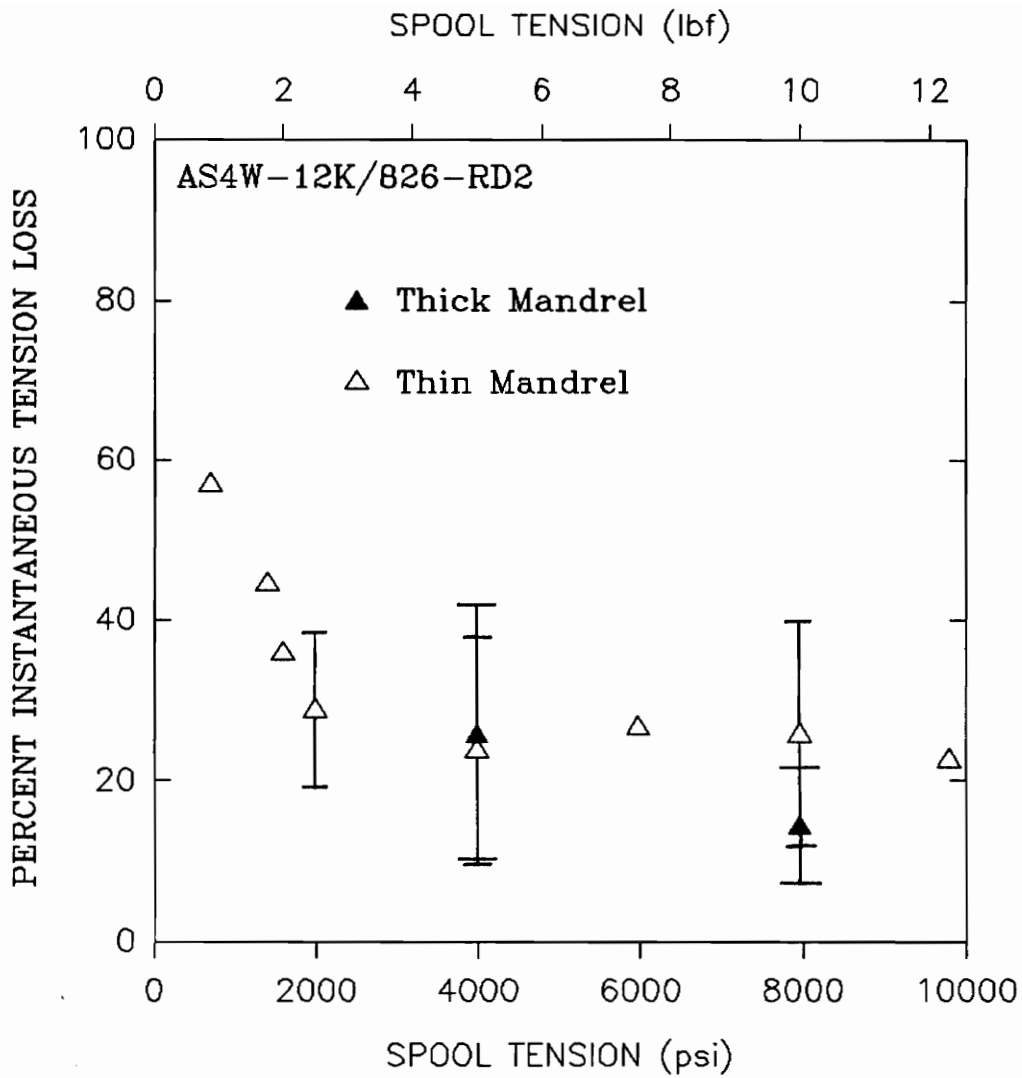


Figure 4.17 Instantaneous Tension Loss Versus Spool Tension for AS4W-12K/826-RD2

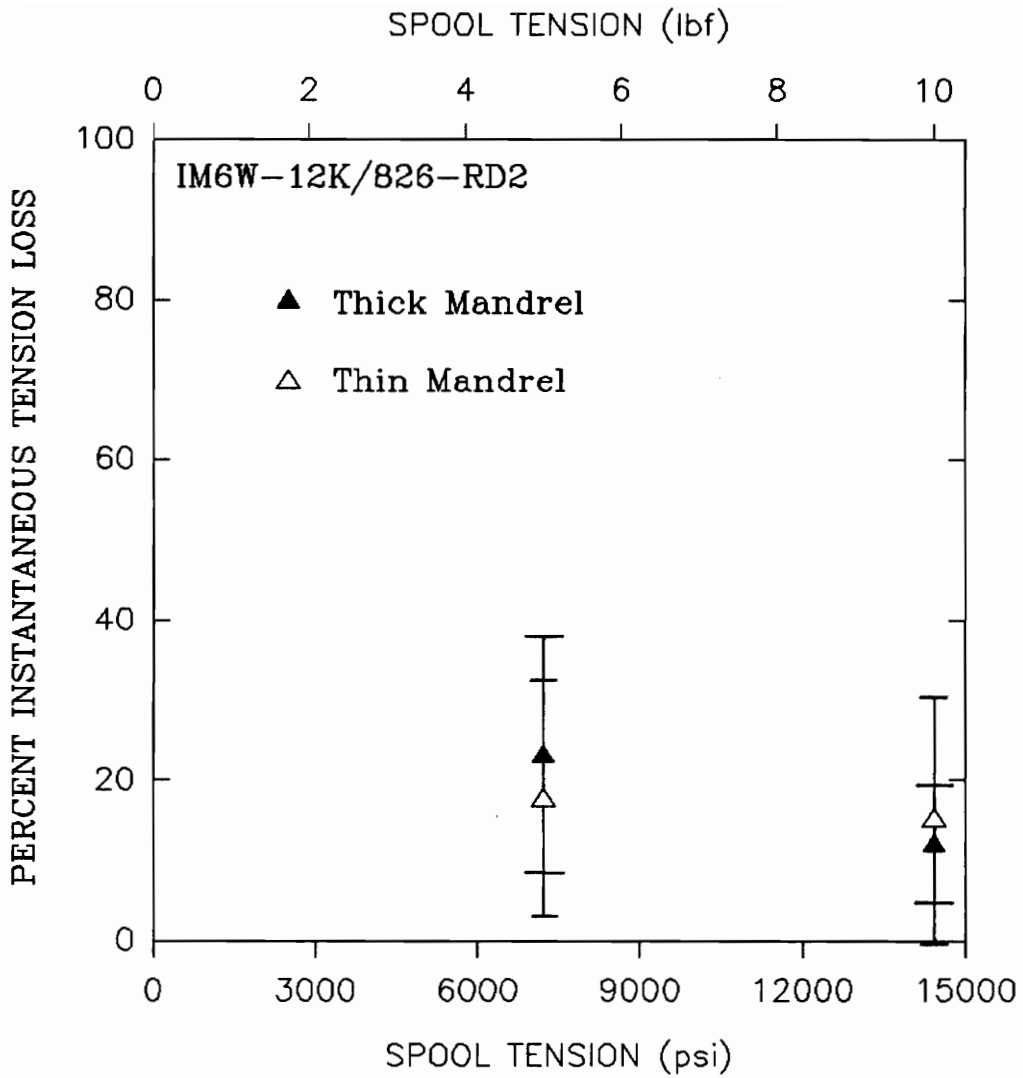


Figure 4.18 Instantaneous Tension Loss Versus Spool Tension for IM6W-12K/826-RD2

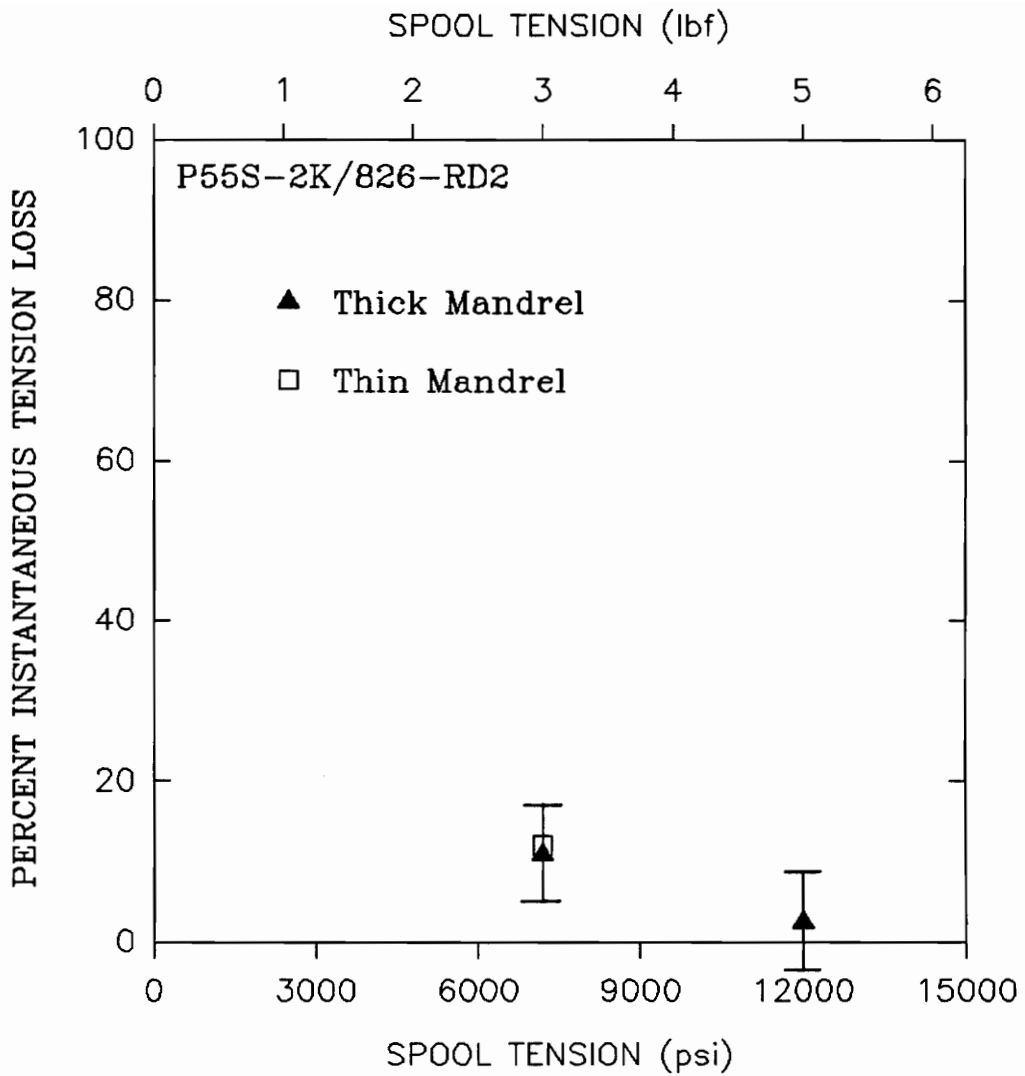


Figure 4.19 Instantaneous Tension Loss Versus Spool Tension for P55S-2K/826-RD2

Nguyen⁷ states that the lay-down tension is a material dependent function of the spool tension. It appears when viewing Figures 4.14 through 4.16 that lay-down tension is also a function of mandrel stiffness. The lay-down tension resulting from the stiffer thick-walled mandrel experiments has different trends and different values than the lay-down tension resulting from the thin-walled mandrel winds for the same spool tensions.

If lay-down tension is a function of mandrel stiffness then for WACSAFE to correctly model the winding process, the instantaneous tension loss (spool tension minus lay-down tension) must be determined for the particular fiber/resin system, spool tension and mandrel being used. This is difficult and costly to do experimentally for each winding prediction. It is suggested that additional work be done to develop a model that will predict the instantaneous tension loss. The model can be validated experimentally and then used in combination with WACSAFE to model the winding process. This work is beyond the scope of this thesis, but is recommend as a follow on research project.

4.3 WACSAFE VERIFICATION

Winding induced mandrel strain predictions were made for the

list of experiments in Table 4.1 using the WACSAFE code. The code modeled the filament winding process by turning on one composite element at a time down the length of the mandrel. The composite elements were pre-stressed at the input tension.

The output mandrel strain values from WACSAFE are average element strains. For the thin-walled mandrel winds this was not a problem. The hoop strain through the mandrel thickness remains almost constant. The thick-walled mandrel predictions required a second order polynomial regression fit to predict the mandrel inside surface hoop strain. Variations in the mandrel hoop strain through the thickness are shown in Figures 4.20 and 4.21. The two plots represent the same mandrel location at two different times during the winding process. Figure 4.20 represents the mandrel strain after eight circuits are wound and Figure 4.21 represents the strain after twenty-one circuits have been wound. The difference between the two strain curve shapes led to the selection of a second order polynomial regression fit rather than a linear. The second order approximates the data more closely for all cases than a linear regression. Excellent correlation between the data and the regression fit can be seen in the figures.

The input tensions, used in the WACSAFE models, used the

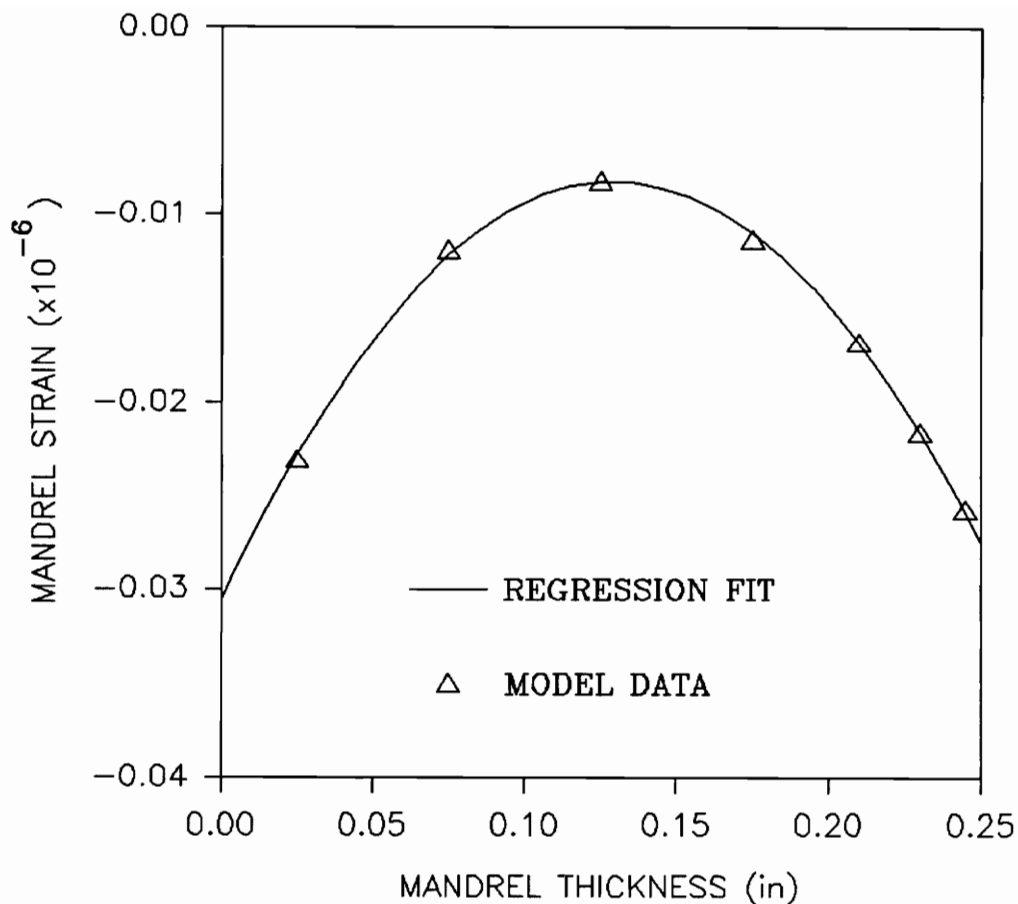


Figure 4.20 Mandrel Hoop Strain Through the Thickness After Eight Circuits

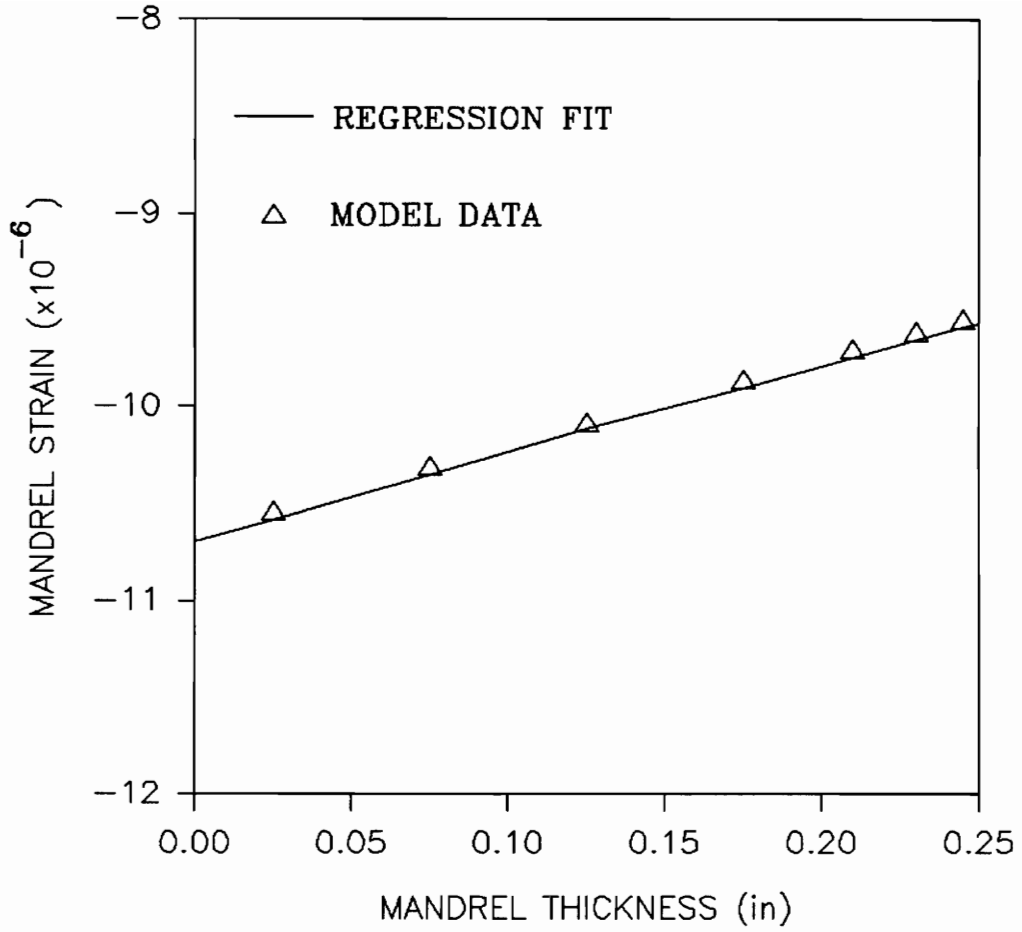


Figure 4.21 Mandrel Hoop Strain Through the Thickness After Twenty-one Circuits

lay-down tension retention factors from Figures 4.14 through 4.16 multiplied by the spool tensions. The input tensions for the AS4 and IM6 thin-walled mandrel winds were averages. For tension levels of five pounds and higher, retention factors of 0.750 and 0.834 were used for AS4 and IM6 winding respectively. For the lower AS4 tension levels a linear regression was used, Equation (4.9).

$$R=0.176989T_s+0.266214 \quad (4.9)$$

R = Retention Factor
T_s = Spool Tension

The correlation between the averaged lay-down tension retention factors and the experimentally measured lay-down tension retention factors are shown in Figures 4.22 and 4.23. The dotted line represents the averaged values.

The winding experiments recorded the inside mandrel hoop strain at the midpoint of the mandrel length. The strain gage was 0.25-inch wide and measured an average strain for its width at that location. Strain gage readings were taken each time the winding progressed one-half-inch down the length of the mandrel.

To correspond to the averaged strain gage readings, the WACSAFE mandrel inside surface analytical strains were

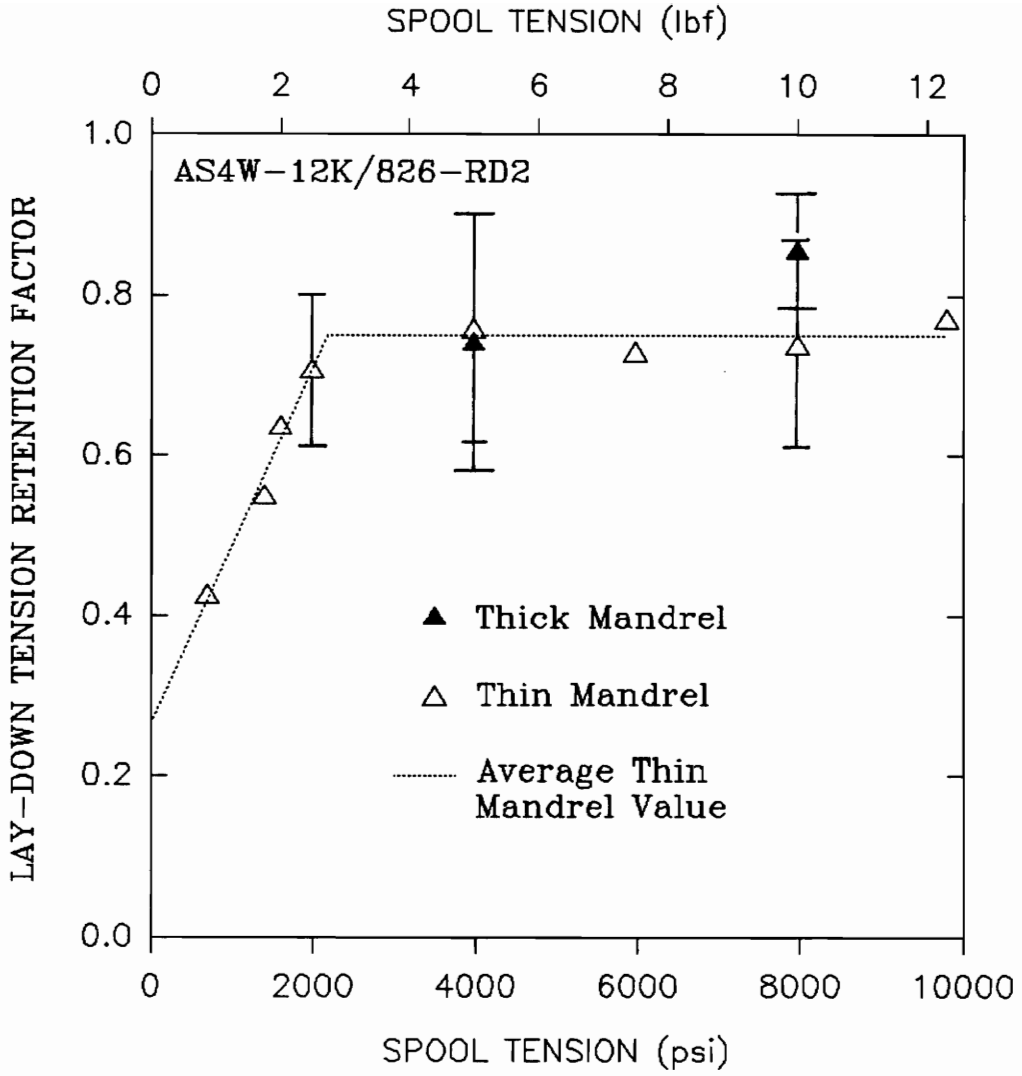


Figure 4.22 Averaged Lay-down Tension Retention Factor for AS4W-12K/826-RD2

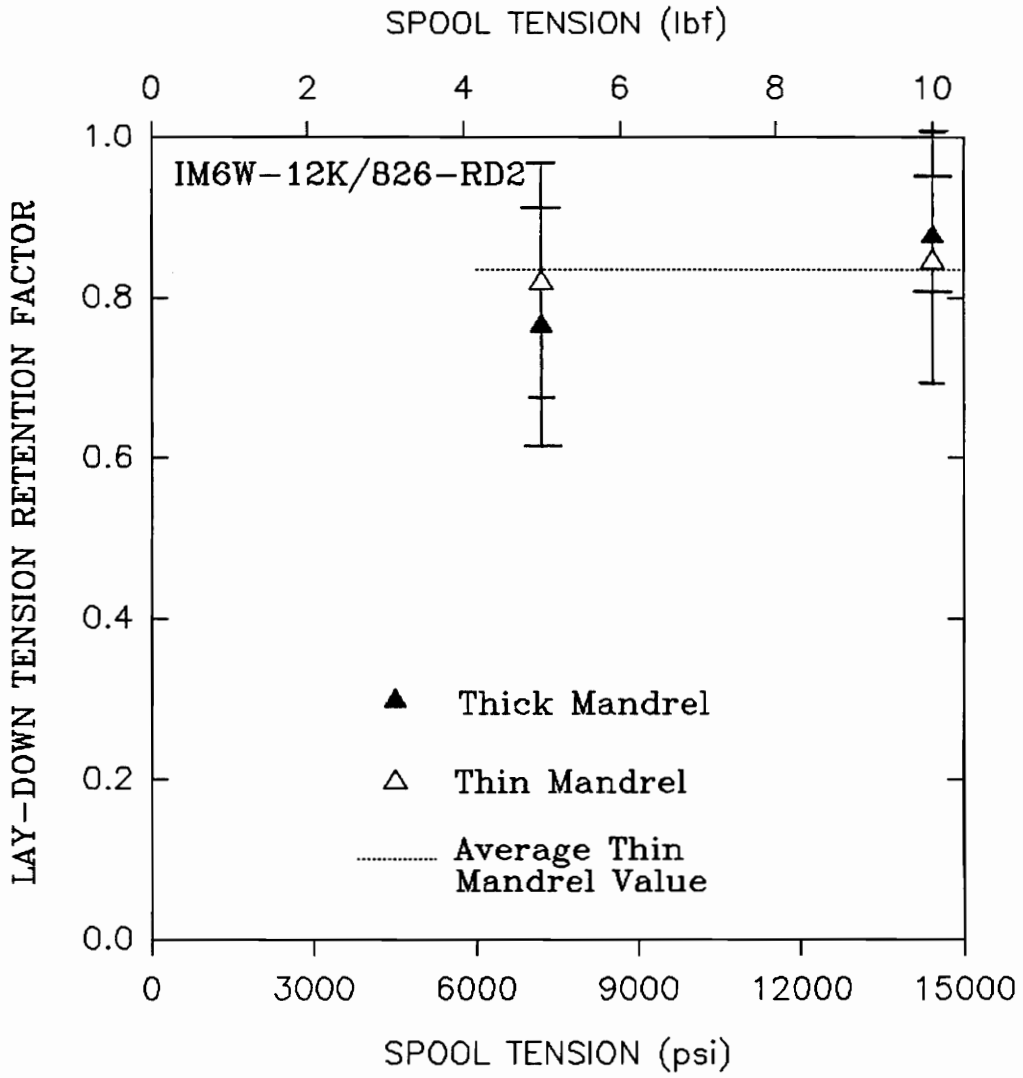


Figure 4.23 Averaged Lay-down Tension Retention Factor for IM6W-12K/826-RD2

averaged over a 0.25-inch width at the midpoint of the mandrel length. The averaged mandrel hoop strains were calculated after each circuit was turned on in the model.

The comparison between the WACSAFE analytical mandrel strains and the experimental strains are shown in Figures 4.24 through 4.27. Excellent agreement is shown in all cases. The small discrepancies between the model and the test data shown in Figure 4.24 for the 12.3-lb and 5.0-lb AS4 thin-walled mandrel wind are due to the difference in the averaged lay-down tension retention factor and the actual shown in Figure 4.22.

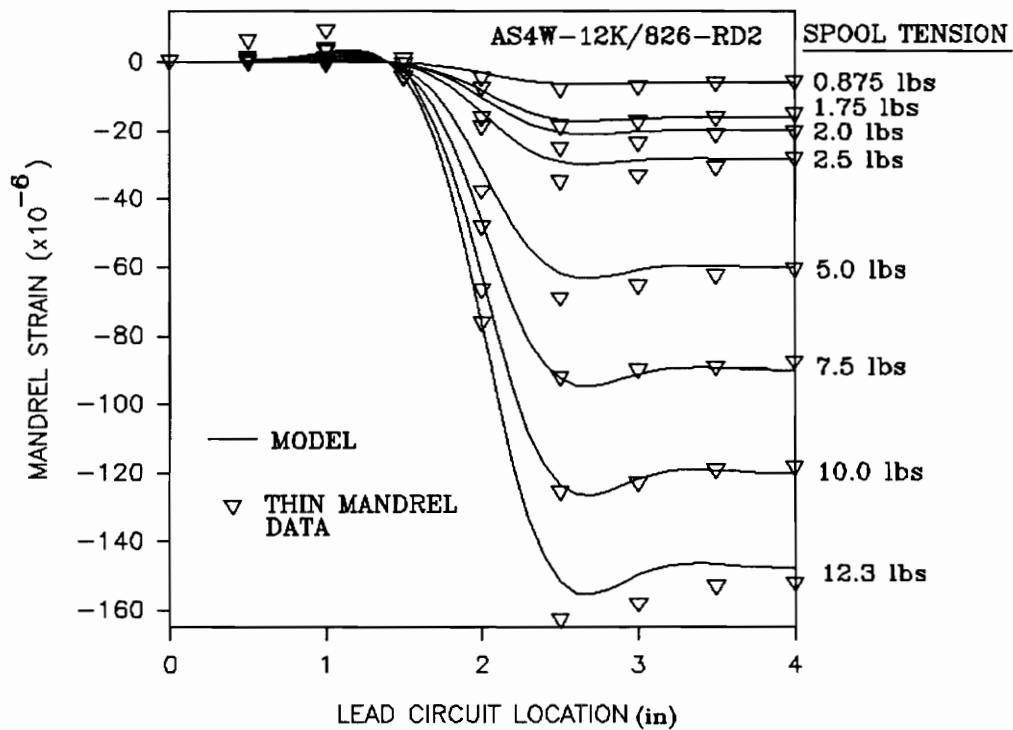


Figure 4.24 Thin-Walled Mandrel Strain Comparisons for AS4W-12K/826-RD2

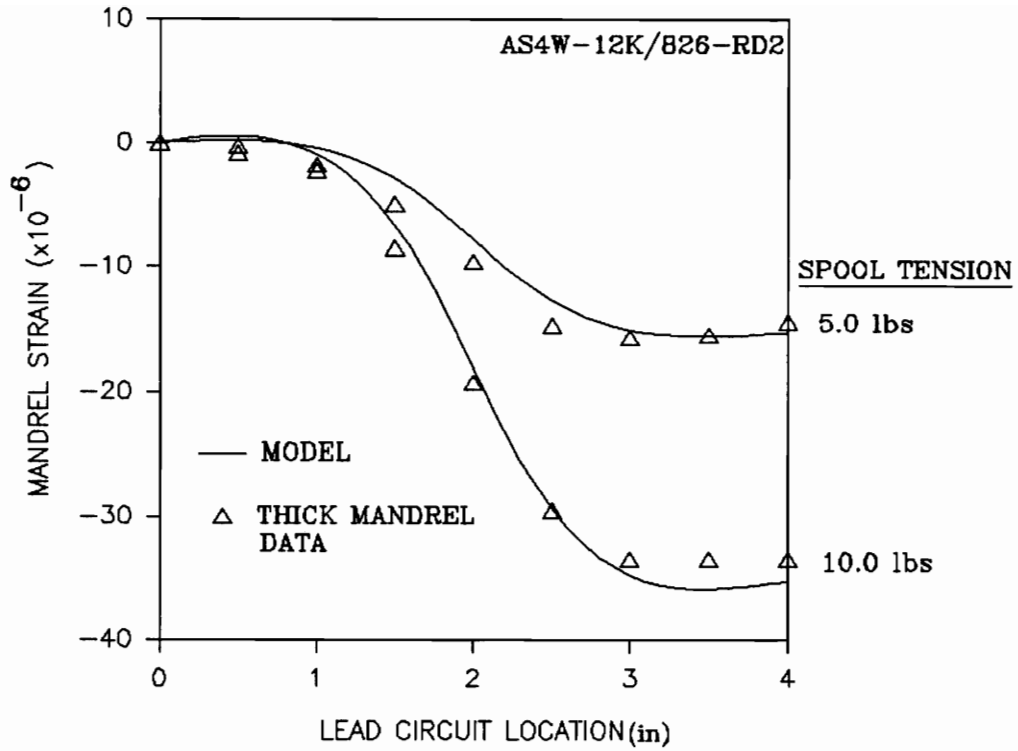


Figure 4.25 Thick-Walled Mandrel Strain Comparisons for AS4W-12K/826-RD2

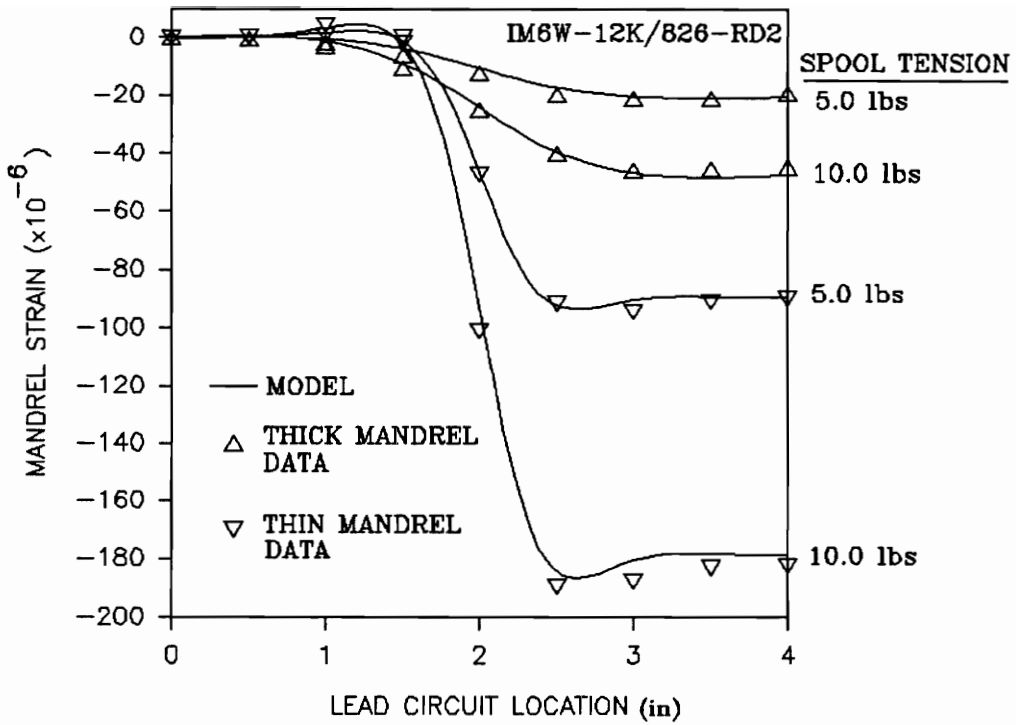


Figure 4.26 Mandrel Strain Comparisons for IM6W-12K/826-RD2

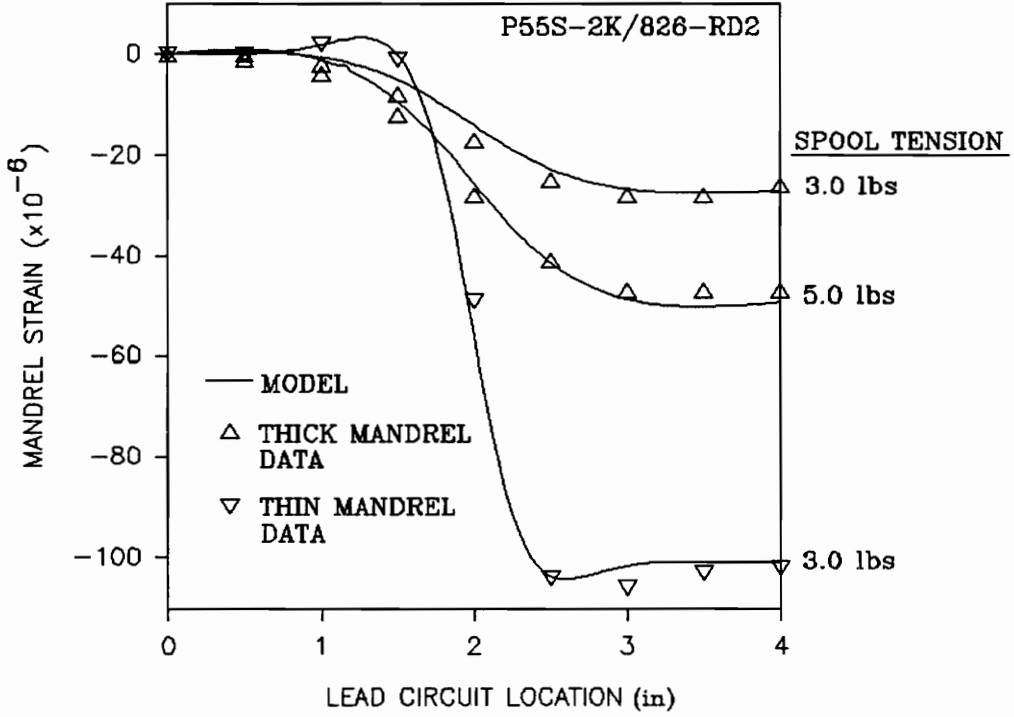


Figure 4.27 Mandrel Strain Comparisons for P55S-2K/826-RD2

5.0 SUMMARY AND CONCLUSIONS

5.1 SUMMARY

During the course of this investigation the following major tasks were completed:

1. A wet winding resin impregnation system was designed and fabricated. The impregnation system is adaptable to different types and sizes of fibers and can be adjusted to deliver the desired resin content. The system demonstrated its capability of maintaining typical resin content tolerances of $\pm 2\%$ by weight.

Equations were derived relating wet fiber weight to percent resin content.

2. A tension measuring device was designed and built. It is adaptable to different types and sizes of fibers.

The location of the load cell is adjustable and can handle large ranges of fiber tension. The tension measuring device was designed to be the last contact the fiber makes prior to mandrel contact. This provides an accurate reading of spool tension without any additional influences on the fiber beyond the point of tension measurement.

Equations were derived relating load cell output to fiber tension.

3. The experimental winding process was optimized to yield repeatable results. Changes were made in the fiber delivery to minimize tension variations caused by the fiber pay-out angle from the spool.
4. Equations were derived relating mandrel strain readings to fiber tension for both thick-walled and thin-walled mandrels.
5. The permeability model of FWCURE was verified by matching experimental data. The permeability constants and a relationship between fiber bundle resin content

and spool tension were found.

6. Percent side-by-side tension losses for the materials and mandrels used in this study were found.
7. The lay-down tension retention factors and the percent instantaneous tension loss were found for the mandrels and materials used in this study.
8. The capability of WACSAFE to model the filament winding process was verified through matching experimental data.

5.2 CONCLUSIONS

The ability of the FWCURE and WACSAFE computer codes to model the filament winding process and the associated tension losses have been verified with good results. A large number of experimental cylinders were wound to generate the needed data. In all cases the predicted values matched the actual data quite well. There were some areas of small mismatch that suggest areas of improvement. These are discussed in section 5.3. Even though there are suggested areas of improvement, this is not to say that the

predictions were bad. They were still reasonably close.

A suggested method of determining uncured composite properties was made in section 4.2.1. The effect that these properties have on side-by-side tension losses were shown to be negligible.

The side-by-side tension losses for a given mandrel and material system were shown to be a constant percentage of the spool tension. A similar analytical study can be performed using different materials and mandrels to determine their side-by-side losses as a function of spool tension.

It was hoped at the beginning of this study that an instantaneous tension loss curve could be generated for each material system as a function of spool tension. The testing and results, presented in section 4.2.3, show that instantaneous tension losses could also be a function of mandrel stiffness. For thin-walled compliant mandrels, the instantaneous loss appears to be constant at higher tension levels. At these same tension levels and using the thicker more rigid mandrel the instantaneous tension loss curve has a downward slope.

5.3 RECOMMENDATIONS

The experimental data and results presented herein were based on wet winding processes. The use of preimpregnated materials in filament winding is gaining popularity. It is suggested that a similar study be repeated using preimpregnated composite materials.

An improvement for relating fiber bundle resin content to spool tension is suggested. The test data for P55 fibers indicated that tows with fewer numbers of filaments and smaller cross sectional areas have more resin migrating to the surface instantaneously than the current relationship predicts. The increased instantaneous resin migration leads to a lower fiber bundle resin content and a flatter tension loss with time curve. The multi-layer winds suggest that when winding on top of previously wound layers, the fiber bundle resin content increases. This allows more resin to migrate to the surface with time resulting in a more pronounced tension loss with time curve.

The development of an instantaneous tension loss model is also recommended. As discussed previously, the test data indicates that the instantaneous tension loss is a function of mandrel stiffness as well as spool tension and the material system used. Currently, for WACSAFE to correctly

model the winding process, the instantaneous tension loss needs to be found experimentally for each fiber/resin system, spool tension and mandrel used. The experimental process of finding the instantaneous loss is too costly and time consuming to be a viable option each time a fabrication stress prediction is desired.

BIBLIOGRAPHY

1. Calius, E. P. and Springer, G. S., "Modeling the Filament Winding Process," *Proceedings of the Fifth International Conference on Composite Materials*, San Diego, CA, July 29-Aug. 1, pp. 1071-1088, (1985).
2. Springer, G. S., "Modeling the Cure Process of Composites," *Materials Sciences for the Future: Proceedings of the 31st SAMPE Symposium*, pp. 776-787, (1986).
3. Calius, E. P. and Springer, G. S., "Validation of the Filament Winding Process Model," *Materials--Pathway to the Future: Proceedings of the 33rd SAMPE Symposium*, pp. 670-676, (1988).
4. Calius, E. P., Kidron, M., Lee, S. Y. and Springer, G. S., "Manufacturing Stresses and Strains in Filament Wound Cylinders," *Materials--Pathway to the Future: Proceedings of the 33rd SAMPE Symposium*, pp. 347-351, (1988).
5. Spencer, B. E., "Prediction of Manufacturing Stresses in Thick Walled Orthotropic Cylinders," *Materials Sciences for the Future: Proceedings of the 31st SAMPE Symposium*, pp. 867-879, (1986).
6. Tzeng, T. S., "A Model of the Winding and Curing Processes for Filament Wound Composites," Ph. D. Dissertation, Virginia Tech, (1988).
7. Nguyen, V. D., "A Fabrication Stress Model for Filament Wound Composite Structures," Ph. D. Dissertation, Virginia Tech, (1988).

8. Timoshenko, S. P. and Goodier, J. N., *Theory of Elasticity*, McGraw-Hill, New York, (1970).
9. Box, G. E. P. and Behnken, D. W., "Some New Three Level Designs for the Study of Quantitative Variables," *Technometrics*, pp. 455-475, (1960).
10. Jones, R. M., *Mechanics of Composite Materials*, Hemisphere Publishing Corporation, New York, (1975).
11. Stein, S. C. and Knight, C. E., "Modeling of the Filament-Winding Fabrication Process Using WACSAFE," Technical Report, Thiokol Corporation, Wasatch Division, (1991)

APPENDIX A

DERIVATION OF WET WEIGHT CALCULATION Equation (2.1)

$$C = R + F$$

C = Composite Volume
 R = Resin Volume
 F = Fiber Volume

Set Volumes to Fractions

$$V_T = V_R + V_F$$

$V_T = 1$
 $V_R =$ Resin Volume Fraction
 $V_F =$ Fiber Volume Fraction

$$V_F = \frac{F}{C} \quad \rightarrow \quad F = C V_F$$

$$V_R = \frac{R}{C} \quad \rightarrow \quad R = C V_R$$

Relate Volume to Weight

$W_F = \rho_F F$ $W_F =$ Fiber Weight (dry)
 $\rho_F =$ Fiber Density

$W_R = \rho_R R$ $W_R =$ Resin Weight
 $\rho_R =$ Resin Density

$W_C = W_F + W_R$ $W_C =$ Composite Weight

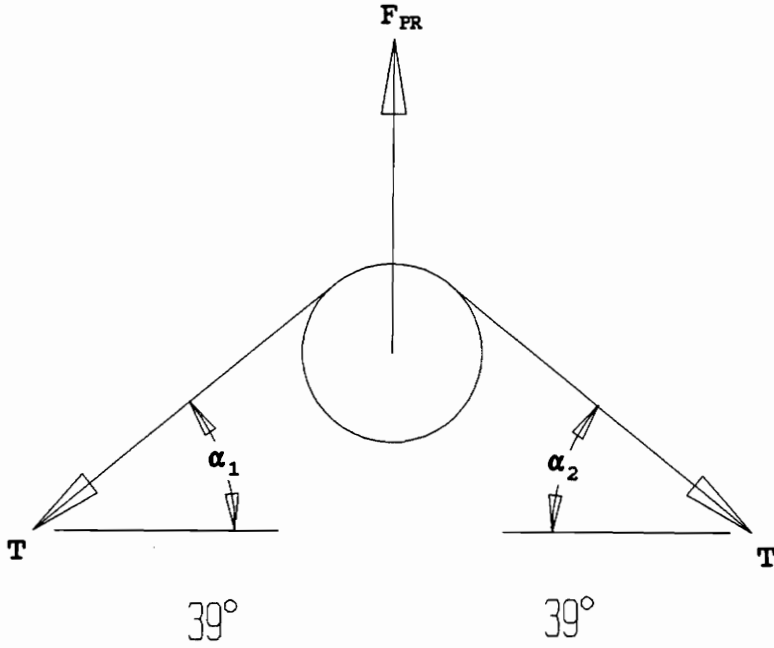
$$W_C = W_F + \rho_R R \quad - \quad W_F + \rho_R C V_R \quad - \quad W_F + \rho_R C V_R \frac{V_F \rho_F}{V_F \rho_F}$$

$$W_C = W_F + \frac{\rho_R V_R (C V_F \rho_F)}{\rho_F V_F} \quad - \quad W_F + \frac{\rho_R V_R W_F}{\rho_F V_F} \quad - \quad W_F \left(1 + \frac{\rho_R V_R}{\rho_F V_F} \right)$$

Let $W_f = D$, Dry Fiber Sample Weight
Let $W_c = W$, Wet Fiber Sample Weight

$$W-D \left(1 + \frac{\rho_R V_R}{\rho_F (1-V_R)} \right) \tag{2.1}$$

DERIVATION OF WINDING TENSION CALCULATION
Equation (2.2)

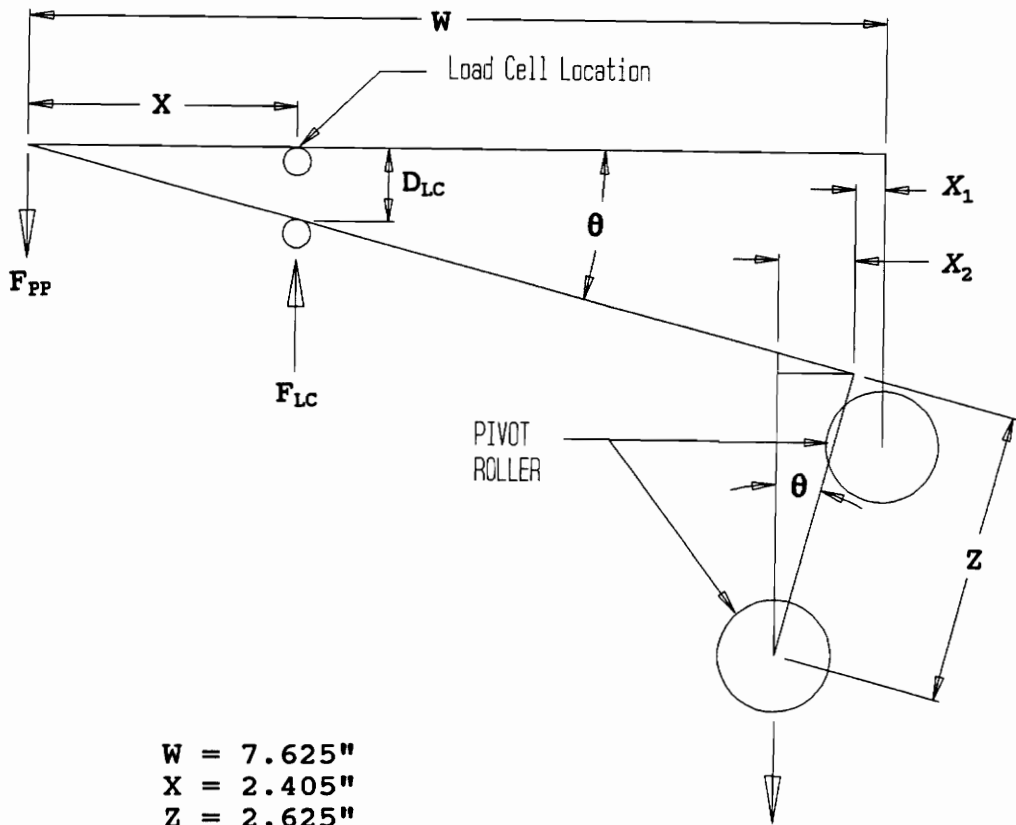


T = Fiber Tension
 F_{PR} = Force on Pivot Roller
 α = Fiber Angle Between Rollers

$$\Sigma F_Y = 0: F_{PR} - T \sin \alpha_1 - T \sin \alpha_2 = 0$$

$$T = \frac{F_{PR}}{\sin \alpha_1 + \sin \alpha_2} \quad (\text{A.1})$$

Determine F_{PR} :



- $W = 7.625''$
- $X = 2.405''$
- $Z = 2.625''$
- F_{LC} = Force on Load Cell
- F_{PP} = Force at Pivot Point
- D_{LC} = Vertical Displacement of Load Cell

$$\Sigma M_{PP} = 0: \quad X F_{LC} - (W - X_1 - X_2) F_{PR} = 0 \quad \rightarrow \quad F_{PR} = \frac{X F_{LC}}{W - X_1 - X_2} \quad (A.2)$$

$$X_1 = W - W \cos \theta = W(1 - \cos \theta) \quad (A.3)$$

$$X_2 = Z \sin \theta \quad (A.4)$$

Incorporate Equations (A.3) and (A.4) into Equation (A.2)

$$F_{PR} = \frac{X F_{LC}}{W - W(1 - \cos \theta) - Z \sin \theta} = \frac{X F_{LC}}{W \cos \theta - Z \sin \theta} \quad (A.5)$$

Determine θ :

$$\theta = \tan^{-1} \frac{D_{LC}}{X} \quad (\text{A.6})$$

From the Manufacturer: Load cell will displace .01-in with a 25-lb load.

Load cell deflection versus load is linear.

$$\therefore \frac{D_{LC}}{F_{LC}} = \frac{.01}{25} \quad \rightarrow \quad D_{LC} = \frac{.01 F_{LC}}{25} \quad (\text{A.7})$$

Incorporate Equation (A.7) into Equation (A.6)

$$\theta = \tan^{-1} \frac{.01 F_{LC}}{25 X} = \tan^{-1} \frac{F_{LC}}{2500 X} \quad (\text{A.8})$$

Incorporate Equation (A.8) into Equation (A.5)

$$F_{PR} = \frac{X F_{LC}}{W \cos\left(\tan^{-1} \frac{F_{LC}}{2500 X}\right) - Z \sin\left(\tan^{-1} \frac{F_{LC}}{2500 X}\right)} \quad (\text{A.9})$$

From Figure 2.3:

$$R = \frac{O_{LC}}{F_{LC}} \quad \rightarrow \quad F_{LC} = \frac{O_{LC}}{R} \quad (\text{A.10})$$

O_{LC} = Load Cell Output
 R = Output/Load Ratio (26.36/lbs)

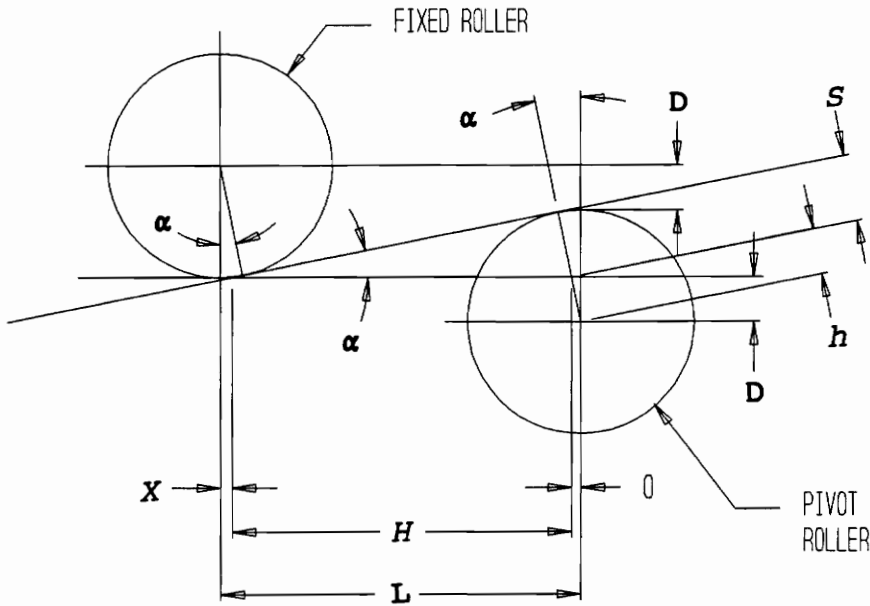
Incorporate Equation (A.10) into Equation (A.9)

$$F_{PR} = \frac{X O_{LC}}{R \left[W \cos \left(\tan^{-1} \frac{O_{LC}}{2500 R X} \right) - Z \sin \left(\tan^{-1} \frac{O_{LC}}{2500 R X} \right) \right]} \quad (\text{A.11})$$

Incorporate Equation (A.11) into Equation (A.1)

$$T = \frac{X O_{LC}}{R (\sin \alpha_1 + \sin \alpha_2) \left[W \cos \left(\tan^{-1} \frac{O_{LC}}{2500 R X} \right) - Z \sin \left(\tan^{-1} \frac{O_{LC}}{2500 R X} \right) \right]} \quad (\text{2.2})$$

DERIVATION OF FIBER ANGLE Equation (2.3)



L = Length between fixed roller and pivot roller

R = Radius of rollers (0.5")

D = Displacement of pivot roller (0.04" @ zero load)

$$\sin\alpha = \frac{S}{H}$$

$$S = R - h$$

$$\cos\alpha = \frac{D}{h} \rightarrow h = \frac{D}{\cos\alpha}$$

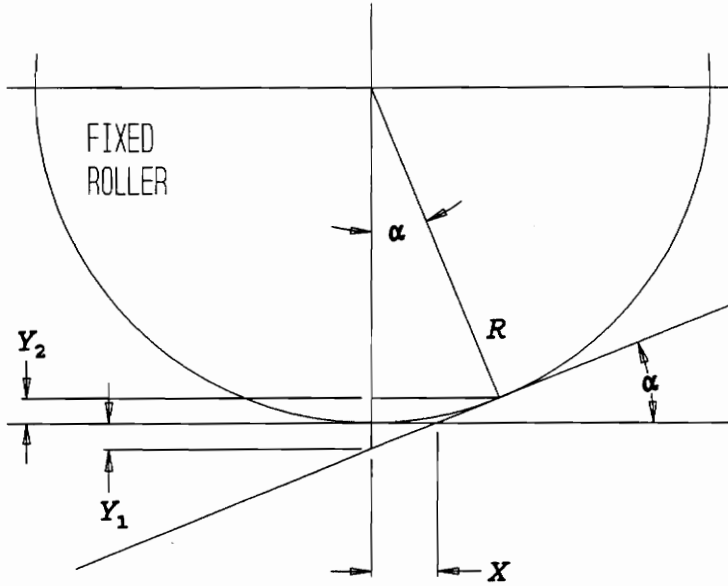
$$H = L - t - X$$

$$\tan\alpha = \frac{t}{D} \rightarrow t = D \tan\alpha$$

$$\sin\alpha = \frac{R - \frac{D}{\cos\alpha}}{L - D \tan\alpha - X}$$

(A.12)

Determine the distance X



$$\tan\alpha = \frac{Y_1}{X} \quad Y_1 = d \tan\alpha - Y_2 \quad d = R \sin\alpha \quad Y_2 = R - R \cos\alpha$$

$$\tan\alpha = \frac{d \tan\alpha - R + R \cos\alpha}{X} = \frac{R \sin\alpha \tan\alpha - R + R \cos\alpha}{X}$$

$$\Rightarrow X = \frac{R \sin\alpha \tan\alpha - R + R \cos\alpha}{\tan\alpha} = \frac{R \sin\alpha \frac{\sin\alpha}{\cos\alpha} - R \frac{\cos\alpha}{\cos\alpha} + R \frac{\cos^2\alpha}{\cos\alpha}}{\frac{\sin\alpha}{\cos\alpha}}$$

$$\Rightarrow X = \frac{R(1 - \cos\alpha)}{\sin\alpha}$$

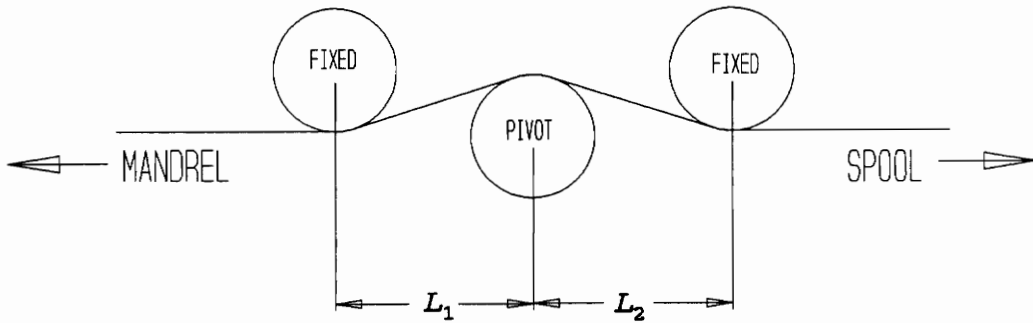
(A.13)

Incorporate Equation (A.13) into Equation (A.12)

$$\sin\alpha = \frac{R - \frac{D}{\cos\alpha}}{L - D \tan\alpha - \frac{R(1 - \cos\alpha)}{\sin\alpha}} = \frac{R - \frac{D}{\cos\alpha}}{L \frac{\sin\alpha}{\sin\alpha} - D \frac{\sin\alpha \tan\alpha}{\sin\alpha} - \frac{R(1 - \cos\alpha)}{\sin\alpha}}$$

$$\begin{aligned}
\rightarrow 1 - \frac{R - \frac{D}{\cos\alpha}}{L \sin\alpha - D \sin\alpha \tan\alpha - R(1 - \cos\alpha)} \\
\rightarrow L \sin\alpha - D \sin\alpha \tan\alpha - R(1 - \cos\alpha) - R - \frac{D}{\cos\alpha} \\
\rightarrow L \sin\alpha - D \sin\alpha \tan\alpha - 2R + R \cos\alpha + \frac{D}{\cos\alpha} = 0 \\
\rightarrow L \sin\alpha \cos\alpha - D \sin^2\alpha - 2R \cos\alpha + R \cos^2\alpha + D = 0 \\
\rightarrow L \sin\alpha \cos\alpha + D(1 - \sin^2\alpha) + R \cos\alpha (\cos\alpha - 2) = 0 \\
\rightarrow L \sin\alpha \cos\alpha + D \cos^2\alpha + R \cos\alpha (\cos\alpha - 2) = 0 \\
\rightarrow L \sin\alpha + D \cos\alpha + R(\cos\alpha - 2) = 0
\end{aligned}$$

$$L \sin\alpha + (D+R) \cos\alpha - 2R = 0$$

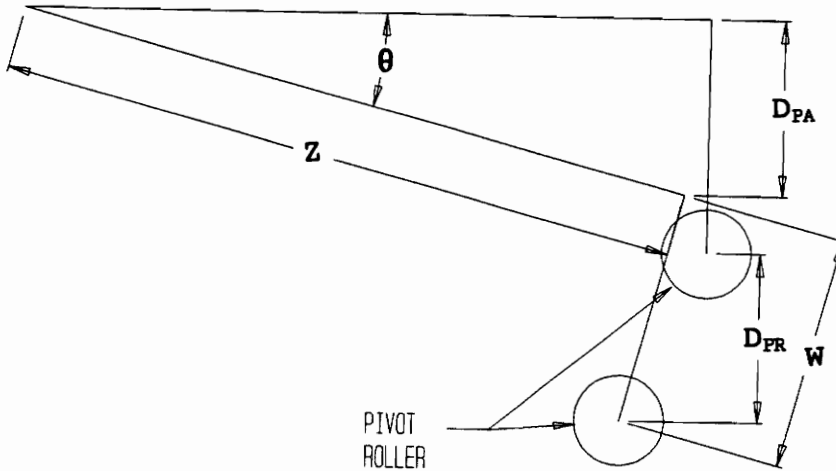


$$L_1 \sin\alpha_1 + (D+R) \cos\alpha_1 - 2R = 0$$

$$L_2 \sin\alpha_2 + (D+R) \cos\alpha_2 - 2R = 0$$

(2.3)

DERIVATION FOR THE PIVOT ROLLER VERTICAL DISPLACEMENT,
CAUSED BY THE APPLIED LOAD Equation (2.5)



D_{PA} = Vertical Displacement of the Pivot Arm
 D_{PR} = Vertical Displacement of the Pivot Roller
 $W = 7.625''$
 $Z = 2.625''$

$$D_{PA} = W \sin \theta$$

$$D_{PR} = D_{PA} - (Z - Z \cos \theta) = D_{PA} - Z(1 - \cos \theta) = W \sin \theta - Z(1 - \cos \theta) \quad (A.14)$$

From Equation (A.8)
$$\theta = \tan^{-1} \frac{F_{LC}}{2500X}$$

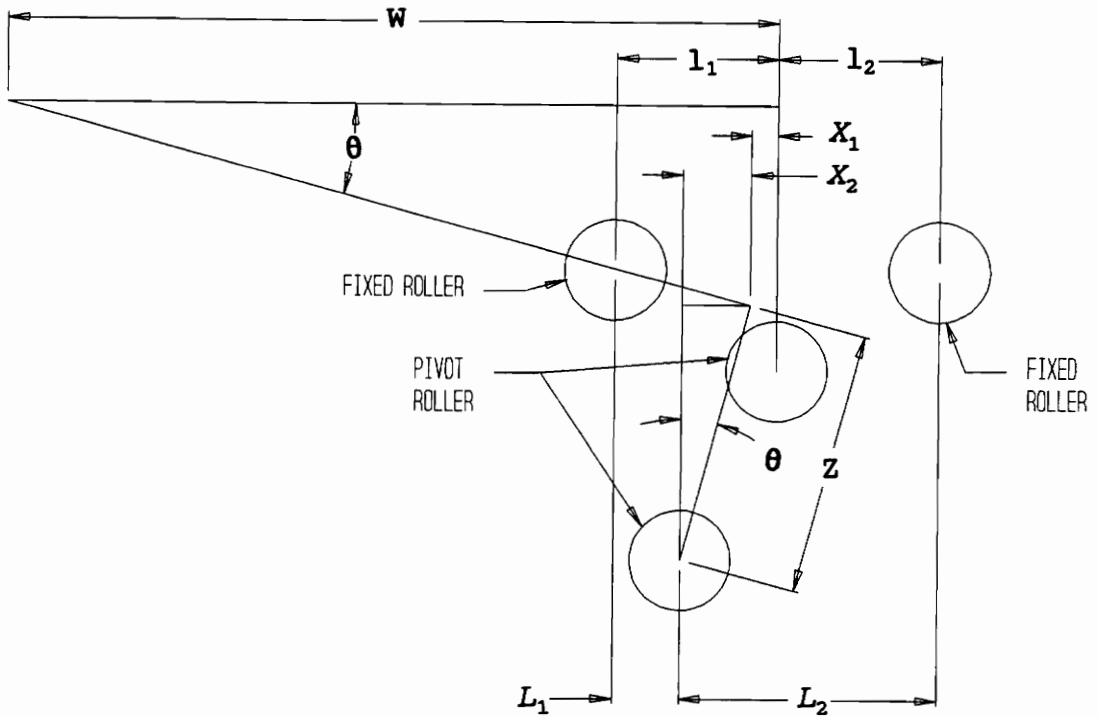
From Equation (A.10)
$$F_{LC} = \frac{O_{LC}}{R}$$

F_{LC} = Force on Load Cell
 O_{LC} = Load Cell Output
 R = Output/Load Ratio

Incorporate Equations (A.8) and (A.9) into (A.14)

$$D_{PR} = W \sin \left(\tan^{-1} \frac{O_{LC}}{2500RX} \right) - Z \left[1 - \cos \left(\tan^{-1} \frac{O_{LC}}{2500RX} \right) \right] \quad (2.5)$$

DERIVATION TO DETERMINE THE DISTANCE BETWEEN THE STATIONARY ROLLERS AND THE PIVOT ROLLER Equation (2.6)



$$\begin{aligned}
 W &= 7.625'' \\
 Z &= 2.625'' \\
 l_1 &= 1.592'' \\
 l_2 &= 1.644''
 \end{aligned}$$

From Equation (A.3)

$$X_1 = W(1 - \cos\theta)$$

From Equation (A.4)

$$X_2 = Z \sin\theta$$

$$L_1 - l_1 - X_1 - X_2 = l_1 - W(1 - \cos\theta) - Z \sin\theta$$

$$L_2 - l_2 + X_1 + X_2 = l_2 + W(1 - \cos\theta) + Z \sin\theta$$

(A.15)

From Equation (A.8) $\theta = \tan^{-1} \frac{F_{LC}}{2500X}$

From Equation (A.10) $F_{LC} = \frac{O_{LC}}{R}$

F_{LC} = Force on Load Cell
 O_{LC} = Load Cell Output
 R = Output/Load Ratio

Incorporate Equations (A.8) and (A.10) into Equation (A.15)

$$L_1 = l_1 - W \left[1 - \cos \left(\tan^{-1} \frac{O_{LC}}{2500RX} \right) \right] - Z \sin \left(\tan^{-1} \frac{O_{LC}}{2500RX} \right)$$

$$L_2 = l_2 + W \left[1 - \cos \left(\tan^{-1} \frac{O_{LC}}{2500RX} \right) \right] + Z \sin \left(\tan^{-1} \frac{O_{LC}}{2500RX} \right)$$

(2.6)

DETERMINATION OF FIBER TENSION FROM MANDREL STRAIN READINGS
Equation (3.2)

For thin-walled mandrels:

$$e = \frac{1}{E} (\sigma_h - \nu \sigma_\theta - \nu \sigma_r) \quad \sigma_\theta = 0 \quad \sigma_r = 0 \quad \therefore \sigma_h = Ee$$

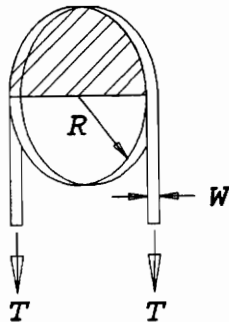
$$\sigma_h = \frac{PR}{t} \quad \rightarrow \quad \sigma_h = \frac{PR}{t} = Ee \quad \rightarrow \quad P = \frac{Eet}{R}$$

From Equation (3.2) $P = \frac{T}{RW}$

$$P = \frac{Eet}{R} = \frac{T}{RW}$$

$$T = EetW \tag{3.1}$$

DETERMINATION OF MANDREL PRESSURE FROM MANDREL STRAIN READINGS
Equation (3.3)



$$P = \frac{\text{Force}}{\text{Area}} = \frac{2T}{2RW}$$

$$P = \frac{T}{RW} \tag{3.2}$$

APPENDIX B

This appendix contains the raw data taken during the winding experiments. The times given during the winding operation are estimates. The times taken after winding to measure tension loss with time are accurate. When residual mandrel strain readings were present, after removing the fiber, they were added back into the data linearly with time. That is to say that a unit of strain per minute was calculated based on the residual strain and the elapsed time. This was multiplied by the time increments in each step and added to the strain value at that time step.

The test data for the EPON 828 wind (Table 3.1 Set #9) and the test data for the 0.5" winds (Table 4.1 Set #18 - 28) are not included. Their absence is due to the problems associated with getting useable values as explained in Section 3.0 and Section 4.0.

WIND #5

FIBER TYPE - AS4W-12K
 FIBER MODULUS - 34E06 psi
 FILAMENT DIA. - 0.000315" / 8μm
 FIBER VOL. - 58.7%
 WIND ANGLE - 90°
 PLY THICKNESS - 0.0128"
 BAND WIDTH - 0.1000"

RESIN TYPE - 826/RD2
 VISCOSITY - 6.16 poise
 RESIN VOL. - 41.3%
 # PLIES - 1
 SPOOL TENSION - 10 lbs

AREA OF TOW WITH RESIN - 1.284E-3 in²
 AREA OF TOW WITHOUT RESIN - 7.540E-4 in²

MANDREL OUTER RADIUS - 3.00"
 MANDREL THICKNESS - 0.05"
 MANDREL MATERIAL - ALUMINUM

MICROSTRAIN		TIME			MANDREL	WIND
GAGE 1	GAGE 2	hrs.	min.	sec.	COVERAGE	STATUS
					inches	
0	1	0	0	0	0.00	START
3	-1	0	0	6	0.54	STOP
		0	0	25	0.54	START
6	8	0	0	30	1.03	STOP
		0	0	54	1.03	START
-4	2	0	1	00	1.52	STOP
		0	1	24	1.52	START
-79	-82	0	1	30	2.03	STOP
		0	1	54	2.03	START
-119	-113	0	2	00	2.54	STOP
		0	2	25	2.54	START
-113	-119	0	2	30	3.00	STOP
		0	2	54	3.00	START
-110	-113	0	3	00	3.50	STOP
		0	3	24	3.50	START
-110	-113	0	3	30	4.00	END
-107	-107	0	5	0	4.00	
-101	-99	0	10	0	4.00	
-99	-93	0	15	0	4.00	
-98	-88	0	20	0	4.00	
-97	-84	0	25	0	4.00	
-95	-80	0	30	0	4.00	
-95	-76	0	35	0	4.00	
-94	-68	0	45	0	4.00	
-92	-61	0	55	0	4.00	
-91	-54	1	5	0	4.00	
-90	-47	1	15	0	4.00	
-90	-40	1	25	0	4.00	
-89	-34	1	35	0	4.00	
-88	-24	1	50	0	4.00	
-87	-14	2	5	0	4.00	
-85	-4	2	20	0	4.00	
-84	4	2	35	0	4.00	
-83	11	2	50	0	4.00	
-82	18	3	5	0	4.00	
8	115	3	9	0	0.00	REMOVED
8	116	3	10	0	0.00	REMOVED

WIND #6

FIBER TYPE - AS4W-12K
 FIBER MODULUS - 34E06 psi
 FILAMENT DIA. - 0.000315" / 8μm
 FIBER VOL. - 55.7%
 WIND ANGLE - 90°
 PLY THICKNESS - 0.0135"
 BAND WIDTH - 0.1000"
 RESIN TYPE - 826/RD2
 VISCOSITY - 6.16 poise
 RESIN VOL. - 44.3%
 # PLIES - 1
 SPOOL TENSION - 10 lbs
 AREA OF TOW WITH RESIN - 1.354E-3 in²
 AREA OF TOW WITHOUT RESIN - 7.540E-4 in²
 MANDREL OUTER RADIUS - 3.00"
 MANDREL THICKNESS - 0.05"
 MANDREL MATERIAL - ALUMINUM

MICROSTRAIN		TIME			MANDREL	WIND
GAGE 1	GAGE 2	hrs.	min.	sec.	COVERAGE	STATUS
					inches	
0	1	0	0	0	0.00	START
4	-1	0	0	6	0.54	STOP
		0	0	25	0.54	START
2	2	0	0	30	1.02	STOP
		0	0	54	1.02	START
-2	-5	0	1	00	1.52	STOP
		0	1	24	1.52	START
-82	-85	0	1	30	2.02	STOP
		0	1	54	2.02	START
-125	-142	0	2	00	2.57	STOP
		0	2	25	2.57	START
-123	-135	0	2	30	3.00	STOP
		0	2	55	3.00	START
-118	-131	0	3	00	3.48	STOP
		0	3	24	3.48	START
-118	-129	0	3	30	4.00	END
-114	-126	0	5	0	4.00	
-112	-124	0	6	0	4.00	
-109	-117	0	11	0	4.00	
-108	-112	0	16	0	4.00	
-106	-109	0	21	0	4.00	
-105	-106	0	26	0	4.00	
-104	-102	0	31	0	4.00	
-103	-99	0	36	0	4.00	
-102	-92	0	46	0	4.00	
-101	-87	0	56	0	4.00	
-100	-81	1	6	0	4.00	
-99	-76	1	16	0	4.00	
-98	-71	1	26	0	4.00	
-97	-63	1	38	0	4.00	
-95	-56	1	51	0	4.00	
-93	-48	2	6	0	4.00	
-92	-40	2	21	0	4.00	
-91	-33	2	36	0	4.00	
-90	-26	2	51	0	4.00	
-90	-19	3	6	0	4.00	
9	93	3	12	0	0.00	REMOVED

WIND #7

FIBER TYPE - AS4W-12K
 FIBER MODULUS - 34E06 psi
 FILAMENT DIA. - 0.000315" / 8 μ m
 FIBER VOL. - 62.1%
 WIND ANGLE - 90°
 PLY THICKNESS - 0.0121"
 BAND WIDTH - 0.1000"

RESIN TYPE - 826/RD2
 VISCOSITY - 6.16 poise
 RESIN VOL. - 37.9%
 # PLIES - 1
 SPOOL TENSION - 10 lbs

AREA OF TOW WITH RESIN - 1.214E-3 in²
 AREA OF TOW WITHOUT RESIN - 7.540E-4 in²

MANDREL OUTER RADIUS - 3.00"
 MANDREL THICKNESS - 0.05"
 MANDREL MATERIAL - ALUMINUM

MICROSTRAIN		TIME			MANDREL	WIND
GAGE 1	GAGE 2	hrs.	min.	sec.	COVERAGE	STATUS
					inches	
0	0	0	0	0	0.00	START
1	-1	0	0	7	0.63	STOP
		0	0	26	0.63	START
5	-1	0	0	30	1.02	STOP
		0	0	55	1.02	START
-6	0	0	1	00	1.46	STOP
		0	1	24	1.46	START
-72	-77	0	1	30	2.03	STOP
		0	1	55	2.03	START
-118	-129	0	2	00	2.51	STOP
		0	2	24	2.51	START
-113	-121	0	2	30	3.00	STOP
		0	2	54	3.00	START
-109	-120	0	3	00	3.50	STOP
		0	3	24	3.50	START
-109	-120	0	3	30	4.00	END
-107	-116	0	5	0	4.00	
-102	-111	0	10	0	4.00	
-100	-108	0	15	0	4.00	
-99	-106	0	20	0	4.00	
-98	-104	0	25	0	4.00	
-97	-103	0	30	0	4.00	
-97	-102	0	35	0	4.00	
-96	-100	0	45	0	4.00	
-95	-98	0	55	0	4.00	
-94	-97	1	5	0	4.00	
-94	-95	1	15	0	4.00	
-93	-94	1	25	0	4.00	
-93	-93	1	35	0	4.00	
-92	-92	1	50	0	4.00	
-92	-90	2	5	0	4.00	
-91	-88	2	20	0	4.00	
-91	-87	2	35	0	4.00	
-90	-87	2	50	0	4.00	
-90	-86	3	5	0	4.00	
1	13	3	10	0	0.00	REMOVED

WIND #8

FIBER TYPE - AS4W-12K
 FIBER MODULUS - 34E06 psi
 FILAMENT DIA. - 0.000315" / 8 μ m
 FIBER VOL. - 62.1%
 WIND ANGLE - 90°
 PLY THICKNESS - 0.0121"
 BAND WIDTH - 0.1000"

RESIN TYPE - 826/RD2
 VISCOSITY - 6.16 poise
 RESIN VOL. - 37.9%
 # PLIES - 1
 SPOOL TENSION - 5 lbs

AREA OF TOW WITH RESIN - 1.214E-3 in²
 AREA OF TOW WITHOUT RESIN - 7.540E-4 in²

MANDREL OUTER RADIUS - 3.00"
 MANDREL THICKNESS - 0.05"
 MANDREL MATERIAL - ALUMINUM

MICROSTRAIN		TIME			MANDREL	WIND
GAGE 1	GAGE 2	hrs.	min.	sec.	COVERAGE	STATUS
					inches	
0	0	0	0	0	0.00	START
2	-2	0	0	7	0.59	STOP
		0	0	25	0.59	START
4	-1	0	0	30	1.02	STOP
		0	0	55	1.02	START
1	-3	0	1	00	1.48	STOP
		0	1	24	1.48	START
-34	-40	0	1	30	2.01	STOP
		0	1	54	2.01	START
-63	-70	0	2	00	2.52	STOP
		0	2	24	2.52	START
-60	-67	0	2	30	3.00	STOP
		0	2	54	3.00	START
-57	-63	0	3	00	3.50	STOP
		0	3	24	3.50	START
-56	-60	0	3	30	4.00	END
-53	-56	0	4	0	4.00	
-46	-47	0	9	0	4.00	
-43	-42	0	14	0	4.00	
-42	-39	0	19	0	4.00	
-40	-35	0	24	0	4.00	
-39	-32	0	29	0	4.00	
-38	-29	0	34	0	4.00	
-37	-23	0	44	0	4.00	
-36	-17	0	54	0	4.00	
-35	-11	1	4	0	4.00	
-33	-5	1	14	0	4.00	
-33	0	1	24	0	4.00	
-32	7	1	34	0	4.00	
-31	17	1	49	0	4.00	
-29	27	2	4	0	4.00	
-29	36	2	19	0	4.00	
-28	46	2	34	0	4.00	
-27	56	2	49	0	4.00	
-26	65	3	4	0	4.00	
8	104	3	9	0	0.00	REMOVED

WIND #9

FIBER TYPE - AS4W-12K
 FIBER MODULUS - 34E06 psi
 FILAMENT DIA. - 0.000315" / 8 μ m
 FIBER VOL. - 58.7%
 WIND ANGLE - 90°
 PLY THICKNESS - 0.0128"
 BAND WIDTH - 0.1000"

RESIN TYPE - 826/RD2
 VISCOSITY - 6.16 poise
 RESIN VOL. - 41.3%
 # PLIES - 1
 SPOOL TENSION - 5 lbs

AREA OF TOW WITH RESIN - 1.284E-3 in²
 AREA OF TOW WITHOUT RESIN - 7.540E-4 in²

MANDREL OUTER RADIUS - 3.00"
 MANDREL THICKNESS - 0.05"
 MANDREL MATERIAL - ALUMINUM

MICROSTRAIN		TIME			MANDREL	WIND
GAGE 1	GAGE 2	hrs.	min.	sec.	COVERAGE	STATUS
					inches	
0	0	0	0	0	0.00	START
1	0	0	0	6	0.52	STOP
		0	0	24	0.52	START
3	0	0	0	30	1.08	STOP
		0	0	54	1.08	START
-3	-1	0	1	00	1.51	STOP
		0	1	25	1.51	START
-43	-39	0	1	30	2.00	STOP
		0	1	54	2.00	START
-74	-72	0	2	00	2.49	STOP
		0	2	24	2.49	START
-68	-72	0	2	30	3.00	STOP
		0	2	54	3.00	START
-66	-67	0	3	00	3.53	STOP
		0	3	25	3.53	START
-64	-66	0	3	30	4.00	END
-60	-61	0	4	0	4.00	
-58	-59	0	6	0	4.00	
-54	-55	0	11	0	4.00	
-52	-52	0	16	0	4.00	
-51	-50	0	21	0	4.00	
-50	-48	0	26	0	4.00	
-49	-47	0	31	0	4.00	
-49	-46	0	36	0	4.00	
-47	-44	0	46	0	4.00	
-47	-42	0	56	0	4.00	
-46	-40	1	6	0	4.00	
-46	-39	1	16	0	4.00	
-45	-37	1	26	0	4.00	
-45	-36	1	36	0	4.00	
-44	-34	1	51	0	4.00	
-44	-32	2	6	0	4.00	
-43	-30	2	21	0	4.00	
-43	-29	2	36	0	4.00	
-42	-28	2	51	0	4.00	
-42	-26	3	6	0	4.00	
1	18	3	11	0	0.00	REMOVED

WIND #13

FIBER TYPE - AS4W-12K
 FIBER MODULUS - 34E06 psi
 FILAMENT DIA. - 0.000315" / 8μm
 FIBER VOL. - 57.2%

RESIN TYPE - 826/RD2
 VISCOSITY - 6.16 poise
 RESIN VOL. - 42.8%

WIND ANGLE - 90°
 # PLIES - 1

PLY THICKNESS - 0.0132"
 BAND WIDTH - 0.1000"
 SPOOL TENSION - 7.5 lbs

AREA OF TOW WITH RESIN - 1.318E-3 in²
 AREA OF TOW WITHOUT RESIN - 7.540E-4 in²

MANDREL OUTER RADIUS - 3.00"
 MANDREL THICKNESS - 0.05"
 MANDREL MATERIAL - ALUMINUM

MICROSTRAIN		TIME			MANDREL	WIND
GAGE 1	GAGE 2	hrs.	min.	sec.	COVERAGE	STATUS
					inches	
0	0	0	0	0	0.00	START
2	0	0	0	5	0.48	STOP
		0	0	24	0.48	START
2	5	0	0	30	1.05	STOP
		0	0	54	1.05	START
-2	-8	0	1	00	1.56	STOP
		0	1	25	1.56	START
-47	-50	0	1	30	2.02	STOP
		0	1	55	2.02	START
-85	-100	0	2	00	2.50	STOP
		0	2	24	2.50	START
-90	-91	0	2	30	3.00	STOP
		0	2	54	3.00	START
-87	-92	0	3	00	3.53	STOP
		0	3	25	3.53	START
-87	-89	0	3	30	4.00	END
-83	-87	0	5	0	4.00	
-79	-83	0	10	0	4.00	
-77	-81	0	15	0	4.00	
-76	-79	0	20	0	4.00	
-75	-78	0	25	0	4.00	
-74	-77	0	30	0	4.00	
-74	-77	0	35	0	4.00	
-72	-76	0	45	0	4.00	
-72	-75	0	55	0	4.00	
-71	-75	1	5	0	4.00	
-71	-74	1	15	0	4.00	
-70	-73	1	25	0	4.00	
-70	-73	1	35	0	4.00	
-69	-72	1	50	0	4.00	
-68	-71	2	5	0	4.00	
-67	-70	2	20	0	4.00	
-67	-70	2	35	0	4.00	
-67	-69	2	50	0	4.00	
-67	-69	3	5	0	4.00	
1	3	3	9	0	0.00	REMOVED

WIND #14

FIBER TYPE - AS4W-12K
 FIBER MODULUS - 34E06 psi
 FILAMENT DIA. - 0.000315" / 8μm
 FIBER VOL. - 54.2%

RESIN TYPE - 826/RD2
 VISCOSITY - 6.16 poise
 RESIN VOL. - 45.8%

WIND ANGLE - 90°
 # PLIES - 1

PLY THICKNESS - 0.0139"
 BAND WIDTH - 0.1000"
 SPOOL TENSION - 12.3 lbs

AREA OF TOW WITH RESIN - 1.391E-3 in²
 AREA OF TOW WITHOUT RESIN - 7.540E-4 in²

MANDREL OUTER RADIUS - 3.00"
 MANDREL THICKNESS - 0.05"
 MANDREL MATERIAL - ALUMINUM

MICROSTRAIN		TIME			MANDREL	WIND
GAGE 1	GAGE 2	hrs.	min.	sec.	COVERAGE	STATUS
					inches	
0	0	0	0	0	0.00	START
5	7	0	0	6	0.50	STOP
		0	0	23	0.50	START
8	10	0	0	30	1.08	STOP
		0	0	55	1.08	START
-1	2	0	1	00	1.55	STOP
		0	1	25	1.55	START
-67	-67	0	1	30	1.95	STOP
		0	1	54	1.95	START
-156	-170	0	2	00	2.52	STOP
		0	2	24	2.52	START
-153	-164	0	2	30	3.02	STOP
		0	2	55	3.02	START
-148	-159	0	3	00	3.50	STOP
		0	3	24	3.50	START
-148	-157	0	3	30	4.00	END
-146	-155	0	4	0	4.00	
-142	-151	0	9	0	4.00	
-140	-149	0	14	0	4.00	
-139	-148	0	19	0	4.00	
-136	-146	0	24	0	4.00	
-136	-145	0	29	0	4.00	
-136	-143	0	34	0	4.00	
-135	-142	0	44	0	4.00	
-134	-141	0	54	0	4.00	
-133	-141	1	4	0	4.00	
-132	-139	1	14	0	4.00	
-131	-138	1	24	0	4.00	
-130	-138	1	34	0	4.00	
-130	-136	1	49	0	4.00	
-129	-135	2	4	0	4.00	
-128	-134	2	19	0	4.00	
-128	-133	2	34	0	4.00	
-128	-132	2	49	0	4.00	
-128	-132	3	4	0	4.00	
0	-3	3	9	0	0.00	REMOVED

WIND #15

FIBER TYPE - IM6W-12K
 FIBER MODULUS - 40.4E06 psi
 FILAMENT DIA. - 0.000205" / 5.2μm
 FIBER VOL. - 56.0%
 WIND ANGLE - 90°
 PLY THICKNESS - 0.0097"
 BAND WIDTH - 0.0769"
 RESIN TYPE - 826/RD2
 VISCOSITY - 6.16 poise
 RESIN VOL. - 44.0%
 # PLIES - 1
 SPOOL TENSION - 5 lbs
 AREA OF TOW WITH RESIN - 0.743E-3 in²
 AREA OF TOW WITHOUT RESIN - 4.160E-4 in²
 MANDREL OUTER RADIUS - 3.00"
 MANDREL THICKNESS - 0.05"
 MANDREL MATERIAL - ALUMINUM

MICROSTRAIN		TIME			MANDREL	WIND
GAGE 1	GAGE 2	hrs.	min.	sec.	COVERAGE	STATUS
					inches	
0	0	0	0	0	0.00	START
3	0	0	0	8	0.52	STOP
		0	0	23	0.52	START
4	0	0	0	30	1.03	STOP
		0	0	53	1.03	START
0	-2	0	1	00	1.51	STOP
		0	1	23	1.51	START
-45	-50	0	1	30	1.97	STOP
		0	1	53	1.97	START
-90	-92	0	2	00	2.48	STOP
		0	2	22	2.48	START
-90	-97	0	2	30	3.01	STOP
		0	2	53	3.01	START
-86	-92	0	3	00	3.50	STOP
		0	3	23	3.50	START
-85	-90	0	3	30	4.00	END
-83	-87	0	5	0	4.00	
-81	-84	0	10	0	4.00	
-79	-83	0	15	0	4.00	
-78	-81	0	20	0	4.00	
-77	-81	0	25	0	4.00	
-76	-80	0	30	0	4.00	
-75	-79	0	35	0	4.00	
-75	-79	0	45	0	4.00	
-74	-78	0	55	0	4.00	
-74	-78	1	5	0	4.00	
-74	-77	1	15	0	4.00	
-74	-77	1	25	0	4.00	
-73	-77	1	35	0	4.00	
-73	-76	1	50	0	4.00	
-73	-76	2	5	0	4.00	
-72	-76	2	20	0	4.00	
-72	-76	2	35	0	4.00	
-72	-75	2	50	0	4.00	
-72	-75	3	5	0	4.00	
0	1	3	9	0	0.00	REMOVED

WIND #16

FIBER TYPE	- P55S-2K	RESIN TYPE	- 826/RD2
FIBER MODULUS	- 55E06 psi	VISCOSITY	- 6.16 poise
FILAMENT DIA.	- 0.000394" / 10 μ m	RESIN VOL.	- 42%
FIBER VOL.	- 58%	# PLIES	- 1
WIND ANGLE	- 90°	SPOOL TENSION	- 3 lbs
PLY THICKNESS	- 0.0108"		
BAND WIDTH	- 0.0400"		
AREA OF TOW WITH RESIN	- 0.431E-3 in ²		
AREA OF TOW WITHOUT RESIN	- 2.500E-4 in ²		
MANDREL OUTER RADIUS	- 3.00"		
MANDREL THICKNESS	- 0.05"		
MANDREL MATERIAL	- ALUMINUM		

MICROSTRAIN		TIME			MANDREL COVERAGE	WIND STATUS
GAGE 1	GAGE 2	hrs.	min.	sec.	inches	
0	0	0	0		0.00	START
2	-1	0	0		0.50	STOP
		0	0		0.50	START
5	1	0	0		0.95	STOP
		0	1		0.95	START
0	-2	0	1		1.48	STOP
		0	1		1.48	START
-62	-58	0	1		2.00	STOP
		0	2		2.00	START
-107	-113	0	2		2.45	STOP
		0	2		2.45	START
-106	-113	0	2		3.00	STOP
		0	3		3.00	START
-105	-109	0	3		3.50	STOP
		0	3		3.50	START
-105	-107	0	4		4.00	END
-102	-105	0	8	0	4.00	
-101	-104	0	13	0	4.00	
-101	-104	0	18	0	4.00	
-101	-104	0	23	0	4.00	
-101	-104	0	28	0	4.00	
-101	-104	0	33	0	4.00	
-102	-105	0	38	0	4.00	
-102	-106	0	48	0	4.00	
-103	-106	0	58	0	4.00	
-103	-107	1	8	0	4.00	
-104	-108	1	18	0	4.00	
-105	-109	1	28	0	4.00	
-106	-110	1	38	0	4.00	
-107	-110	1	53	0	4.00	
-107	-111	2	8	0	4.00	
-107	-111	2	23	0	4.00	
-106	-110	2	38	0	4.00	
-106	-110	2	53	0	4.00	
-106	-110	3	8	0	4.00	
3	5	3	18	0	0.00	REMOVED

WIND #18

FIBER TYPE	- AS4W-12K	RESIN TYPE	- 826/RD2
FIBER MODULUS	- 34E06 psi	VISCOSITY	- 6.16 poise
FILAMENT DIA.	- 0.000315" / 8 μ m	RESIN VOL.	- 42.8%
FIBER VOL.	- 57.2%	# PLIES	- 1
WIND ANGLE	- 90°	SPOOL TENSION	- 2 lbs
PLY THICKNESS	- 0.0132"		
BAND WIDTH	- 0.1000"		
AREA OF TOW WITH RESIN	- 1.318E-3 in ²		
AREA OF TOW WITHOUT RESIN	- 7.540E-4 in ²		
MANDREL OUTER RADIUS	- 3.00"		
MANDREL THICKNESS	- 0.05"		
MANDREL MATERIAL	- ALUMINUM		

MICROSTRAIN		TIME			MANDREL	WIND
GAGE 1	GAGE 2	hrs.	min.	sec.	COVERAGE	STATUS
					inches	
0	0	0	0	0	0.00	START
0	0	0	0	6	0.55	STOP
		0	0	34	0.55	START
1	-1	0	0	39	1.02	STOP
		0	1	07	1.02	START
0	-2	0	1	13	1.52	STOP
		0	1	40	1.52	START
-14	-19	0	1	46	2.05	STOP
		0	2	14	2.05	START
-24	-27	0	2	20	2.53	STOP
		0	2	48	2.53	START
-21	-27	0	2	53	3.00	STOP
		0	3	21	3.00	START
-20	-23	0	3	27	3.55	STOP
		0	3	55	3.55	START
-19	-22	0	4	0	4.00	END

WIND #26

FIBER TYPE	- IM6W-12K	RESIN TYPE	- 826/RD2
FIBER MODULUS	- 40.4E06 psi	VISCOSITY	- 6.16 poise
FILAMENT DIA.	- 0.000205" / 5.2 μ m	RESIN VOL.	- 45.2%
FIBER VOL.	- 54.8%	# PLIES	- 1
WIND ANGLE	- 90°	SPOOL TENSION	- 10 lbs
PLY THICKNESS	- 0.0099"		
BAND WIDTH	- 0.0769"		
AREA OF TOW WITH RESIN	- 0.759E-3 in ²		
AREA OF TOW WITHOUT RESIN	- 4.160E-4 in ²		
MANDREL OUTER RADIUS	- 3.00"		
MANDREL THICKNESS	- 0.05"		
MANDREL MATERIAL	- ALUMINUM		

MICROSTRAIN		TIME			MANDREL	WIND
GAGE 1	GAGE 2	hrs.	min.	sec.	COVERAGE	STATUS
					inches	
0	0	0	0	0	0.00	START
5	0	0	0	8	0.53	STOP
		0	0	34	0.53	START
14	1	0	0	40	0.95	STOP
		0	1	06	0.95	START
3	-1	0	1	14	1.50	STOP
		0	1	40	1.50	START
-104	-115	0	1	47	2.00	STOP
		0	2	13	2.00	START
-174	-189	0	2	21	2.54	STOP
		0	2	47	2.54	START
-171	-187	0	2	54	3.00	STOP
		0	3	19	3.00	START
-168	-183	0	3	27	3.50	STOP
		0	3	53	3.50	START
-168	-182	0	4	0	4.00	END

WIND #27

FIBER TYPE - AS4W-12K
 FIBER MODULUS - 34E06 psi
 FILAMENT DIA. - 0.000315" / 8 μ m
 FIBER VOL. - 60.4%
 WIND ANGLE - 90°
 PLY THICKNESS - 0.0125"
 BAND WIDTH - 0.1000"
 RESIN TYPE - 826/RD2
 VISCOSITY - 6.16 poise
 RESIN VOL. - 39.6%
 # PLIES - 1
 SPOOL TENSION - 2.5 lbs
 AREA OF TOW WITH RESIN - 1.248E-3 in²
 AREA OF TOW WITHOUT RESIN - 7.540E-4 in²
 MANDREL OUTER RADIUS - 3.00"
 MANDREL THICKNESS - 0.05"
 MANDREL MATERIAL - ALUMINUM

MICROSTRAIN		TIME			MANDREL	WIND
GAGE 1	GAGE 2	hrs.	min.	sec.	COVERAGE	STATUS
					inches	
0	0	0	0	0	0.00	START
1	-1	0	0	7	0.62	STOP
		0	0	26	0.62	START
0	-2	0	0	39	1.00	STOP
		0	0	50	1.00	START
1	-3	0	0	55	1.46	STOP
		0	1	14	1.46	START
-21	-21	0	1	21	2.03	STOP
		0	1	40	2.03	START
-37	-41	0	1	46	2.57	STOP
		0	2	05	2.57	START
-35	-40	0	2	11	3.08	STOP
		0	2	30	3.08	START
-33	-37	0	2	35	3.53	STOP
		0	2	54	3.53	START
-30	-29	0	3	0	4.00	END

WIND #28

FIBER TYPE	- IM6W-12K	RESIN TYPE	- 826/RD2
FIBER MODULUS	- 40.4E06 psi	VISCOSITY	- 6.16 poise
FILAMENT DIA.	- 0.000205" / 5.2 μ m	RESIN VOL.	- 42.6%
FIBER VOL.	- 57.4%	# PLIES	- 1
WIND ANGLE	- 90°	SPOOL TENSION	- 10 lbs
PLY THICKNESS	- 0.0094"		
BAND WIDTH	- 0.0769"		
AREA OF TOW WITH RESIN	- 0.725E-3 in ²		
AREA OF TOW WITHOUT RESIN	- 4.160E-4 in ²		
MANDREL OUTER RADIUS	- 3.00"		
MANDREL THICKNESS	- 0.25"		
MANDREL MATERIAL	- ALUMINUM		

MICROSTRAIN		TIME			MANDREL	WIND
GAGE 1	GAGE 2	hrs.	min.	sec.	COVERAGE	STATUS
					inches	
0	0	0	0	0	0.00	START
0	-1	0	0	7	0.47	STOP
		0	0	31	0.47	START
-2	-4	0	0	40	1.10	STOP
		0	1	3	1.10	START
-10	-11	0	1	9	1.46	STOP
		0	1	32	1.46	START
-24	-27	0	1	39	1.95	STOP
		0	2	3	1.95	START
-38	-40	0	2	10	2.45	STOP
		0	2	34	2.45	START
-45	-46	0	2	42	3.00	STOP
		0	3	6	3.00	START
-44	-45	0	3	13	3.50	STOP
		0	3	37	3.50	START
-45	-43	0	3	44	4.00	END

WIND #31

FIBER TYPE - IM6W-12K
 FIBER MODULUS - 40.4E06 psi
 FILAMENT DIA. - 0.000205" / 5.2μm
 FIBER VOL. - 57.4%
 WIND ANGLE - 90°
 PLY THICKNESS - 0.0094"
 BAND WIDTH - 0.0769"
 RESIN TYPE - 826/RD2
 VISCOSITY - 6.16 poise
 RESIN VOL. - 42.6%
 # PLIES - 1
 SPOOL TENSION - 5 lbs
 AREA OF TOW WITH RESIN - 0.725E-3 in²
 AREA OF TOW WITHOUT RESIN - 4.160E-4 in²
 MANDREL OUTER RADIUS - 3.00"
 MANDREL THICKNESS - 0.25"
 MANDREL MATERIAL - ALUMINUM

MICROSTRAIN		TIME			MANDREL	WIND
GAGE 1	GAGE 2	hrs.	min.	sec.	COVERAGE	STATUS
					inches	
0	0	0	0	0	0.00	START
0	-1	0	0	7	0.48	STOP
		0	0	32	0.48	START
-1	-3	0	0	40	1.01	STOP
		0	1	5	1.01	START
-5	-8	0	1	13	1.53	STOP
		0	1	38	1.53	START
-11	-14	0	1	44	1.96	STOP
		0	2	9	1.96	START
-18	-22	0	2	17	2.53	STOP
		0	2	42	2.53	START
-20	-22	0	2	49	2.99	STOP
		0	3	14	2.99	START
-21	-21	0	3	21	3.48	STOP
		0	3	46	3.48	START
-19	-18	0	3	54	4.00	END

WIND #34

FIBER TYPE	- P55S-2K	RESIN TYPE	- 826/RD2
FIBER MODULUS	- 55E06 psi	VISCOSITY	- 6.16 poise
FILAMENT DIA.	- 0.000394" / 10 μ m	RESIN VOL.	- 30%
FIBER VOL.	- 70%	# PLIES	- 1
WIND ANGLE	- 90°	SPOOL TENSION	- 5 lbs
PLY THICKNESS	- 0.0089"		
BAND WIDTH	- 0.0400"		
AREA OF TOW WITH RESIN	- 0.357E-3 in ²		
AREA OF TOW WITHOUT RESIN	- 2.500E-4 in ²		
MANDREL OUTER RADIUS	- 3.00"		
MANDREL THICKNESS	- 0.25"		
MANDREL MATERIAL	- ALUMINUM		

MICROSTRAIN		TIME			MANDREL	WIND
GAGE 1	GAGE 2	hrs.	min.	sec.	COVERAGE	STATUS
					inches	
0	0	0	0	0	0.00	START
0	-1	0	0	13	0.47	STOP
		0	0	40	0.47	START
-2	-5	0	0	54	0.97	STOP
		0	1	21	0.97	START
-11	-14	0	1	36	1.50	STOP
		0	2	6	1.50	START
-28	-30	0	2	19	2.10	STOP
		0	2	46	2.10	START
-41	-40	0	2	56	2.45	STOP
		0	3	23	2.45	START
-48	-46	0	3	38	3.00	STOP
		0	4	5	3.00	START
-49	-46	0	4	19	3.50	STOP
		0	4	46	3.50	START
-48	-46	0	5	0	4.00	END

WIND #37

FIBER TYPE - P55S-2K
 FIBER MODULUS - 55E06 psi
 FILAMENT DIA. - 0.000394" / 10 μ m
 FIBER VOL. - 64%
 WIND ANGLE - 90°
 PLY THICKNESS - 0.0098"
 BAND WIDTH - 0.0400"
 RESIN TYPE - 826/RD2
 VISCOSITY - 6.16 poise
 RESIN VOL. - 36%
 # PLIES - 1
 SPOOL TENSION - 3 lbs
 AREA OF TOW WITH RESIN - 0.391E-3 in²
 AREA OF TOW WITHOUT RESIN - 2.500E-4 in²
 MANDREL OUTER RADIUS - 3.00"
 MANDREL THICKNESS - 0.25"
 MANDREL MATERIAL - ALUMINUM

MICROSTRAIN		TIME			MANDREL	WIND
GAGE 1	GAGE 2	hrs.	min.	sec.	COVERAGE	STATUS
					inches	
0	0	0	0	0	0.00	START
0	0	0	0	14	0.51	STOP
		0	0	41	0.51	START
-1	-3	0	0	54	0.95	STOP
		0	1	20	0.95	START
-6	-9	0	1	36	1.50	STOP
		0	2	3	1.50	START
-15	-19	0	2	17	2.00	STOP
		0	2	43	2.00	START
-23	-26	0	2	56	2.46	STOP
		0	3	23	2.46	START
-27	-27	0	3	38	3.00	STOP
		0	4	5	3.00	START
-27	-27	0	4	19	3.50	STOP
		0	4	46	3.50	START
-26	-25	0	5	0	4.00	END

WIND #40

FIBER TYPE	- AS4W-12K	RESIN TYPE	- 826/RD2
FIBER MODULUS	- 34E06 psi	VISCOSITY	- 6.16 poise
FILAMENT DIA.	- 0.000315" / 8 μ m	RESIN VOL.	- 36.0%
FIBER VOL.	- 64.0%	# PLIES	- 1
WIND ANGLE	- 90°	SPOOL TENSION	- 5 lbs
PLY THICKNESS	- 0.0118"		
BAND WIDTH	- 0.1000"		
AREA OF TOW WITH RESIN	- 1.178E-3 in ²		
AREA OF TOW WITHOUT RESIN	- 7.540E-4 in ²		
MANDREL OUTER RADIUS	- 3.00"		
MANDREL THICKNESS	- 0.25"		
MANDREL MATERIAL	- ALUMINUM		

MICROSTRAIN		TIME			MANDREL	WIND
GAGE 1	GAGE 2	hrs.	min.	sec.	COVERAGE	STATUS
					inches	
0	0	0	0	0	0.00	START
0	-1	0	0	6	0.50	STOP
		0	0	29	0.50	START
-1	-2	0	0	35	1.02	STOP
		0	0	59	1.02	START
-4	-5	0	1	5	1.55	STOP
		0	1	28	1.55	START
-7	-9	0	1	33	1.94	STOP
		0	1	56	1.94	START
-14	-14	0	2	3	2.57	STOP
		0	2	27	2.57	START
-15	-16	0	2	32	3.02	STOP
		0	2	55	3.02	START
-15	-14	0	3	1	3.50	STOP
		0	3	25	3.50	START
-14	-13	0	3	30	4.00	END

WIND #40A

FIBER TYPE	- AS4W-12K	RESIN TYPE	- 826/RD2
FIBER MODULUS	- 34E06 psi	VISCOSITY	- 6.16 poise
FILAMENT DIA.	- 0.000315" / 8 μ m	RESIN VOL.	- 39.6%
FIBER VOL.	- 60.4%	# PLIES	- 1
WIND ANGLE	- 90°	SPOOL TENSION	- 5 lbs
PLY THICKNESS	- 0.0125"		
BAND WIDTH	- 0.1000"		
AREA OF TOW WITH RESIN	- 1.248E-3 in ²		
AREA OF TOW WITHOUT RESIN	- 7.540E-4 in ²		
MANDREL OUTER RADIUS	- 3.00"		
MANDREL THICKNESS	- 0.25"		
MANDREL MATERIAL	- ALUMINUM		

MICROSTRAIN		TIME			MANDREL	WIND
GAGE 1	GAGE 2	hrs.	min.	sec.	COVERAGE	STATUS
					inches	
0	0	0	0	0	0.00	START
0	-2	0	0	6	0.53	STOP
		0	0	30	0.53	START
-1	-3	0	0	35	1.00	STOP
		0	0	58	1.00	START
-4	-7	0	1	4	1.52	STOP
		0	1	27	1.52	START
-9	-11	0	1	32	2.00	STOP
		0	1	56	2.00	START
-13	-17	0	2	2	2.53	STOP
		0	2	26	2.53	START
-16	-17	0	2	31	3.00	STOP
		0	2	55	3.00	START
-15	-17	0	3	0	3.50	STOP
		0	3	24	3.50	START
-15	-15	0	3	30	4.00	END

WIND #41

FIBER TYPE	- AS4W-12K	RESIN TYPE	- 826/RD2
FIBER MODULUS	- 34E06 psi	VISCOSITY	- 6.16 poise
FILAMENT DIA.	- 0.000315" / 8 μ m	RESIN VOL.	- 41.3%
FIBER VOL.	- 58.7%	# PLIES	- 1
WIND ANGLE	- 90°	SPOOL TENSION	- 10 lbs
PLY THICKNESS	- 0.0129"		
BAND WIDTH	- 0.1000"		
AREA OF TOW WITH RESIN	- 1.128E-3 in ²		
AREA OF TOW WITHOUT RESIN	- 7.540E-4 in ²		
MANDREL OUTER RADIUS	- 3.00"		
MANDREL THICKNESS	- 0.25"		
MANDREL MATERIAL	- ALUMINUM		

MICROSTRAIN		TIME			MANDREL	WIND
GAGE 1	GAGE 2	hrs.	min.	sec.	COVERAGE	STATUS
					inches	
0	0	0	0	0	0.00	START
0	-1	0	0	6	0.54	STOP
		0	0	30	0.54	START
-2	-3	0	0	35	1.00	STOP
		0	0	58	1.00	START
-7	-10	0	1	4	1.50	STOP
		0	1	28	1.50	START
-17	-21	0	1	34	2.10	STOP
		0	1	58	2.10	START
-29	-30	0	2	2	2.50	STOP
		0	2	26	2.50	START
-33	-34	0	2	32	3.03	STOP
		0	2	56	3.03	START
-32	-34	0	3	1	3.53	STOP
		0	3	25	3.53	START
-32	-33	0	3	30	4.00	END

WIND #42

FIBER TYPE	- AS4W-12K	RESIN TYPE	- 826/RD2
FIBER MODULUS	- 34E06 psi	VISCOSITY	- 6.16 poise
FILAMENT DIA.	- 0.000315" / 8 μ m	RESIN VOL.	- 34.0%
FIBER VOL.	- 66.0%	# PLIES	- 1
WIND ANGLE	- 90°	SPOOL TENSION	- 10 lbs
PLY THICKNESS	- 0.0114"		
BAND WIDTH	- 0.1000"		
AREA OF TOW WITH RESIN	- 1.142E-3 in ²		
AREA OF TOW WITHOUT RESIN	- 7.540E-4 in ²		
MANDREL OUTER RADIUS	- 3.00"		
MANDREL THICKNESS	- 0.25"		
MANDREL MATERIAL	- ALUMINUM		

MICROSTRAIN		TIME			MANDREL	WIND
GAGE 1	GAGE 2	hrs.	min.	sec.	COVERAGE	STATUS
					inches	
0	0	0	0	0	0.00	START
0	0	0	0	6	0.53	STOP
		0	0	30	0.53	START
-1	-3	0	0	35	1.03	STOP
		0	0	59	1.03	START
-8	-9	0	1	4	1.52	STOP
		0	1	28	1.52	START
-19	-20	0	1	33	2.03	STOP
		0	1	57	2.03	START
-29	-30	0	2	2	2.50	STOP
		0	2	26	2.50	START
-33	-34	0	2	32	3.03	STOP
		0	2	55	3.03	START
-34	-34	0	3	1	3.55	STOP
		0	3	25	3.55	START
-34	-34	0	3	30	4.00	END

WIND #43

FIBER TYPE - AS4W-12K
 FIBER MODULUS - 34E06 psi
 FILAMENT DIA. - 0.000315" / 8 μ m
 FIBER VOL. - 66.0%
 WIND ANGLE - 90°
 PLY THICKNESS - 0.0114"
 BAND WIDTH - 0.1000"
 RESIN TYPE - 826/RD2
 VISCOSITY - 6.16 poise
 RESIN VOL. - 34.0%
 # PLIES - 1
 SPOOL TENSION - 5 lbs
 AREA OF TOW WITH RESIN - 1.142E-3 in²
 AREA OF TOW WITHOUT RESIN - 7.540E-4 in²
 MANDREL OUTER RADIUS - 3.00"
 MANDREL THICKNESS - 0.25"
 MANDREL MATERIAL - ALUMINUM

MICROSTRAIN		TIME			MANDREL	WIND
GAGE 1	GAGE 2	hrs.	min.	sec.	COVERAGE	STATUS
					inches	
0	0	0	0	0	0.00	START
0	-2	0	0	6	0.49	STOP
		0	0	29	0.49	START
-1	-3	0	0	35	1.05	STOP
		0	0	59	1.05	START
-4	-6	0	1	4	1.50	STOP
		0	1	28	1.50	START
-9	-11	0	1	34	2.03	STOP
		0	1	57	2.03	START
-15	-17	0	2	3	2.56	STOP
		0	2	27	2.56	START
-17	-17	0	2	32	3.00	STOP
		0	2	55	3.00	START
-17	-17	0	3	0	3.56	STOP
		0	3	24	3.56	START
-16	-16	0	3	29	4.00	END

WIND #44

FIBER TYPE	- AS4W-12K	RESIN TYPE	- 826/RD2
FIBER MODULUS	- 34E06 psi	VISCOSITY	- 6.16 poise
FILAMENT DIA.	- 0.000315" / 8 μ m	RESIN VOL.	- 45.8%
FIBER VOL.	- 54.2%	# PLIES	- 1
WIND ANGLE	- 90°	SPOOL TENSION	- 5 lbs
PLY THICKNESS	- 0.0139"		
BAND WIDTH	- 0.1000"		
AREA OF TOW WITH RESIN	- 1.391E-3 in ²		
AREA OF TOW WITHOUT RESIN	- 7.540E-4 in ²		
MANDREL OUTER RADIUS	- 3.00"		
MANDREL THICKNESS	- 0.25"		
MANDREL MATERIAL	- ALUMINUM		

MICROSTRAIN		TIME			MANDREL	WIND
GAGE 1	GAGE 2	hrs.	min.	sec.	COVERAGE	STATUS
					inches	
0	0	0	0	0	0.00	START
0	-1	0	0	6	0.55	STOP
		0	0	29	0.55	START
-1	-3	0	0	35	1.02	STOP
		0	0	59	1.02	START
-4	-6	0	1	4	1.52	STOP
		0	1	28	1.52	START
-9	-12	0	1	33	2.03	STOP
		0	1	57	2.03	START
-13	-16	0	2	3	2.57	STOP
		0	2	27	2.57	START
-16	-14	0	2	32	3.05	STOP
		0	2	56	3.05	START
-14	-17	0	3	1	3.50	STOP
		0	3	24	3.50	START
-14	-14	0	3	30	4.00	END

WIND #44A

FIBER TYPE - AS4W-12K
 FIBER MODULUS - 34E06 psi
 FILAMENT DIA. - 0.000315" / 8 μ m
 FIBER VOL. - 60.4%
 WIND ANGLE - 90°
 PLY THICKNESS - 0.0125"
 BAND WIDTH - 0.1000"
 RESIN TYPE - 826/RD2
 VISCOSITY - 6.16 poise
 RESIN VOL. - 39.6%
 # PLIES - 1
 SPOOL TENSION - 5 lbs
 AREA OF TOW WITH RESIN - 1.248E-3 in²
 AREA OF TOW WITHOUT RESIN - 7.540E-4 in²
 MANDREL OUTER RADIUS - 3.00"
 MANDREL THICKNESS - 0.25"
 MANDREL MATERIAL - ALUMINUM

MICROSTRAIN		TIME			MANDREL	WIND
GAGE 1	GAGE 2	hrs.	min.	sec.	COVERAGE	STATUS
					inches	
0	0	0	0	0	0.00	START
0	-2	0	0	6	0.53	STOP
		0	0	30	0.53	START
0	-3	0	0	35	1.03	STOP
		0	0	59	1.03	START
-3	-6	0	1	4	1.51	STOP
		0	1	28	1.51	START
-8	-11	0	1	33	2.01	STOP
		0	1	57	2.01	START
-12	-16	0	2	4	2.60	STOP
		0	2	27	2.60	START
-13	-16	0	2	32	3.05	STOP
		0	2	56	3.05	START
-14	-15	0	3	1	3.55	STOP
		0	3	25	3.55	START
-14	-13	0	3	30	4.00	END

WIND #45

FIBER TYPE	- P55S-2K	RESIN TYPE	- 826/RD2
FIBER MODULUS	- 55E06 psi	VISCOSITY	- 6.16 poise
FILAMENT DIA.	- 0.000394" / 10 μ m	RESIN VOL.	- 42%
FIBER VOL.	- 58%	# PLIES	- 1
WIND ANGLE	- 90°	SPOOL TENSION	- 3 lbs
PLY THICKNESS	- 0.0108"		
BAND WIDTH	- 0.0400"		
AREA OF TOW WITH RESIN	- 0.431E-3 in ²		
AREA OF TOW WITHOUT RESIN	- 2.500E-4 in ²		
MANDREL OUTER RADIUS	- 3.00"		
MANDREL THICKNESS	- 0.25"		
MANDREL MATERIAL	- ALUMINUM		

MICROSTRAIN		TIME			MANDREL	WIND
GAGE 1	GAGE 2	hrs.	min.	sec.	COVERAGE	STATUS
					inches	
0	0	0	0	0	0.00	START
0	-1	0	0	14	0.48	STOP
		0	0	40	0.48	START
-2	-3	0	0	55	1.00	STOP
		0	1	22	1.00	START
-6	-10	0	1	35	1.49	STOP
		0	2	2	1.49	START
-15	-20	0	2	17	2.00	STOP
		0	2	43	2.00	START
-22	-28	0	2	56	2.45	STOP
		0	3	23	2.45	START
-26	-30	0	3	39	3.02	STOP
		0	4	6	3.02	START
-27	-29	0	4	18	3.46	STOP
		0	4	45	3.46	START
-26	-25	0	5	0	4.00	END

WIND #46

FIBER TYPE	- P55S-2K	RESIN TYPE	- 826/RD2
FIBER MODULUS	- 55E06 psi	VISCOSITY	- 6.16 poise
FILAMENT DIA.	- 0.000394" / 10 μ m	RESIN VOL.	- 42%
FIBER VOL.	- 58%	# PLIES	- 1
WIND ANGLE	- 90°	SPOOL TENSION	- 5 lbs
PLY THICKNESS	- 0.0108"		
BAND WIDTH	- 0.0400"		
AREA OF TOW WITH RESIN	- 0.431E-3 in ²		
AREA OF TOW WITHOUT RESIN	- 2.500E-4 in ²		
MANDREL OUTER RADIUS	- 3.00"		
MANDREL THICKNESS	- 0.25"		
MANDREL MATERIAL	- ALUMINUM		

MICROSTRAIN		TIME			MANDREL COVERAGE	WIND STATUS
GAGE 1	GAGE 2	hrs.	min.	sec.	inches	
0	0	0	0	0	0.00	START
0	-1	0	0	13	0.46	STOP
		0	0	40	0.46	START
-2	-5	0	0	55	1.01	STOP
		0	1	22	1.01	START
-10	-13	0	1	35	1.50	STOP
		0	2	3	1.50	START
-26	-29	0	2	17	2.00	STOP
		0	2	43	2.00	START
-39	-43	0	2	56	2.46	STOP
		0	3	23	2.46	START
-46	-49	0	3	38	3.00	STOP
		0	4	5	3.00	START
-48	-46	0	4	19	3.50	STOP
		0	4	46	3.50	START
-46	-46	0	5	0	4.00	END

WIND #47

FIBER TYPE - IM6W-12K
 FIBER MODULUS - 40.4E06 psi
 FILAMENT DIA. - 0.000205" / 5.2μm
 FIBER VOL. - 58.8%
 WIND ANGLE - 90°
 PLY THICKNESS - 0.0092"
 BAND WIDTH - 0.0769"
 RESIN TYPE - 826/RD2
 VISCOSITY - 6.16 poise
 RESIN VOL. - 41.2%
 # PLIES - 1
 SPOOL TENSION - 5 lbs
 AREA OF TOW WITH RESIN - 0.707E-3 in²
 AREA OF TOW WITHOUT RESIN - 4.160E-4 in²
 MANDREL OUTER RADIUS - 3.00"
 MANDREL THICKNESS - 0.25"
 MANDREL MATERIAL - ALUMINUM

MICROSTRAIN		TIME			MANDREL	WIND
GAGE 1	GAGE 2	hrs.	min.	sec.	COVERAGE	STATUS
					inches	
0	0	0	0	0	0.00	START
0	-1	0	0	7	0.50	STOP
		0	0	32	0.50	START
-1	-2	0	0	39	0.98	STOP
		0	1	3	0.98	START
-5	-7	0	1	11	1.53	STOP
		0	1	36	1.53	START
-11	-13	0	1	42	1.98	STOP
		0	2	7	1.98	START
-19	-20	0	2	15	2.56	STOP
		0	2	40	2.56	START
-21	-22	0	2	47	3.04	STOP
		0	3	11	3.04	START
-21	-21	0	3	19	3.53	STOP
		0	3	43	3.53	START
-21	-20	0	3	50	4.00	END

WIND #48

FIBER TYPE	- IM6W-12K	RESIN TYPE	- 826/RD2
FIBER MODULUS	- 40.4E06 psi	VISCOSITY	- 6.16 poise
FILAMENT DIA.	- 0.000205" / 5.2 μ m	RESIN VOL.	- 41.2%
FIBER VOL.	- 58.8%	# PLIES	- 1
WIND ANGLE	- 90°	SPOOL TENSION	- 10 lbs
PLY THICKNESS	- 0.0092"		
BAND WIDTH	- 0.0769"		
AREA OF TOW WITH RESIN	- 0.707E-3 in ²		
AREA OF TOW WITHOUT RESIN	- 4.160E-4 in ²		
MANDREL OUTER RADIUS	- 3.00"		
MANDREL THICKNESS	- 0.25"		
MANDREL MATERIAL	- ALUMINUM		

MICROSTRAIN		TIME			MANDREL	WIND
GAGE 1	GAGE 2	hrs.	min.	sec.	COVERAGE	STATUS
					inches	
0	0	0	0	0	0.00	START
0	-1	0	0	8	0.55	STOP
		0	0	31	0.55	START
-2	-4	0	0	38	1.02	STOP
		0	1	1	1.02	START
-9	-12	0	1	7	1.46	STOP
		0	1	31	1.46	START
-24	-26	0	1	38	1.96	STOP
		0	2	1	1.96	START
-41	-42	0	2	10	2.55	STOP
		0	2	33	2.55	START
-45	-47	0	2	39	2.97	STOP
		0	3	2	2.97	START
-47	-46	0	3	10	3.50	STOP
		0	3	33	3.50	START
-46	-45	0	3	40	4.00	END

WIND #49

FIBER TYPE - IM6W-12K
 FIBER MODULUS - 40.4E06 psi
 FILAMENT DIA. - 0.000205" / 5.2μm
 FIBER VOL. - 58.8%
 WIND ANGLE - 90°
 PLY THICKNESS - 0.0092"
 BAND WIDTH - 0.0769"
 RESIN TYPE - 826/RD2
 VISCOSITY - 6.16 poise
 RESIN VOL. - 41.2%
 # PLIES - 1
 SPOOL TENSION - 5 lbs
 AREA OF TOW WITH RESIN - 0.708E-3 in²
 AREA OF TOW WITHOUT RESIN - 4.160E-4 in²
 MANDREL OUTER RADIUS - 3.00"
 MANDREL THICKNESS - 0.05"
 MANDREL MATERIAL - ALUMINUM

MICROSTRAIN		TIME			MANDREL	WIND
GAGE 1	GAGE 2	hrs.	min.	sec.	COVERAGE	STATUS
					inches	
0	0	0	0	0	0.00	START
-1	-1	0	0	8	0.53	STOP
		0	0	32	0.53	START
0	0	0	0	38	0.97	STOP
		0	1	2	0.97	START
-1	-4	0	1	8	1.54	STOP
		0	1	32	1.54	START
-43	-51	0	1	39	2.00	STOP
		0	2	3	2.00	START
-87	-97	0	2	10	2.50	STOP
		0	2	34	2.50	START
-90	-101	0	2	42	3.00	STOP
		0	3	6	3.00	START
-88	-97	0	3	14	3.54	STOP
		0	3	38	3.54	START
-87	-97	0	3	44	4.00	END

WIND #50

FIBER TYPE	- IM6W-12K	RESIN TYPE	- 826/RD2
FIBER MODULUS	- 40.4E06 psi	VISCOSITY	- 6.16 poise
FILAMENT DIA.	- 0.000205" / 5.2μm	RESIN VOL.	- 41.2%
FIBER VOL.	- 58.8%	# PLIES	- 1
WIND ANGLE	- 90°	SPOOL TENSION	- 10 lbs
PLY THICKNESS	- 0.0092"		
BAND WIDTH	- 0.0769"		
AREA OF TOW WITH RESIN	- 0.708E-3 in ²		
AREA OF TOW WITHOUT RESIN	- 4.160E-4 in ²		
MANDREL OUTER RADIUS	- 3.00"		
MANDREL THICKNESS	- 0.05"		
MANDREL MATERIAL	- ALUMINUM		

MICROSTRAIN		TIME			MANDREL	WIND
GAGE 1	GAGE 2	hrs.	min.	sec.	COVERAGE	STATUS
					inches	
0	0	0	0	0	0.00	START
-2	-1	0	0	8	0.53	STOP
		0	0	33	0.53	START
2	0	0	0	40	1.04	STOP
		0	1	05	1.04	START
1	-2	0	1	12	1.48	STOP
		0	1	37	1.48	START
-75	-110	0	1	44	2.00	STOP
		0	2	9	2.00	START
-189	-207	0	2	17	2.50	STOP
		0	2	42	2.50	START
-191	-202	0	2	48	2.95	STOP
		0	3	13	2.95	START
-186	-196	0	3	21	3.50	STOP
		0	3	46	3.50	START
-187	-194	0	3	54	4.00	END

WIND #51

FIBER TYPE	- AS4W-12K	RESIN TYPE	- 826/RD2
FIBER MODULUS	- 34E06 psi	VISCOSITY	- 6.16 poise
FILAMENT DIA.	- 0.000315" / 8 μ m	RESIN VOL.	- 39.6%
FIBER VOL.	- 60.4%	# PLIES	- 1
WIND ANGLE	- 90°	SPOOL TENSION	- 10 lbs
PLY THICKNESS	- 0.0125"		
BAND WIDTH	- 0.1000"		
AREA OF TOW WITH RESIN	- 1.248E-3 in ²		
AREA OF TOW WITHOUT RESIN	- 7.540E-4 in ²		
MANDREL OUTER RADIUS	- 3.00"		
MANDREL THICKNESS	- 0.05"		
MANDREL MATERIAL	- ALUMINUM		

MICROSTRAIN		TIME			MANDREL	WIND
GAGE 1	GAGE 2	hrs.	min.	sec.	COVERAGE	STATUS
					inches	
0	0	0	0	0	0.00	START
-1	-1	0	0	7	0.59	STOP
		0	0	31	0.59	START
2	0	0	0	36	1.00	STOP
		0	1	00	1.00	START
-10	-9	0	1	6	1.53	STOP
		0	1	31	1.53	START
-61	-72	0	1	36	2.00	STOP
		0	2	0	2.00	START
-120	-137	0	2	5	2.43	STOP
		0	2	29	2.43	START
-126	-133	0	2	35	2.97	STOP
		0	3	0	2.97	START
-122	-128	0	3	6	3.50	STOP
		0	3	30	3.50	START
-122	-125	0	3	35	4.00	END

WIND #52

FIBER TYPE - AS4W-12K
 FIBER MODULUS - 34E06 psi
 FILAMENT DIA. - 0.000315" / 8µm
 FIBER VOL. - 64.0%
 WIND ANGLE - 90°
 PLY THICKNESS - 0.0118"
 BAND WIDTH - 0.1000"
 RESIN TYPE - 826/RD2
 VISCOSITY - 6.16 poise
 RESIN VOL. - 36.0%
 # PLIES - 1
 SPOOL TENSION - 5 lbs
 AREA OF TOW WITH RESIN - 1.178E-3 in²
 AREA OF TOW WITHOUT RESIN - 7.540E-4 in²
 MANDREL OUTER RADIUS - 3.00"
 MANDREL THICKNESS - 0.05"
 MANDREL MATERIAL - ALUMINUM

MICROSTRAIN		TIME			MANDREL	WIND
GAGE 1	GAGE 2	hrs.	min.	sec.	COVERAGE	STATUS
					inches	
0	0	0	0	0	0.00	START
-1	-3	0	0	6	0.52	STOP
		0	0	29	0.52	START
3	-2	0	0	34	1.02	STOP
		0	0	57	1.02	START
-2	-7	0	1	3	1.56	STOP
		0	1	26	1.56	START
-28	-43	0	1	31	2.00	STOP
		0	1	54	2.00	START
-65	-71	0	2	0	2.54	STOP
		0	2	23	2.54	START
-62	-65	0	2	28	3.00	STOP
		0	2	51	3.00	START
-58	-64	0	2	57	3.50	STOP
		0	3	19	3.50	START
-58	-60	0	3	25	4.00	END

WIND #53

FIBER TYPE - AS4W-12K
 FIBER MODULUS - 34E06 psi
 FILAMENT DIA. - 0.000315" / 8 μ m
 FIBER VOL. - 60.4%
 WIND ANGLE - 90°
 PLY THICKNESS - 0.0125"
 BAND WIDTH - 0.1000"
 RESIN TYPE - 826/RD2
 VISCOSITY - 6.16 poise
 RESIN VOL. - 39.6%
 # PLIES - 1
 SPOOL TENSION - 2.5 lbs
 AREA OF TOW WITH RESIN - 1.248E-3 in²
 AREA OF TOW WITHOUT RESIN - 7.540E-4 in²
 MANDREL OUTER RADIUS - 3.00"
 MANDREL THICKNESS - 0.05"
 MANDREL MATERIAL - ALUMINUM

MICROSTRAIN		TIME			MANDREL	WIND
GAGE 1	GAGE 2	hrs.	min.	sec.	COVERAGE	STATUS
					inches	
0	0	0	0	0	0.00	START
0	0	0	0	6	0.56	STOP
		0	0	29	0.56	START
0	-1	0	0	35	1.04	STOP
		0	0	57	1.04	START
0	-2	0	1	3	1.50	STOP
		0	1	25	1.50	START
-16	-18	0	1	32	2.06	STOP
		0	1	55	2.06	START
-30	-33	0	2	0	2.57	STOP
		0	2	23	2.57	START
-29	-30	0	2	29	3.10	STOP
		0	2	52	3.10	START
-27	-28	0	2	58	3.60	STOP
		0	3	21	3.60	START
-27	-28	0	3	25	4.00	END

WIND #54

FIBER TYPE	- AS4W-12K	RESIN TYPE	- 826/RD2
FIBER MODULUS	- 34E06 psi	VISCOSITY	- 6.16 poise
FILAMENT DIA.	- 0.000315" / 8 μ m	RESIN VOL.	- 39.6%
FIBER VOL.	- 60.4%	# PLIES	- 1
WIND ANGLE	- 90°	SPOOL TENSION	- 1.75 lbs
PLY THICKNESS	- 0.0125"		
BAND WIDTH	- 0.1000"		
AREA OF TOW WITH RESIN	- 1.248E-3 in ²		
AREA OF TOW WITHOUT RESIN	- 7.540E-4 in ²		
MANDREL OUTER RADIUS	- 3.00"		
MANDREL THICKNESS	- 0.05"		
MANDREL MATERIAL	- ALUMINUM		

MICROSTRAIN		TIME			MANDREL	WIND
GAGE 1	GAGE 2	hrs.	min.	sec.	COVERAGE	STATUS
					inches	
0	0	0	0	0	0.00	START
0	0	0	0	6	0.52	STOP
		0	0	29	0.52	START
1	0	0	0	35	1.00	STOP
		0	0	58	1.00	START
1	0	0	1	4	1.49	STOP
		0	1	27	1.49	START
-7	-9	0	1	33	1.96	STOP
		0	1	56	1.96	START
-18	-20	0	2	2	2.47	STOP
		0	2	26	2.47	START
-17	-18	0	2	32	3.00	STOP
		0	2	55	3.00	START
-16	-17	0	3	1	3.50	STOP
		0	3	24	3.50	START
-15	-16	0	3	30	4.00	END

WIND #55

FIBER TYPE	- AS4W-12K	RESIN TYPE	- 826/RD2
FIBER MODULUS	- 34E06 psi	VISCOSITY	- 6.16 poise
FILAMENT DIA.	- 0.000315" / 8 μ m	RESIN VOL.	- 37.9%
FIBER VOL.	- 62.1%	# PLIES	- 1
WIND ANGLE	- 90°	SPOOL TENSION	- .875 lbs
PLY THICKNESS	- 0.0121"		
BAND WIDTH	- 0.1000"		
AREA OF TOW WITH RESIN	- 1.214E-3 in ²		
AREA OF TOW WITHOUT RESIN	- 7.540E-4 in ²		
MANDREL OUTER RADIUS	- 3.00"		
MANDREL THICKNESS	- 0.05"		
MANDREL MATERIAL	- ALUMINUM		

MICROSTRAIN		TIME			MANDREL	WIND
GAGE 1	GAGE 2	hrs.	min.	sec.	COVERAGE	STATUS
					inches	
0	0	0	0	0	0.00	START
0	0	0	0	6	0.55	STOP
		0	0	29	0.55	START
0	0	0	0	34	1.00	STOP
		0	0	57	1.00	START
0	-2	0	1	3	1.50	STOP
		0	1	25	1.50	START
-4	-6	0	1	31	2.00	STOP
		0	1	54	2.00	START
-8	-9	0	2	0	2.53	STOP
		0	2	23	2.53	START
-7	-8	0	2	29	3.10	STOP
		0	2	52	3.10	START
-6	-7	0	2	57	3.50	STOP
		0	3	19	3.50	START
-6	-6	0	3	25	4.00	END

WIND #57

FIBER TYPE - P55S-2K
 FIBER MODULUS - 55E06 psi
 FILAMENT DIA. - 0.000394" / 10µm
 FIBER VOL. - 58%
 WIND ANGLE - 90°
 PLY THICKNESS - 0.0108"
 BAND WIDTH - 0.0400"
 RESIN TYPE - 826/RD2
 VISCOSITY - 6.16 poise
 RESIN VOL. - 42%
 # PLIES - 1
 SPOOL TENSION - 3 lbs
 AREA OF TOW WITH RESIN - 0.431E-3 in²
 AREA OF TOW WITHOUT RESIN - 2.500E-4 in²
 MANDREL OUTER RADIUS - 3.00"
 MANDREL THICKNESS - 0.05"
 MANDREL MATERIAL - ALUMINUM

MICROSTRAIN		TIME			MANDREL	WIND
GAGE 1	GAGE 2	hrs.	min.	sec.	COVERAGE	STATUS
					inches	
0	0	0	0	0	0.00	START
0	-1	0	0	15	0.53	STOP
		0	0	42	0.53	START
2	0	0	0	55	1.00	STOP
		0	1	24	1.00	START
1	-2	0	1	38	1.50	STOP
		0	2	5	1.50	START
-44	-32	0	2	19	2.00	STOP
		0	2	45	2.00	START
-98	-99	0	2	59	2.50	STOP
		0	3	26	2.50	START
-100	-103	0	3	41	3.03	STOP
		0	4	8	3.03	START
-97	-99	0	4	21	3.50	STOP
		0	4	46	3.50	START
-96	-98	0	5	0	4.00	END
-95	-98	0	7	0	4.00	
-93	-96	0	12	0	4.00	
-93	-95	0	17	0	4.00	
-94	-95	0	22	0	4.00	
-94	-95	0	27	0	4.00	
-93	-94	0	32	0	4.00	
-93	-93	0	37	0	4.00	
-93	-90	0	47	0	4.00	
-93	-90	0	57	0	4.00	
-92	-88	1	7	0	4.00	
-92	-84	1	17	0	4.00	
-91	-82	1	27	0	4.00	
-91	-79	1	37	0	4.00	
-91	-77	1	52	0	4.00	
-91	-74	2	7	0	4.00	
-89	-72	2	22	0	4.00	
-89	-68	2	37	0	4.00	
-89	-64	2	52	0	4.00	
-89	-58	3	7	0	4.00	
0	38	3	12	0	0.00	REMOVED

WIND #58

FIBER TYPE - AS4W-12K
 FIBER MODULUS - 34E06 psi
 FILAMENT DIA. - 0.000315" / 8 μ m
 FIBER VOL. - 57.2%
 WIND ANGLE - 90°
 PLY THICKNESS - 0.0132"
 BAND WIDTH - 0.1000"
 RESIN TYPE - 826
 VISCOSITY - 80 poise
 RESIN VOL. - 42.8%
 # PLIES - 1
 SPOOL TENSION - 5 lbs
 AREA OF TOW WITH RESIN - 1.318E-3 in²
 AREA OF TOW WITHOUT RESIN - 7.540E-4 in²
 MANDREL OUTER RADIUS - 3.00"
 MANDREL THICKNESS - 0.05"
 MANDREL MATERIAL - ALUMINUM

MICROSTRAIN		TIME			MANDREL	WIND
GAGE 1	GAGE 2	hrs.	min.	sec.	COVERAGE	STATUS
					inches	
-1	0	0	0	0	0.00	START
-3	-1	0	0	7	0.53	STOP
		0	0	25	0.53	START
-8	-2	0	0	30	1.00	STOP
		0	0	55	1.00	START
-5	-2	0	1	00	1.50	STOP
		0	1	24	1.50	START
-33	-14	0	1	30	2.00	STOP
		0	1	54	2.00	START
-64	-62	0	2	00	2.60	STOP
		0	2	24	2.60	START
-62	-62	0	2	30	3.02	STOP
		0	2	54	3.02	START
-59	-60	0	3	00	3.52	STOP
		0	3	24	3.52	START
-57	-59	0	3	30	4.00	END
-57	-59	0	5	0	4.00	
-56	-55	0	10	0	4.00	
-55	-55	0	15	0	4.00	
-54	-55	0	20	0	4.00	
-54	-54	0	25	0	4.00	
-53	-54	0	30	0	4.00	
-53	-54	0	35	0	4.00	
-52	-54	0	45	0	4.00	
-52	-52	0	55	0	4.00	
-51	-52	1	5	0	4.00	
-51	-52	1	15	0	4.00	
-51	-52	1	25	0	4.00	
-51	-51	1	35	0	4.00	
-50	-51	1	50	0	4.00	
-50	-51	2	5	0	4.00	
-50	-50	2	20	0	4.00	
-50	-50	2	35	0	4.00	
-50	-50	2	50	0	4.00	
-50	-50	3	5	0	4.00	
1	6	3	10	0	4.00	REMOVED

WIND #62

FIBER TYPE	- AS4W-12K	RESIN TYPE	- 826/RD2
FIBER MODULUS	- 34E06 psi	VISCOSITY	- 6.16 poise
FILAMENT DIA.	- 0.000315" / 8μm	RESIN VOL.	- 39.6%
FIBER VOL.	- 58.7%	# PLIES	- 19
WIND ANGLE	- 90°	SPOOL TENSION	- 5 lbs
PLY THICKNESS	- 0.0128"		
BAND WIDTH	- 0.1000"		
AREA OF TOW WITH RESIN	- 1.284E-3 in ²		
AREA OF TOW WITHOUT RESIN	- 7.540E-4 in ²		
MANDREL OUTER RADIUS	- 3.00"		
MANDREL THICKNESS	- 0.05"		
MANDREL MATERIAL	- ALUMINUM		

MICROSTRAIN		TIME min.	MANDREL COVERAGE inches	LAYER No.
GAGE 1	GAGE 2			
-65	-65	0	4.00	1
-58	-62	1	4.00	1
-54	-56	6	4.00	1
-53	-54	11	4.00	1
-52	-53	16	4.00	1
-51	-52	21	4.00	1
-51	-50	26	4.00	1
-82	-82	31	4.00	2
-76	-76	36	4.00	2
-74	-74	41	4.00	2
-73	-73	46	4.00	2
-73	-73	51	4.00	2
-72	-73	56	4.00	2
-90	-89	61	4.00	3
-83	-86	66	4.00	3
-81	-81	71	4.00	3
-80	-81	76	4.00	3
-80	-81	81	4.00	3
-80	-81	86	4.00	3
-90	-92	91	4.00	4
-83	-85	96	4.00	4
-82	-84	101	4.00	4
-81	-83	106	4.00	4
-81	-82	111	4.00	4
-80	-82	116	4.00	4
-91	-89	121	4.00	5
-84	-84	126	4.00	5
-82	-84	131	4.00	5
-82	-83	136	4.00	5
-81	-83	141	4.00	5
-81	-83	146	4.00	5

MICROSTRAIN		TIME min.	MANDREL	LAYER No.
GAGE 1	GAGE 2		COVERAGE inches	
-90	-88	151	4.00	6
-83	-83	156	4.00	6
-82	-83	161	4.00	6
-82	-83	166	4.00	6
-82	-83	171	4.00	6
-82	-83	176	4.00	6
-87	-86	179	4.00	7
-83	-84	181	4.00	7
-82	-84	186	4.00	7
-82	-80	191	4.00	7
-81	-80	196	4.00	7
-81	-80	201	4.00	7
-81	-80	206	4.00	7
-85	-82	211	4.00	8
-80	-80	216	4.00	8
-80	-80	221	4.00	8
-80	-80	226	4.00	8
-80	-80	231	4.00	8
-79	-80	236	4.00	8
-84	-80	244	4.00	9
-81	-79	246	4.00	9
-80	-79	251	4.00	9
-81	-78	256	4.00	9
-80	-78	261	4.00	9
-80	-78	266	4.00	9
-83	-80	271	4.00	10
-81	-80	276	4.00	10
-80	-77	281	4.00	10
-80	-77	286	4.00	10
-83	-79	291	4.00	11
-81	-78	296	4.00	11
-80	-78	301	4.00	11
-80	-78	306	4.00	11
-82	-78	311	4.00	12
-80	-77	316	4.00	12
-80	-76	321	4.00	12
-80	-76	326	4.00	12
-81	-76	331	4.00	13
-79	-76	336	4.00	13
-79	-76	341	4.00	13
-79	-76	346	4.00	13
-81	-76	351	4.00	14
-80	-76	356	4.00	14
-80	-76	361	4.00	14
-79	-76	366	4.00	14

MICROSTRAIN		TIME min.	MANDREL	LAYER No.
GAGE 1	GAGE 2		COVERAGE inches	
-80	-76	371	4.00	15
-79	-76	376	4.00	15
-78	-76	381	4.00	15
-79	-76	386	4.00	15
-79	-76	396	4.00	16
-79	-76	401	4.00	16
-79	-76	406	4.00	16
-78	-76	411	4.00	16
-80	-76	416	4.00	17
-80	-76	421	4.00	17
-79	-76	426	4.00	17
-78	-76	431	4.00	17
-78	-76	436	4.00	18
-78	-76	441	4.00	18
-78	-76	446	4.00	18
-78	-76	451	4.00	18
-78	-76	456	4.00	19
-78	-76	461	4.00	19
-78	-76	466	4.00	19
-78	-76	471	4.00	19
-78	-76	476	4.00	19
-78	-76	481	4.00	19

WIND #63

FIBER TYPE	- AS4W-12K	RESIN TYPE	- 826/RD2
FIBER MODULUS	- 34E06 psi	VISCOSITY	- 6.16 poise
FILAMENT DIA.	- 0.000315" / 8 μ m	RESIN VOL.	- 39.6%
FIBER VOL.	- 58.7%	# PLIES	- 18
WIND ANGLE	- 90°	SPOOL TENSION	- 5 lbs
PLY THICKNESS	- 0.0128"		
BAND WIDTH	- 0.1000"		

AREA OF TOW WITH RESIN - 1.284E-3 in²
 AREA OF TOW WITHOUT RESIN - 7.540E-4 in²

MANDREL OUTER RADIUS - 3.00"
 MANDREL THICKNESS - 0.05"
 MANDREL MATERIAL - ALUMINUM

MICROSTRAIN		TIME	MANDREL COVERAGE	LAYER
GAGE 1	GAGE 2	min.	inches	No.
-58	-60	0	4.00	1
-50	-53	5	4.00	1
-48	-49	10	4.00	1
-46	-48	15	4.00	1
-45	-48	20	4.00	1
-45	-46	25	4.00	1
-78	-78	32	4.00	2
-68	-70	35	4.00	2
-66	-70	40	4.00	2
		45	4.00	2
-63	-64	50	4.00	2
-63	-64	55	4.00	2
-86	-89	60	4.00	3
-75	-77	65	4.00	3
-73	-76	70	4.00	3
-72	-76	75	4.00	3
-71	-75	80	4.00	3
-70	-74	85	4.00	3
-87	-90	90	4.00	4
-77	-82	95	4.00	4
-74	-78	100	4.00	4
-74	-78	105	4.00	4
-73	-78	110	4.00	4
-72	-76	115	4.00	4
-88	-90	120	4.00	5
-82	-86	125	4.00	5
-80	-83	130	4.00	5
-79	-83	135	4.00	5
-79	-83	140	4.00	5
-79	-83	145	4.00	5

MICROSTRAIN		TIME min.	MANDREL COVERAGE inches	LAYER No.
GAGE 1	GAGE 2			
-91	-90	150	4.00	6
-84	-86	155	4.00	6
-82	-86	160	4.00	6
-82	-85	165	4.00	6
-81	-85	170	4.00	6
-81	-85	175	4.00	6
-88	-90	180	4.00	7
-85	-88	185	4.00	7
-84	-88	190	4.00	7
-83	-84	195	4.00	7
-83	-84	200	4.00	7
-83	-84	205	4.00	7
-88	-86	210	4.00	8
-86	-86	215	4.00	8
-84	-86	220	4.00	8
-84	-86	225	4.00	8
-84	-86	230	4.00	8
-84	-86	235	4.00	8
-86	-86	240	4.00	9
-85	-86	245	4.00	9
-84	-86	250	4.00	9
-84	-86	255	4.00	9
-83	-86	260	4.00	9
-83	-82	265	4.00	9
-85	-84	270	4.00	10
-84	-84	275	4.00	10
-83	-84	280	4.00	10
-83	-83	285	4.00	10
-85	-85	290	4.00	11
-84	-85	295	4.00	11
-84	-85	300	4.00	11
-83	-85	305	4.00	11
-85	-85	310	4.00	12
-84	-85	315	4.00	12
-84	-85	320	4.00	12
-83	-85	325	4.00	12
-85	-85	330	4.00	13
-85	-83	335	4.00	13
-84	-83	340	4.00	13
-83	-83	345	4.00	13
-84	-84	350	4.00	14
-84	-84	355	4.00	14
-83	-84	360	4.00	14
-83	-84	365	4.00	14
-85	-84	370	4.00	15
-84	-84	375	4.00	15
-85	-84	380	4.00	15
-84	-84	385	4.00	15

MICROSTRAIN		TIME min.	MANDREL	LAYER
GAGE 1	GAGE 2		COVERAGE inches	
-85	-84	390	4.00	16
-84	-84	395	4.00	16
-84	-84	400	4.00	16
-84	-84	405	4.00	16
-84	-84	410	4.00	17
-84	-84	415	4.00	17
-84	-84	420	4.00	17
-84	-84	425	4.00	17
-84	-84	430	4.00	18
-84	-84	435	4.00	18
-84	-84	440	4.00	18
-84	-84	445	4.00	18
-84	-84	456	4.00	18
-84	-84	461	4.00	18
-84	-84	466	4.00	18

WIND #67

FIBER TYPE	- AS4W-12K	RESIN TYPE	- 826-A
FIBER MODULUS	- 34E06 psi	VISCOSITY	- VARIABLE
FILAMENT DIA.	- 0.000315" / 8 μ m	TEMPERATURE	- 23°C
FIBER VOL.	- 60.3%	RESIN VOL.	- 39.6%
WIND ANGLE	- 90°	# PLIES	- 1
PLY THICKNESS	- 0.0125"	SPOOL TENSION	- 5 lbs
BAND WIDTH	- 0.1000"		
AREA OF TOW WITH RESIN	- 1.250E-3 in ²		
AREA OF TOW WITHOUT RESIN	- 7.540E-4 in ²		
MANDREL OUTER RADIUS	- 3.00"		
MANDREL THICKNESS	- 0.05"		
MANDREL MATERIAL	- ALUMINUM		

MICROSTRAIN		TIME			MANDREL	WIND	VISCOSITY
GAGE 1	GAGE 2	hrs.	min.	sec.	COVERAGE	STATUS	poise
					inches		
0	0	0	0	0	0.00	START	24
-58	-62	0	1	0	4.00	END	24
-56	-60	0	3	0	4.00		25
-55	-58	0	8	0	4.00		29
-53	-56	0	13	0	4.00		30
-53	-56	0	18	0	4.00		29
-52	-57	0	23	0	4.00		36
-52	-56	0	28	0	4.00		38
-51	-54	0	33	0	4.00		41
-51	-54	0	43	0	4.00		47
-50	-54	0	53	0	4.00		54
-51	-54	1	3	0	4.00		70
-50	-53	1	13	0	4.00		88
-50	-53	1	23	0	4.00		106
-50	-53	1	33	0	4.00		132
-50	-53	1	48	0	4.00		177
-49	-52	2	3	0	4.00		262
-49	-52	2	18	0	4.00		363
		2	33	0	4.00		
-49	-51	2	48	0	4.00		788
-49	-51	3	3	0	4.00		1261

WIND #69

FIBER TYPE	- AS4W-12K	RESIN TYPE	- 826
FIBER MODULUS	- 34E06 psi	VISCOSITY	- 80 poise
FILAMENT DIA.	- 0.000315" / 8 μ m	RESIN VOL.	- 41.3%
FIBER VOL.	- 58.7%	# PLIES	- 1
WIND ANGLE	- 90°	SPOOL TENSION	- 5 lbs
PLY THICKNESS	- 0.0128"		
BAND WIDTH	- 0.1000"		
AREA OF TOW WITH RESIN	- 1.284E-3 in ²		
AREA OF TOW WITHOUT RESIN	- 7.540E-4 in ²		
MANDREL OUTER RADIUS	- 3.00"		
MANDREL THICKNESS	- 0.05"		
MANDREL MATERIAL	- ALUMINUM		

MICROSTRAIN		TIME			MANDREL	WIND
GAGE 1	GAGE 2	hrs.	min.	sec.	COVERAGES	STATUS
					inches	
0		0	0	0	0.00	START
0		0	0	7	0.53	STOP
		0	0	25	0.53	START
1		0	0	30	1.00	STOP
		0	0	55	1.00	START
-2		0	1	00	1.50	STOP
		0	1	24	1.50	START
-29		0	1	30	2.00	STOP
		0	1	54	2.00	START
-60		0	2	00	2.60	STOP
		0	2	24	2.60	START
-60		0	2	30	3.02	STOP
		0	2	54	3.02	START
-59		0	3	00	3.52	STOP
		0	3	24	3.52	START
-58		0	3	30	4.00	END
-55		0	5	0	4.00	
-54		0	10	0	4.00	
-52		0	15	0	4.00	
-50		0	20	0	4.00	
-49		0	25	0	4.00	
-49		0	30	0	4.00	
-48		0	35	0	4.00	
-46		0	45	0	4.00	
-46		0	55	0	4.00	
-45		1	5	0	4.00	
-44		1	15	0	4.00	
-43		1	25	0	4.00	
-43		1	35	0	4.00	
-42		1	50	0	4.00	
-42		2	5	0	4.00	
-41		2	20	0	4.00	
-41		2	35	0	4.00	
-41		2	50	0	4.00	
-40		3	5	0	4.00	
1		3	10	0	4.00	REMOVED

VITA

Russell Kent Call was born in 1956 in Ogden, Utah. He graduated from Morgan High School, Morgan, Utah in 1975. He graduated Magna Cum Laude from Weber State College in 1981 receiving a Bachelor of Science degree in Manufacturing Engineering Technology. After graduation, Mr. Call was employed by Hercules Aerospace Inc. He worked in the Composite Structures Development Laboratory, where he was promoted to supervisor over Research and Development Filament Winding.

In 1984 Mr. Call went to work for Atlantic Research Corporation. He aided in the setting up and start up of their filament winding facility.

In 1986 Mr. Call left Atlantic Research to pursue graduate studies at Virginia Tech. In 1988, after the course work was completed, Mr. Call left VPI&SU for employment with Thiokol Corporation. The remaining requirements for the Masters degree were completed while in their employ.



R. Kent Call